

---

**I can see it in your eyes:**

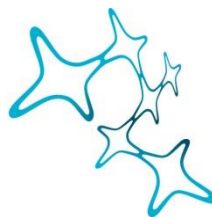
**What the *Xenopus laevis* eye can teach us**

**about motion perception**

---

Dissertation der Graduate School of Systemic Neurosciences

der Ludwig-Maximilians-Universität München



Graduate School of  
Systemic Neurosciences  
LMU Munich

**Céline Gravot**

München, 07.07.2017



Supervisor and first reviewer: Prof. Dr. Hans Straka

Second reviewer: Prof. Dr. Anja Horn-Bochtler

Third reviewer: Prof. Dr. Ansgar Büschges

Date of oral defense: 25.10.2017

*“L’essentiel est invisible pour les yeux.”*

Antoine de Saint-Exupéry

# Table of Contents

1	Introduction.....	1
1.1	Motion detectors .....	1
1.1.1	Modalities of motion detection .....	1
1.1.2	Motion-detecting sensory systems .....	2
1.2	Motion detection during locomotion .....	4
1.2.1	Object motion and self-motion .....	4
1.2.2	Visuo-vestibular interaction .....	5
1.2.3	The physiology of the vestibular system .....	6
1.2.4	The physiology of the visual system .....	8
1.3	Gaze stabilization .....	12
1.3.1	The vestibulo-ocular reflex .....	13
1.3.2	The optokinetic reflex.....	13
1.4	Visual motion detection is context-dependent .....	14
1.4.1	Characteristics of a visual scene .....	15
1.4.2	Image stabilization during self-motion.....	17
1.5	I can see it in your eye.....	18
1.5.1	<i>Xenopus laevis</i> tadpoles.....	18
1.5.2	Virtual reality setups.....	19
1.6	Aim of the thesis .....	21
2	Manuscript 1.....	23
3	Manuscript 2.....	59
4	Manuscript 3.....	83
5	Discussion .....	95
5.1	Motion information.....	95
5.1.1	Detecting different forms of motion .....	95
5.1.2	Visual motion detection.....	96
5.2	Gaze-stabilizing reflexes.....	97
5.2.1	A behavioral correlate .....	97
5.3	Speed estimation .....	98
5.3.1	A velocity signal present at the retinal level.....	98
5.3.2	The influence of visual scene parameters .....	99

5.4	Comparative aspect of visual motion processing .....	102
5.4.1	Through the eye of <i>Xenopus laevis</i> tadpoles .....	103
5.4.2	Human experiments .....	104
5.4.3	Comparative approach .....	105
5.4.4	Different speed estimates .....	105
5.5	Internal representation of self-motion .....	106
5.5.1	Nature versus nurture .....	108
5.6	From biology to technology .....	109
5.7	Outlook.....	111
6	Appendix 1: Human Experiments.....	112
7	References.....	117
8	Acknowledgements .....	i
9	List of publications.....	ii
10	Eidesstattliche Versicherung .....	iii
11	Author contributions .....	iv

# 1 Introduction

## 1.1 Motion detectors

Miniaturized motion detecting systems are all around us: Whether they are sitting quietly on our wrist while we are jogging, embedded in our smartphone when wiping on the screen or mounted behind the windshield of self-driving cars. A large range of sensors are nowadays able to precisely detect basic motion metrics, such as step counts or the position and trajectories of pedestrians on the sidewalk. These new technologies drastically change how we monitor our environments and control our own lives: Commonly used in security systems (e.g. remote alarms), they are also applied for a variety of clinical applications (e.g. rehabilitation and monitoring of neurological patients, (Appelboom et al., 2014)) or for road safety (e.g. autonomous cars, (Bayat et al., 2017)). However, it is often neglected that many of the mechanisms underlying modern motion sensor technologies can also be found in highly sophisticated biological systems, that evolved and developed millions of years ago (Kaas, 1989).

### 1.1.1 Modalities of motion detection

Sensory systems enable animals to gather information about the physical world they live in (Keeley, 2002). Motion detectors, in particular, are tasked with detecting motion, i.e. changes in position, be it their own motion through space or the motion of other objects. Therefore, it is important to emphasize the physical modalities by which sensory systems, in particular motion detecting systems, can be stimulated.

When moving through a liquid or gaseous environment, the movement of an object must be accompanied by a relative motion of the surrounding medium in the opposite direction, thus, the first method to detect motion is to estimate the velocity of bulk flow fluctuations (see Fig. 1, upper row). This mass rate measurement is applicable in different media, such as water or oil but poses greater challenges at low speeds in media with lower densities, such as air.

A second way to detect motion is to sense acceleration, which is the net result of inertial forces acting on an object (see Fig. 1, middle row). Thus, any acceleration is accompanied

by inertial forces, which mathematically relate to the strength of the acceleration. However, this method only applies for accelerated movements. Movements at a constant velocity, however, cannot be distinguished from standstill, since the acceleration in both cases is zero.

A third way to detect motion is by comparing visual images taken at slightly different timepoints. If an object has changed position in two successive images, this means it must have been moving relative to the sensor. Functionally, this requires the sensor to detect the shift of an edge in a visual scene, relying on brightness changes of light and consequently calculate the velocity of the motion by determining the magnitude of the shift and the time it took for it (see Fig. 1, lower row).

The first two methods, that rely on mechanical forces (bulk flow and inertial force), are particularly suitable for the detection of dynamical motion changes, due to the immediacy of their signal transduction and their temporal dynamics. On the other hand, the third method (vision-based) is less direct, as this process needs to encode the shift between two consecutive events, and therefore perform complex computations to extract a motion signal. This illustrates the reason why at least two motion detecting sensors need to be involved for the intricate process of faithful motion detection in animals.

### 1.1.2 Motion-detecting sensory systems

During the course of evolution, sensory systems evolved to respond to the demands of animals in their specific environments. In particular, motion detecting sensors developed to provide living organisms with relevant information about motion changes in their surrounding and of their own (Butler & Hodos, 2005). Interestingly, the development of these sensory systems reflects the major steps in the evolutionary history of life.

#### The lateral line system

Animals evolved in the ocean (Erwin et al., 2011). Thereby it is not surprising that one of the phylogenetically most ancient motion detecting system evolved under water and is specifically suited to aquatic environments: Flow sensors of the lateral line system

detect weak water motion and enable navigation using hydrodynamic cues. Sensors of the lateral line system are still present in most anamniotes and are involved in orientation and navigation (Goulet et al., 2008). The smallest sensory unit of the lateral line system, the neuromast, is a structure lying in or just beneath the skin. The biological motion sensors of the neuromasts are hair cells with mechanically sensitive organelles, called stereocilia. The latter protrude into a gelatinous substance called cupula, that is exposed to the surrounding water. When water current displaces the cupula and concurrently the stereocilia, the mechanical energy is transduced into an electrical energy, that is signaled by afferent nerves towards the central nervous system of the animals (see Fig. 1, upper row).

### The vestibular system

After the Cambrian explosion, changes in atmospheric oxygen levels as well as the development of complex body structures, enabled life to venture on land. This event put a strong selective pressure on the lateral line organ, which became obsolete in terrestrial/aerial habitats. Now, animals had to support their body weight against the pull of gravity to stay upright, and therefore relied even more heavily on specific graviceptive sensors, i.e. sensors that respond to gravitational acceleration. These sensory structures were suited to detect not only gravity, but also inertial forces caused by accelerated motion of the animal through space (see Fig. 1, middle row). The vestibular system, embedded in the inner ear, detects angular and linear acceleration by means of ciliated mechanosensitive hair cells (Hudspeth, 2005). These structures, like in the lateral line system, respond to physical displacements of the stereocilia and convert the mechanical stimulus into a neuronal signal, which is then processed by the central nervous system. Because acceleration is zero during periods of constant motion, this sensor is unable to detect motion at constant velocities. This drawback is however compensated by a third kind of motion detecting system that is particularly suited for detecting constant motion and will be the main focus of this thesis: the visual system.

### The visual system

Parallel to the vestibular system, the evolution of image-forming eyes during the Cambrian Period suddenly enabled organisms to perceive their environments in a

completely new way (Parker, 2003). The development of vision triggered an explosion of life diversity, with an enormous variety of new body forms, life styles and colors. Whichever animals possessed eyes could detect motion in the surrounding area and had huge advantages, such as seeing into the distance, thereby ensuring greater success at finding food or avoiding predators. In particular, if an animal is able to estimate the speed and direction of a prey's trajectory, this greatly increases the repertoire of strategies it can employ while hunting. These capabilities came along with the evolution of the ocular motor system, which allowed motion tracking and maintaining a stable eye position in space during locomotion.

Unlike the lateral line or vestibular system, motion sensors in the visual system are not purely mechanically driven, but rely on substantial computations based on the activity patterns of photoreceptor cells in the retina of the eye, to be able to infer the velocity of structures in any moving image (see Fig. 1, lower row).

## 1.2 Motion detection during locomotion

### 1.2.1 Object motion and self-motion

Especially when actively locomoting through the world, animals strongly rely on their motion detecting sensory systems to estimate the motion of objects in the world (e.g. other animals, predators or prey) as well as their own motion relative to their environments (DeAngelis & Angelaki, 2012). Although the detection of object motion is particularly important for the avoidance of obstacles and the interaction with other animals, an accurate estimation of the own movement in space is crucial for self- or body motion perception and permits effective navigation in space as well as the control of posture and gaze (Campos & Bühlhoff, 2012).

While the modus operandi of the vestibular sense restricts it to detecting only self-motion uninfluenced by the motion of outside objects, the sense of vision can detect both the motion of small objects, as well as provide information about self-motion in space. This is a challenge for the central nervous system, as it must distinguish between these different sources of visual motion and keep two major components apart: Small-field visual motion can typically be attributed to the movement of individual objects.

Large-field visual motion on the other hand is evoked when the entire visual world changes place with respect to the animal and typically means that the animal itself is in motion. Thus, large-field visual motion signals are cues for self- or body motion.

Typically, self-motion perception is experienced when an animal locomotes, i.e. actively moves within and throughout the environment, but can also be perceived when being passively moved (Campos & Bühlhoff, 2012). This is why a large-field movement of a visual scene induces a sense of self-motion even when actually it is the environment that is moving relative to the organism. Most humans have experienced this illusionary phenomenon, while sitting in a stationary train: When a neighboring train begins to move, vision alone can sometimes create a compelling illusion of self-motion (Campos & Bühlhoff, 2012).

### 1.2.2 Visuo-vestibular interaction

When actively moving through space during daily behaviors, a percept of self-motion is obtained by the interplay of different sensory systems and their respective motion-detecting sensors. The interaction of these sensory systems provides animals with a reliable estimate about the extent, speed and direction of egocentric movements to correctly navigate and control posture in space (Campos & Bühlhoff, 2012).

In most vertebrates, the two main systems that provide the most sensitive information for judging self- or body motion are the vestibular and the visual systems: While the vestibular system provides powerful clues about head (body) position in space, the visual system reports the relative motion between an observer and a visual scene. One main aim of the visuo-vestibular interaction is to maintain a high level of visual acuity during locomotion, when there is movement in either the outside world or of the observer (Barnes, 1983). To understand the interaction between these sensory systems, it is vital to know how their anatomical structure and functional connectivity to the central nervous system enables them to detect motion in three-dimensional space.

### 1.2.3 The physiology of the vestibular system

The vestibular system is one of the most predominant but often underestimated motion detecting systems in most animal species. This system is highly conserved among vertebrates (Straka & Dieringer, 2004) and contributes to a large range of functions, ranging from reflexes to navigation and motor coordination (Angelaki & Cullen, 2008). The vestibular apparatus lies within the inner ear of vertebrates, a highly complex anatomical structure in the evolution of vertebrates and a fabulous example of the “engineering” capabilities of nature (Graf, 2007). In mammals, one part of the inner ear, the cochlea, is able to detect minimal fluctuations in air pressure, a mechanism that enables them to hear. Although hearing is often considered the primary function of the inner ear, it also provides important signals about self- or body motion using two sophisticated receptive structures, the semicircular canals and the otolith organs, that evolved to measure angular and linear acceleration components of head movements, respectively.

#### The semicircular canals

Angular acceleration components of head movements are detected in all vertebrates by sense organs in the inner ear, called semicircular canals (Fritsch & Straka, 2014). The three perpendicularly oriented semicircular canals are the anterior vertical, the posterior vertical and the horizontal canal. They cover all planes in the three-dimensional world and thereby maximize the ability to detect three directions of angular rotations of the head. Each canal is filled with an inert fluid, called endolymph, that moves relative to the canal at each acceleration of the head. Due to the inertia of the fluid, a force is applied to a structure called cupula, that in turn bends the mechanosensing hair cell bundles, composed of several stereocilia and one tall kinocilium. Hair cells are extremely sensitive to deflections: Bending the stereocilia towards the kinocilium causes the opening of mechanically gated transduction channels and depolarizes the cell. The depolarization causes the release of neurotransmitters onto the vestibular nerve afferents and an increase in nerve activity, that is conveyed to the central nervous system (Wersäll, 1956). Conversely, bending the stereocilia away

from the kinocilium causes a reduction of the vestibular nerve activity, and thereby enables the vestibular organs to continuously encode rotational acceleration signals.

### The otolith organs

Linear acceleration components of head movements are detected by two main otolith organs, named utricle and saccule, that are common to most mammals. In frogs and nonmammals, a third otolith organ, the lagena, is present and sensitive to both vestibular and auditory stimulation (de Burlet, 1929). Like the semicircular canals, the otolith organs are arranged in a way that enables them to respond maximally to head position changes: While the utricle, oriented within the horizontal plane, is sensitive to lateral acceleration as well as anterior-posterior motion, the saccule, vertically arranged, can sense acceleration along the occipitocaudal axis as well as linear motion along the anterior-posterior axis (Hain et al., 2007). The lagena possesses a dual function and supplements the function of the saccule, by identifying gravitation forces as well as substrate vibrations. Each otolith organ contains a sensory epithelium, called macula, on which many mechanosensitive hair cells lie. The stereocilia of the hair cells project into a gelatinous cap, the otoconia, which is itself weighted by crystals of calcium carbonate. In contrast to the semicircular canals, where the inertia of the endolymph is important for the detection of acceleration, the mass of the otoconia is the key to the sensitivity of the maculae: When the position of the head changes, the inertia of the heavy mass produces a force that bends the stereocilia of the hair cells and thus leads to a change of nerve activity. While hair cells in the semicircular canals all have the same directional sensitivity, otolith hair cells cover an orientation range of  $360^\circ$  (Wersäll, 1956).

### Vestibular processing

The biological motion sensors of the vestibular system, the hair cells, are involved in different processing pathways, that control the positions of head, body and eyes. Hair cells synapse onto vestibular afferent nerve fibers of the eight cranial nerve (Goldberg, 2000), that transmit the incoming acceleration information to central vestibular neurons in the hindbrain. The vestibular nucleus is the primary processor of vestibular inputs: Afferent information is encoded in separate groups of vestibular neurons. The sensory

structure, which a vestibular neuron originates from, determines its response characteristics (Straka et al., 2002). The different areas of the vestibular nucleus are relay stations for compensatory reflexes, that generate neck, body and eye movements in response to head motion, thereby providing stability of the head, postural control and clear vision, respectively. The vestibular nucleus also processes information from other parts of the brain, such as the cerebellum, the somatic as well as the visual sensory systems and therefore is an important multi-sensory nucleus. Moreover, it also projects to the brainstem and the spinal cord. This extensive connectivity is required to establish appropriate efferent signals and generate an adequate output to control the motor effector organs, the extraocular and skeletal muscles. The vestibular system connects to the thalamus and higher cortical areas if present: At this level, complex information integration about movements of the body, the eyes and the visual scene is performed, providing a continuous internal representation of body position and orientation in space (Angelaki & Cullen, 2008; Pfeiffer et al., 2014).

#### 1.2.4 The physiology of the visual system

While we are often unaware of our vestibular system, that gives us an “invisible” sensation about our own motion in space, vision, however, provides us with a window to the outside world: The visual system allows us to detect relative movements of objects’ and our own position in the environment.

Vision is a primary sensory modality of many vertebrates and invertebrates (Gibson, 1979) and is involved in a large range of behavioral tasks. The constraints imposed by the physics of light and specific ecological environments influenced the evolution and led to an overwhelming variation of image-forming eyes in different taxa: While some animals adapted to night vision by increasing the pupil size, others evolved binocular vision to gain depth perception and chase prey more effectively. Nevertheless, the visual circuits and pathways are remarkably similar between species, which enables researchers to elucidate general strategies of this system using a variety of model organisms (Borst et al., 2015; Lamb et al., 2007).

## General anatomy

The visual system uses light that impinges on the earth to form images and provide us with the sense of sight. From a physical point of view, light is an electromagnetic wave which is absorbed by specialized cells of the visual system, the photoreceptors. These specialized sense cells are found in the retina at the back of the eye. Each photoreceptor possesses a specialized outer segment, named cilium, that contains the phototransduction machinery (Sung et al., 1994). The outer segment houses light-sensitive photopigments, the opsins, proteins that are able to change their conformation from a resting state to a signaling state upon light absorption (Shichida & Matsuyama, 2009).

To cope with the massive dynamic range of light intensities in bright day *versus* moonlight, that extends over nine orders of magnitude, the visual system possesses two types of photoreceptors, rods and cones, that work in tandem to adjust vision at varying light levels. While the rods are highly sensitive to small light changes, respond to single photons and provide the basis for scotopic (night) vision, the cones, which are less sensitive to light, mediate vision above a certain luminance level ( $0.03 \text{ cd/m}^2$ , (Kihara et al., 2006)) and are specialized to photopic (daylight) vision.

Cones mediate color vision, by responding to different wavelengths of light, a capability that depends on the conformation change of their visual pigment opsin. Each different pigment is thereby especially sensitive and responds to a certain wavelength of light. Most vertebrates, including humans, possess three types of cones: S-cones respond to short-wavelengths, M-cones to medium-wavelengths and L-cones to long-wavelengths, with their peak wavelengths around 420-440 nm (blue), 534-545 nm (green) and 564-580 nm (red), respectively. In humans, the *visible* light therefore ranges from approximately 400 nm (violet) to 700 nm (red). Other animals possess different number and types of cones and are thereby able to detect other wavelengths, such as ultraviolet (down to 300 nm) or infrared (up to 800 nm) light. Seeing ultraviolet light can for instance help pollinating insects, such as bumblebees, to detect nectar on flowering plants (Macior, 1971). Animals, such as salmons, have evolved the ability to detect

infrared light, enabling them to better navigate in murky water during migration (Enright et al., 2015).

## Visual processing

The process of biological vision begins within the eye, more precisely in the photoreceptors of the retina. In the dark, photoreceptors are in a depolarized state and, in contrast to other sensory receptor cells, the shining of light on these cells leads to a membrane hyperpolarization (Oakley, 1977). In the first step of visual transduction, the opsins of the photoreceptors absorb photons and tune the molecule's absorption of light to a specific region in the spectrum. Light-activation induces a change in the configuration of opsins and triggers a series of alterations, such as the regulation of the nucleotide cyclic guanosine monophosphate (cGMP) level as well as the activation of voltage-sensitive  $\text{Ca}^{2+}$  channels. In light, cGMP levels drop and  $\text{Ca}^{2+}$  channels close, leading to a hyperpolarization of the membrane and a reduction of transmitter release.

In the downstream network, a parallel, retinotopic arrangement connects the photoreceptors with bipolar cells and the bipolar cells with ganglion cells. Moreover, inhibitory horizontal and amacrine cells shape the responses of photoreceptor and bipolar cells as well as bipolar and ganglion cells, respectively (Gollisch & Meister, 2010). Together, all axons of ganglion cells form the optic nerve, that carries the final retinal signal from the eye to the brain. The signal of ganglion cells is conveyed to higher brain structures, such as the pretectum, the lateral geniculate nucleus (LGN) and subsequently to area V1 or area V5/MT of the visual cortex, depending on species. The different pathways serve several different purposes, such as reflexively controlling compensatory, low-latency eye movements, extracting complex pattern information (e.g. inferring surface properties such as smoothness from an object's color and texture) or extrapolating trajectories of moving objects into the future to perform goal-directed actions (Basili et al., 2009; Seymour et al., 2009).

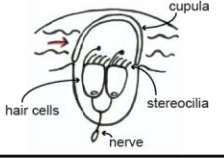
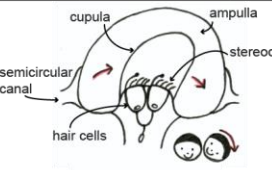
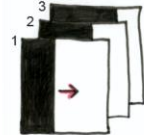
## Motion vision

Visual motion processing, the extraction of real-world speed and direction information from a moving retinal image, is performed at an early stage of visual processing. At the

retinal level, bipolar and ganglion cells already detect temporal brightness increments and decrements of light, i.e. changes of brightness in certain parts of the retinal image. The response patterns are processed in two parallel processing streams, known as the ON (light increment) and the OFF (light decrement) pathways (Schiller et al., 1986).

During motion, the brightness pattern of a visual scene changes in space. Therefore, motion can be computed by detecting the temporal brightness fluctuations of a coherently moving stimulus pattern, e.g. by comparing the brightness increment at a particular location and at a given time with the brightness increment at a neighboring location measured some time later. A motion estimate can thereby be calculated by relating the spatial change of brightness to the temporal change at a given location of the image (Borst & Egelhaaf, 1993), and the speed can be computed as the ratio of displacement over time.

This thesis aims at investigating whether a retinal signal provides an accurate speed estimate of a moving image to animals under different visual conditions and how this estimate is transduced into behaviorally relevant tasks.

Modality	Sensory system	Stimulus	Illustration
Mass flow measurement	Lateral line system	Deflection of hair cells due to water flow	
Acceleration	Vestibular system	Deflection of hair cells due to inertial forces and gravity	
Optic flow	Visual system	Spatio-temporal changes of image characteristics	

**Figure 1: Modalities of motion detection**

Sensory systems are stimulated by different physical modalities, that enable them to detect different sorts of motion.

### 1.3 Gaze stabilization

When interacting with their environment, animals combine and integrate the information of different sensory modalities to generate appropriate behaviors. In particular, motion cues provided by the different sensory systems are crucial inputs, that enable animals to form an estimate of their own movements within the world and the motion of objects around them.

The correct estimation of motion is a demanding task for the central nervous system, as different information, such as vestibular, visual, proprioceptive or somatosensory cues must be encoded, combined and interpreted correctly (DeAngelis & Angelaki, 2012; Dichgans & Brandt, 1978). A key challenge for the visual system is therefore to distinguish between small-field motion components caused by moving objects and large-field visual motion due to self- or world-motion respectively, and simultaneously preserve gaze stability and visual acuity.

Indeed, when interacting within the environment, self-generated body displacements always provoke disturbances and image displacements of the visual world on the retina, impairing drastically visual acuity. Animals therefore need an internal representation of their movements in space, to perform adequate compensatory eye movements and thereby ensure a stable visual image on the retina while locomoting. To achieve this task during active and passive self-motion, the oculomotor system draws upon both visual and vestibular (self)-motion information, both of which drive associated eye movement reflexes: The vestibulo-ocular reflex (VOR), driven by motion sensors of the semicircular canals and otolith organs, operates at high frequencies and effectively detect head movements with high accelerations. On the contrary, the optokinetic reflex (OKR) relies on motion sensitive retinal ganglion cells, that are optimally sensitive at lower movement frequencies and can detect constant velocity motion. The VOR and OKR are therefore ideal complements to ensure image stabilization over a large dynamic working range during self- or world motion, respectively.

### 1.3.1 The vestibulo-ocular reflex

The vestibular sensory periphery provides the central nervous system with a powerful source of information about head motion in space (DeAngelis & Angelaki, 2012). To ensure gaze stability, the vestibulo-ocular reflex generates rapid, compensatory eye movements in the opposite direction of head movements. The functional organization of the VOR network has been highly conserved during evolution from early vertebrates to mammals (Straka & Baker, 2013) and the relative simplicity of its pathway makes it an excellent model system to bridge the gap between the function of neuronal circuits and the resulting behavior (Cullen, 2012). The VOR is one of the fastest reflexes observed in vertebrates, generating compensatory eye movements with a response latency of only 7 ms (Huterer & Cullen, 2002). This property is due to a three-neuron pathway, which ensures minimal axonal and synaptic delays: Vestibular afferent nerve fibers carry motion signals of head turns from the mechanosensitive hair cells to second-order vestibular neurons, which in turn project to extraocular motoneurons, that drive oculomotor neurons to produce compensatory eye movements. The three semicircular canals, which sense angular accelerations of the head drive the angular VOR, whereas the otolith organs, which sense linear acceleration drive the translational VOR (Cullen, 2012).

During natural behavior, such as walking or running, the VOR needs to detect very high frequencies up to 20 Hz (Hirasaki et al., 1999). Due to the mechanical sensitivity of the motion sensors and the low-latency neuronal network, the VOR evolved to perfectly respond to a large range of physiologically relevant dynamics of head movements (Sadeghi et al., 2007). Thus, while higher frequencies are more appropriately compensated by this reflex, the VOR cooperates with another reflex, the optokinetic reflex, that stabilizes gaze at lower frequencies.

### 1.3.2 The optokinetic reflex

The optokinetic reflex, which assists the VOR at lower frequencies, plays a crucial role in stabilizing visual images on the retina. This brainstem-mediated reflex generates characteristic compensatory eye movements, induced by large-field optic flow: Slow

following eye movements in the direction of the current optic flow field motion, and fast, resetting eye movements that maintain the eye within its working range.

The sensory basis of the OKR are motion- and direction-sensitive retinal ganglion cells that provide information about how fast a visual image moves across the retina. This velocity signal of the large-field moving visual scene directly determines the performance of the OKR (Cohen et al., 1981).

In most vertebrates, information from the ganglion cells projects *via* the optic nerve to the accessory optic system (AOS), a nuclear complex in the pretectum of the midbrain. Two main nuclei of the AOS, the nucleus of the optic tract (NOT) and the dorsal terminal nucleus (DTN) provide the neuronal basis for eye movement control during the OKR in the horizontal plane (Masseck & Hoffmann, 2009). Neurons in the medial terminal nucleus and lateral terminal nucleus are involved in vertical optokinetic responses. This relatively short circuitry could explain why a certain degree of image processing is already happening within the retina. Main efferent projections from the NOT-DTN complex reach preculomotor and precerebellar structures, such as the nucleus prepositus hypoglossi, the vestibular nuclei, the inferior olive and the pontine nuclei (Masseck & Hoffmann, 2009).

#### 1.4 Visual motion detection is context-dependent

Comparable to the fitness tracker and the autonomous cars mentioned initially, the vestibular and visual systems rely on different physical modalities to detect motion. The vestibular system, like a fitness tracker, detects motion by detecting inertial forces caused by any acceleration. Although the vestibular system must deal with a large range of head dynamics, the transduction process of this mechanosensitive motion sensors is relatively easy to follow and computationally simple. In contrast, the visual system, whose motion sensor is a spatially distributed array of light-sensitive photoreceptors, deals with the steady variation and complexity of visual sceneries, a complication that is also encountered by autonomous cars.

However, as many animals mainly rely on vision to interact with their environment (Gibson, 1979), the importance of an accurate visual motion detection to elicit adequate

behavioral response places high demands on the robustness of this process to changing visual scenes: Whether an animal needs to detect a prey in clear water or in a murky pond, or a pedestrian needs to avoid a car on a sunny or foggy day, their motion computation needs to be robust under different visual conditions. In particular, when animals actively locomote through space, the perception of their own motion should be precise, regardless of the steady variation of features in the environment.

But how are characteristics of a visual scene detected and interpreted in different environments to control behavior? How do biological visual motion sensors extract features of visual images to form a robust internal representation of the moving world and perform behavioral tasks accordingly?

#### 1.4.1 Characteristics of a visual scene

Different environments possess vastly different visual scene characteristics. Generally, luminance (or color) contrast are essential components to make sense of a natural visual scene, as without contrast the visual image would be a homogeneous surface devoid of any structure (see Fig. 2). Contrast can be defined as the difference in light intensity (or chromatic composition) between two different places in a visual image. Visual contrasts between objects in the environment not only shape the perception to make sense of a visual scene but are also required for motion perception and can influence how the motion of objects in the world or the world moving around oneself is perceived.

Some of the features of a visual scene were already shown to individually influence how motion is detected (Stone et al., 1990; Vaziri-Pashkam & Cavanagh, 2008). Early studies (Hawken et al., 1994; Stone et al., 1990) found for example that differences in *contrast intensities* influence how humans perceive the speed of a moving image: The “Thompson effect” stipulates that a reduction in contrast leads to a reduction in the perceived speed. A similar effect, based on contrast intensity, was observed for visual motion reflexes in insects (Dvorak et al., 1980; Nityananda et al., 2015; Straw et al., 2008) and vertebrates (Donaghy, 1980; Lisberger & Westbrook, 1985). *Contrast polarity* was also shown to influence motion detection processes: An asymmetry with respect to the perception of bright and dark objects was observed in human temporal delay thresholds (Komban et al., 2014). The role of *color contrast* in motion perception has

however been a matter of debate for over 20 years (Gegenfurtner & Hawken, 1996) and it is still unclear whether and how color information contribute to luminance cues in the process of motion perception.

Taken together, a variety of features of a visual scene can influence the detection and perception of motion. However, it still remains unclear how these different image features are interpreted by the visual system to form a coherent representation of the motion of a full-field visual scene and how this speed estimate is used to control behavioral tasks. This accurate motion estimate of a full-field visual scene is particularly important when animals need to stabilize their gaze in space to ensure visual acuity during locomotion.

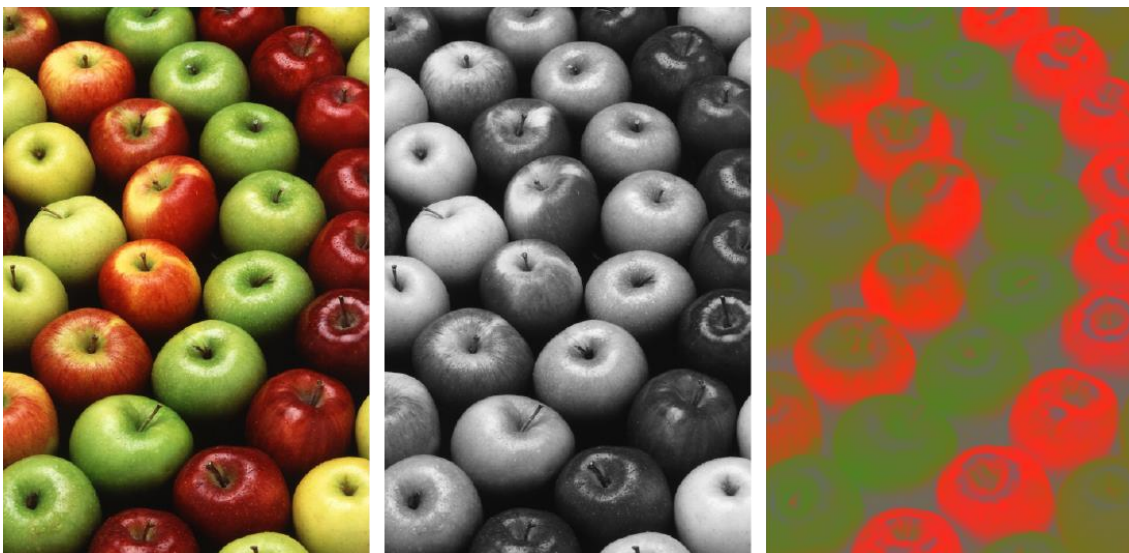


**Figure 2: Color and luminance contrast**

The original image (left panel, adapted from US Department of Agriculture, public domain) includes both color- and luminance contrasts: The apples can be easily distinguished. The black-and-white conversion of the original image (middle panel, only luminance contrast) and the equiluminant image (right panel, only color contrast), highlight different features of the original image.

### 1.4.2 Image stabilization during self-motion

Two gaze stabilizing reflexes make an important contribution to image stabilization during self-motion: While the VOR is elicited by head movements during active and passive motion of animals within their environment, the OKR is driven by large-field motion of the visual scene. As gaze-stabilizing reflexes rely on an internal estimate of how an animal is moving within its environment, both reflexes can give insights about how this motion estimate is formed based on visual and vestibular motion information. An accurate motion estimate and self-motion percept is a necessary requirement for gaze-stabilizing reflexes to keep the eyes of animals stable in space and thereby minimize retinal image slip and maximize visual acuity. But what are the prerequisites for an effective motion estimate? And how are the steadily changing features of our dynamic world influencing self-motion perception?

During behaviors in daily life, the multi-modal integration of inputs from different sensory modalities makes the discrimination of each systems' contribution difficult. However, in the laboratory, the VOR and the OKR can be studied in isolation (Beck et al., 2004; Robinson, 1968). In particular, to study how features of a visual scene influence visual motion estimates under a variety of different scene conditions, the OKR presents several advantages: This brainstem-mediated reflex can be elicited by large-field motion stimuli, does not require any training and is easy to monitor experimentally. Since this reflex is exclusively driven by a visually-generated neuronal correlate of the velocity of the moving scene (Cohen et al., 1981b; Maioli, 1988; Raphan et al., 1979), the optokinetic response relates monotonously to the internal visual motion estimate (see chapter 2, manuscript 1). Thus, for dynamically similar stimuli, a higher internal estimate of stimulus velocity translates into a stronger optokinetic response. Accordingly, the magnitude of the OKR offers a convenient behavioral substrate to reveal influences of various image characteristics on visual motion perception. In this thesis, the optokinetic reflex was therefore used as a behavioral measure to investigate how features of a moving visual scene influence speed estimation processes.

## 1.5 I can see it in your eye

All living beings, whether vertebrates or invertebrates, large or small, share the same world and are therefore confronted with similar challenges to extract meaningful information from their surroundings and perform adequate behavioral tasks. Examining the integration of visual and mechanosensory information in different animals can thereby give interesting insights into how animals combine signals from qualitatively different sensors in their central nervous systems. However, animals with simpler central nervous systems are still often underestimated in terms of significance for comparative studies (Prete, 2004), whereas especially these animals can give us crucial insights into basic and likely common information-processing mechanisms in different species. In the last years, more and more studies have been performed in animals with “simpler” brains and demonstrated that these organisms can reveal valuable information about organizational commonalities of sensory systems (Prete, 2004). This increasing evidence that visual motion perception depends on similar features across the animal kingdom (Borst & Helmstaedter, 2015) shows that simpler organisms, such as fruit flies (Borst, 2009), frogs (Lettvin et al., 1959) or zebrafishes (Gestri et al., 2012) are an auspicious avenue of research.

### 1.5.1 *Xenopus laevis* tadpoles

In this thesis, I used the amphibian *Xenopus laevis*, more specifically semi-intact preparations of *Xenopus laevis* tadpoles at mid-larval stages, to investigate motion processing mechanisms of the visual system. *Xenopus laevis* tadpoles offer many advantages, including facilitated experimental access (Straka & Simmers, 2012) to both visual and vestibular sensory systems. In the last years, this animal model was a key factor in elucidating the functional mechanisms of the vestibular sense, providing new insight into developmental and adaptive processes of this system (Straka & Simmers, 2012). Concerning the visual system of *Xenopus* tadpoles, one crucial advantage is that they possess the basic layout of vertebrates’ eyes, including rods and different types of cones with three distinct absorption spectra (Witkovsky, 2000). Further, the relative simplicity of *Xenopus* tadpoles’ visual system and the short-latency pathway through the accessory optic system, pretectal nuclei and extraocular motor nuclei (Cochran et al.,

1984), offers the unique possibility to study visual motion processes at the brainstem level. Indeed, the absence of cortical areas in these animals in contrast to mammals (Busse et al., 2011; Pinto & Enroth-Cugell, 2000), specifically allows elucidating the role of retinal and brainstem computations (see chapter 2, manuscript 1).

Another advantage of isolated *Xenopus* tadpole preparations is that they evoke robust and easily measurable sensory-driven motor behaviors, such as the vestibulo-ocular reflex and the optokinetic reflex. Both reflexes were shown to be functionally present at mid-larval stages (Branoner et al., 2016; Schuller et al., 2014) and robustly elicit characteristic eye movements. While the VOR provokes compensatory eye movements in the opposite direction of head motion, the OKR is evoked by large-field visual sceneries and elicit slow, following eye movements in the direction of the image motion, interrupted by fast, resetting eye movements when necessary. Like many other vertebrates, *Xenopus laevis* does not possess a fovea, i.e. a point of sharpest vision on the retina: This characteristic presents a great advantage to monitor pure OKR responses, in contrast to e.g. humans, where optokinetically-induced eye movements can be suppressed by smooth pursuit eye movements or visual fixation.

All these features make *Xenopus laevis* tadpoles an ideal animal model in vision and oculomotor research, to provide further insight into common image processing mechanisms across species.

### 1.5.2 Virtual reality setups

Over the last decades, a whole range of novel experimental setups have been developed to investigate multi-sensory integration mechanisms in different species. In particular, virtual reality technologies and self-motion simulators (Campos & Bühlhoff, 2012) developed rapidly, providing researchers with the opportunity to present well-controlled stimulus conditions and life-like environments to their subjects. Virtual reality setups are therefore valuable tools for investigating a wide spectrum of behaviors, as these technologies close the loop between sensory stimulation and motor actions (Thurley et al., 2017).

The experiments reported in this thesis were performed on such a virtual reality setup, consisting of a motion platform with three projectors projecting on a cylindrical large-field screen. The semi-intact *Xenopus* tadpole preparations were placed in the center of the platform and an IR-camera permitted the online tracking of VOR and OKR eye movement responses during stimulation of the motion platform and large-field visual image, respectively. The performance measure of both gaze-stabilizing reflexes was given by the ratio of eye speed to the respective stimulus speed. A crucial advantage of this setup is to simultaneously and precisely be able to control and monitor both sensory stimulation and motor output of *in-vivo* like semi-intact *Xenopus* preparations.

### Natural environments

When attempting to elucidate common sensorimotor processes between different species in virtual reality setups, a crucial question arises: Are the used virtual reality devices recreating a natural environment to the species? Computer screens used in virtual reality setups show an image composed of individual pixels, each of which is composed of the three colors, red, green and blue. These devices are based on knowledge about the trichromatic vision of humans, which possess three types of color-sensitive cones, with peak sensitivities in the red, green and blue spectrum, respectively. Computer displays are able to simulate a large variety of different colors on a screen by choosing the red-green-blue ratio that mimics the activation of human cones under natural lighting conditions. The relationship between the ratio of red, green and blue light and the perceptual experience of that light was defined by psychophysical experiments performed in human subjects (Tedore & Johnsen, 2017). Therefore, this relationship is specific to humans and is not generally applicable to other species. Indeed, different animals can possess different numbers of cones or have different peak sensitivities over the light spectrum (Osorio & Vorobyev, 2008). Therefore, when using virtual reality devices, a correct calibration of these setups to the “color intensity perception” of a particular species should be taken into account. As sometimes the exact anatomical composition or spectral sensitivity of retinal photoreceptors is not available in an animal species, the monitoring of low-level optomotor responses, such as the optokinetic reflex, provides a relatively simple tool to test how animals perceive the brightness of presented colors in virtual reality devices. By tracking the optomotor

responses in an animal model for different colored visual motion stimuli, the relative sensitivities to the red, green and blue channels of a monitor screen can be estimated.

In this thesis, I introduce this simple assay (see chapter 4, manuscript 3) that permits researchers to calibrate the colors of their virtual reality setups to the eye of their studied species. This increased control over the visual stimuli used for different species will help to elucidate more reliably common traits between species (Levy et al., 2014; Tedore & Johnsen, 2017).

## 1.6 Aim of the thesis

To obtain information from their dynamic world and guide behavior, animals possess different sensory systems and a variety of sensors that inform them about their own movements and the motion of objects in their environment. In particular, when actively locomoting through the environment, animals predominantly rely on sensory cues from their vestibular and visual systems.

In this thesis, I focused on the visual system and aimed at elucidating how characteristics of a moving large-field visual scenery influence an animal's internal representation of self- or world motion, respectively. Features of a visual scene were already shown to strongly influence how animals perceive and interpret motion in their environments (e.g. (Rinner et al., 2005)). However, it still remains unclear how the visual system extracts characteristics of a moving visual image to form a reliable estimate of large-field visual motion. This task is however crucial in daily life to control behavioral performances, such as gaze stabilization, navigation or goal-directed actions.

Since visual motion processing in vertebrates is a distributed process across multiple hierarchical levels – from the retina to various areas of the central nervous system – the question arises as to whether and how different scene qualities of a full-field visual image impact the speed estimation process in these animals and how these biases translate into behavioral output.

A suitable tool to test for the influence of visual scene characteristics on visual performance, is to monitor gaze-stabilizing responses, such as the optokinetic reflex. As

the reflex correlates with the velocity of a moving image, the OKR response relates to the internal motion estimate of an animal. Monitoring eye movement reflexes and recording neuronal signals of the optic nerve can thus give crucial insights into how a speed estimate is encoded on a retinal level and how this internal representation translates into behavior.

In the first manuscript of this thesis, I specifically investigated how the manipulation of *contrast polarity* in a visual scene influences retinal signaling and how these biases translate into the optokinetic reflex performance of *Xenopus* tadpoles.

In the second manuscript, the question of whether the retina already exploits *color contrast* of a visual scene for motion vision was researched. Based on behavioral observations of the optokinetic reflex and recordings of the optic nerve, this study investigated whether and how luminance and color information interact on a brainstem-mediated reflex.

In the field of neurosciences, virtual reality setups facilitate the investigation and comparison of sensory-motor behaviors of different animal species. However, whether these virtual reality setups actually mimic natural environments of the animal models is still a matter of debate and presents a serious limitation of these devices. In the third manuscript, I therefore propose a simple behavioral assay to test for *color sensitivity* of different animal models in virtual reality setups, that will help in calibrating the devices accordingly.

## 2 Manuscript 1

It's not all black and white: Contrast polarity influences optokinetic reflex performance in *Xenopus laevis* tadpoles

Céline M. Gravot<sup>1,2,\*</sup>, Alexander G. Knorr<sup>3,4,\*</sup>, Stefan Glasauer<sup>3</sup> and Hans Straka<sup>1</sup>

<sup>1</sup> Department Biology II, Ludwig-Maximilians-University Munich, Großhaderner Str. 2, 82152 Planegg

<sup>2</sup> Graduate School of Systemic Neurosciences, Ludwig-Maximilians-University Munich, Großhaderner Str. 2, 82152 Planegg

<sup>3</sup> Center for Sensorimotor Research, University Hospital Großhadern, Feodor-Lynen-Str. 19, 81377 Munich

<sup>4</sup> Institute for Cognitive Systems, TUM Department of Electrical and Computer Engineering, Technical University of Munich, Karlstraße 45/II, 80333 München

\* C.M.G. and A.G.K. contributed equally to this work.

**Acknowledgments:** The authors acknowledge financial support from the German Science Foundation (CRC 870; STR 478/3-1, GL 342/2-1 and RTG 2175), the German Federal Ministry of Education and Research under the Grant code 01 EO 0901 and the Bernstein Center for Computational Neuroscience Munich (BT-1). The authors also thank the mechanical workshop of the Biocenter Martinsried for their help in assembling the experimental setup.

**Abstract**

The maintenance of visual acuity during active and passive locomotion is ensured by gaze stabilizing reflexes that aim at minimizing retinal image slip. For the optokinetic reflex (OKR), large-field visual motion patterns form the essential stimuli that activate eye movements that follow the motion of the visual surround. Since properties of the visual world are known to influence cognitive motion perception, estimation of visual image velocity and thus the performance of brainstem mediated visuo-motor behaviors might also depend on various characteristics of the image scene. Employing semi-intact preparations of mid-larval stages of *Xenopus laevis* tadpoles, we studied the influence of contrast polarity, intensity, contour shape and motion stimulus patterns on the performance of the OKR and multi-unit optic nerve discharge during motion of a large-field visual scene. At high contrast intensities, the OKR amplitude was significantly larger for visual scenes with a positive contrast compared to those with a negative contrast. This effect persisted for luminance-matched pairs of stimuli, and was independent of contour shape. The relative biases of OKR performance as well as the independence of the responses from contour shape was closely mirrored by the discharge of the optic nerve in response to the respective stimuli. However, the multi-unit activity of the latter in response to a single moving vertical edge with a height of 2.5 mm was strongly influenced by the light intensity in the vertical neighborhood. This suggests that the underlying mechanism of OKR biases related to contrast polarity directly derives from visual motion processing properties of retinal circuits.

## Introduction

Most vertebrates live and locomote within highly dynamic and structured environments of animate and inanimate objects. To ensure adequate visual acuity during locomotion and passive perturbations of the head/body, retinal images are stabilized by two brainstem-mediated ocular motor reflexes: the vestibulo-ocular reflex (VOR), which operates best at high frequencies and accelerations and elicits compensatory eye movements following stimulation of the vestibular sensory system (Straka and Dieringer, 2004) and the optokinetic reflex (OKR), which is activated by large-field visual image motion and triggers eye movements that aim at stabilizing the residual retinal image drift (Collewijn, 1969; Dieringer and Precht, 1982). During prolonged artificial visual stimulation in one direction, an optokinetic nystagmus emerges, in which tracking movements are interrupted by rapid eye movements in the opposite direction (Collewijn, 1969). These fast phases reset the eyes to a central position from which the tracking movements are repetitively activated.

The OKR in all vertebrates is subject to two requirements: providing a rapid processing of image motion while maintaining a faithful representation of the actual image velocity over a broad range of viewing conditions that can range from e.g. bright sunlight to dusk/dawn or from clear to murky water in aquatic environments. These different conditions have vastly different visual scene characteristics such as contrast intensity and polarity as well as total luminance. Some of these characteristics are already known to influence visual motion driven reflexes and perception capabilities in vertebrates (Donaghy, 1980; Lisberger and Westbrook, 1985) as well as insects (Dvorak et al., 1980; Straw et al., 2008; Nityananda et al., 2015). At variance, the influence of contrast polarity, i.e. the sign of brightness differences between objects and background, or contrast intensity on the performance of the optokinetic reflex is only poorly understood so far.

Moreover, it is unknown if an influence of the various visual scene properties on OKR performance is due to a differential processing within the underlying brainstem network or if it derives already from an immanent feature of the retinal motion detection system. As support for the latter, manipulation of visual scene characteristics

can lead to a differential excitation of retinal photoreceptors, which in turn might elicit different activation patterns in motion-sensitive ganglion cells (Enroth-Cugell and Robson, 1966) and thus generate a different velocity estimate. Furthermore, the center-surround organizational structure of retinal edge detectors allows the assumption that the properties of a uniform background in the particles' neighborhood influences the extraction of motion information from the small moving edges. In fact, within visual image textures, only the edges of moving particles generate a motion percept, while the large uniform areas of the large-field image (which is construed as background) make no immediate contribution to visual motion perception (Adelson and Bergen, 1985). These possible scene-related differences in retinal speed estimations might then translate into differences in signal processing within brainstem circuits and thus into behavioral responses, such as the OKR.

Here, we studied the influence of contrast polarity on OKR performance in tadpoles of the African clawed toad *Xenopus laevis*. These vertebrates allow studying respective visuo-motor transformations in semi-intact preparations that offer a facilitated accessibility to all synaptic levels of the underlying brainstem neuronal network (Straka and Simmers, 2012; von Uckermann et al., 2016). Presentation of visual scenes, randomly scattered with particles defined by filled closed contours (e.g. solid dots, squares or crescent shapes), elicited optokinetically driven eye movements of different amplitudes that depended on contrast polarity and intensity as well as luminance levels. Recordings of multi-unit spike discharge from the optic nerve of isolated eyes revealed similar dependencies from the various stimulus parameters, suggesting that major differences in OKR performance derive from the signal processing with retinal circuits.

## Methods

### *Animal Experiments*

*Animals.* Experiments were performed *in vitro* on isolated, semi-intact preparations of *Xenopus laevis* tadpoles ( $n = 42$ ) and comply with the National Institute of Health publication entitled "Principles of animal care", No. 86-23, revised 1985. Permission for these experiments was granted by the governmental institution at the Regierung von Oberbayern/Government of Upper Bavaria (55.2-1-54-2532.3-59-12). Animals at developmental stages 52-55 (Nieuwkoop and Faber, 1994) were obtained from the in-house animal breeding facility at the Biocenter-Martinsried of the Ludwig-Maximilians-University Munich. For all experiments, tadpoles were anesthetized in 0.05% MS-222 (Pharmaq Ltd., UK) in frog Ringer (75 mM NaCl, 25 mM NaHCO<sub>3</sub>, 2 mM CaCl<sub>2</sub>, 2 mM KCl, 0.5 mM MgCl<sub>2</sub>, and 11 mM glucose, pH 7.4) and decapitated at the level of the upper spinal cord.

*Experimental approach.* For behavioral experiments, the skin covering the dorsal head was removed, the soft skull tissue opened and the forebrain disconnected (Lambert et al., 2012). This surgical procedure anatomically preserved the remaining CNS and the eyes including the optic nerve, extraocular motor innervation and eye muscles. Such preparations allowed prolonged behavioral and neuronal recordings and *in vivo*-like activation of the OKR by horizontal large-field image motion under controlled *in vitro* conditions. For electrophysiological recordings of retinal ganglion cell axons in these preparations, the optic nerve of the right eye was cleaned from surrounding connective tissue and transected at the level of the optic chiasm. All extraocular muscles of this eye were transected at their proximal insertion to immobilize the eye in its natural position within the head. Semi-intact preparations were allowed to recover from the surgical intervention at 14°C for 3 hours (Ramlochansingh et al., 2014).

*Setup.* Semi-intact preparations were fixed with insect pins to the Sylgard floor of a Petri dish (5 cm diameter). The chamber, which was constantly perfused with oxygenated frog Ringer solution at a rate of 3.0 - 5.0 ml/min, was mechanically secured in the center of an open cylindrical screen with a height of 5 cm and a diameter of 8 cm, encompassing 275° of the visual field (Fig. 1A). Three digital light processing (DLP) video projectors

(Aiptek V60), installed in 90° angles to each other projected visual motion stimuli onto the screen (Packer et al., 2001) at a refresh rate of 60 Hz. For behavioral recordings, a CCD camera (Grasshopper 0.3 MP Mono FireWire 1394b, PointGrey), mounted 20 cm above the center of the recording chamber, permitted on-line tracking of horizontal eye movements by custom-written software (Beck et al., 2004). The chamber was illuminated from above using an 840 nm infrared light source. An infrared long-pass filter in the camera ensured selective transmission of infrared light and a high contrast of the eyes for motion tracking and online analysis of induced eye movements.

Electrophysiological recordings of multi-unit optic nerve spike activity were performed in the same setup. The spike discharge was recorded extracellularly (EXT 10-2F, npf electrodes, Tamm, Germany) with glass microelectrodes. Electrodes were produced with a horizontal puller (P-87 Brown/Flaming, Sutter Instruments Company, USA) and the tips were broken and individually adjusted to fit the respective optic nerve diameter. The multi-unit spike discharge was digitized at a sampling rate of 28.6 kHz (CED Micro1401-3, Cambridge Electronic Design Ltd., UK) along with the visual motion stimulus and the horizontal position of both eyes, respectively. Data were recorded by a data acquisition program (Spike2 version 7.04, Cambridge Electronic Design Ltd., United Kingdom).

*Data Acquisition.* To assess the performance of the horizontal OKR during sinusoidal large-field visual motion stimulation, the position of both eyes was preprocessed by a Gaussian low-pass filter at a frequency of 5 Hz, and segmented into individual cycles of the stimulus, excluding all cycles with a peak eye velocity  $>50^\circ/\text{s}$ . Thereby, cycles with oculomotor behaviors other than optokinetic slow phase responses, such as high-frequency horizontal oscillations during spontaneous episodes of locomotor activity (Lambert et al., 2012) were discarded. Also, four out of 42 preparations with very small optokinetic response amplitudes ( $<0.5^\circ/\text{s}$ ) during the initial screening, likely due to prior surgical complications, were excluded. The remaining 38 tadpoles were used for subsequent experiments. For horizontal optokinetic motion stimulation at constant speed, the velocity of the slow-phase following eye movement was computed in a window of  $\pm 5^\circ$  around the resting position of the eye by evaluating the slope of a least-squares fit of a straight line to the eye position trace. Additionally, the number of fast-

phases over the duration of the applied stimulus (i.e. 120 s) was counted.

The rate of spontaneous and motion-evoked multi-unit spike discharge was extracted from optic nerve recordings using a threshold method. The resulting spike train was then convolved with a raised cosine window (FWHM = 0.5 s) to compute the firing rate. The modulation depth during sinusoidal visual motion stimulation was then computed by averaging the firing rate (FR) over all cycles of a single trial, approximating the resulting average curve by a function

$$FR = a + b * \left| \sin\left(\frac{t}{T}\right) \right|,$$

in which  $b$  is the modulation depth,  $a$  is the baseline firing rate and  $T$  is the period. For constant velocity visual motion stimuli, the modulation depth was computed as the difference between the maximum and the baseline firing rate.

*Stimulus paradigm.* Horizontal eye movements were elicited by large-field visual motion stimuli using one of two stimulus velocity profiles: Sinusoidal visual motion stimuli with a peak velocity of  $10^\circ/\text{s}$  and a frequency of 0.125 Hz triggered sinusoidally modulated slow conjugate following movements of both eyes (Fig. 1B). Constant velocity visual motion stimuli (120 s in each direction, respectively) with a velocity of  $\pm 10^\circ/\text{s}$  provoked a nystagmic OKR with slow following eye movements (\* in Fig. 1C) and intermittent resetting fast-phases in the opposite direction (> in Fig. 1C).

Large-field horizontal visual motion stimuli consisted of gray scale random-dot ( $\phi$  2.5 mm, visual angle  $1.8^\circ$ ) patterns with different tones of grey for the dots and background and light intensities between 251 and 6428  $\text{cd}/\text{m}^2$  (Photo Research, SpectraScan PR655). Sample sizes were based on a-priori power analysis performed in G\*Power 3.1.9.2 (Faul et al., 2007, 2009) using effect sizes from pilot experiments. *Contrast polarity* was defined as the sign of the difference between dots and background (i.e. *positive* contrast for bright dots on a dark background and *negative* contrast for dark dots on a bright background; see left and right visual scene in Fig. 1A).

*Influence of visual scene properties on OKR performance.* To test how scene properties such as contrast intensity and total luminance influence the OKR in scenes with positive and negative contrast, semi-intact preparations of *Xenopus* tadpoles were presented

with sinusoidal large-field motion stimuli, in which contrast intensity and total luminance were systematically manipulated (Fig. 1D).

*Effect of contrast intensity.* The effect of contrast intensity was tested in preparations ( $n = 8$ ) using sinusoidally moving random-dot scenes. Eight different visual scenes (contrast intensities between -100% for black dots on a white background and +100% for white dots on a dark background, four negative, four positive; see left panel in Fig. 1D) were presented in sparsely populated random-dot images (fill rate 13%).

*Effect of total luminance.* To explicitly test the effect of total luminance on OKR performance under both contrast polarity conditions, preparations ( $n = 10$ ) were presented with five different textures (fill rate 35%) with positive contrast and the same contrast magnitude but different total luminance levels (middle panel in Fig. 1D). In addition, five visual motion stimuli of different total luminance were presented with the same contrast magnitude but negative contrast. This resulted in a total of 10 stimuli. These stimuli were chosen such that eight stimuli formed four pairs (\* in panel scheme in Fig. 1D): For each pair, the stimulus had a different contrast polarity but the same total luminance. The remaining two stimuli (# in middle panel in Fig. 1D) had no match with opposite contrast polarity stimuli due to technical limitations of the display device.

*Effect of contrast polarity.* The third set of stimuli investigated the effect of contrast polarity on OKR amplitude. Preparations ( $n = 12$ ) were presented with two random-dot scenes, in which the total luminance was identical between both contrast polarities by filling 50% of the screen area with dots, while leaving the other 50% as background (right panel in Fig. 1D). Thereby, inverting contrast polarity did not change the ratio of bright vs dark patches on the screen and thus preserved the total luminance.

*Influence of contour shapes on OKR performance.* To test if biases related to contrast polarity in the previous experimental conditions can be explained, at least partly, by the different structural organization of contours in positive as compared to negative contrast stimuli (concave vs convex edges), two additional stimulus protocols were presented to semi-intact *Xenopus* preparations ( $n = 8$ ). These stimuli were identical to the 50% fill rate stimuli in the previous condition, except that in the first of the two sets of experiments all dots were replaced by squares of the same area (left panel in Fig. 1E).

This allowed identifying whether an influence of contrast polarity on the OKR is related to the shape of contours or rather to a foreground/background distinction.

To test whether the direction of the curvature of the contours (concave vs convex) influences OKR performance, the dots in the two maximal-contrast conditions ( $\pm 100\%$ ; see left panel in Fig. 1D) were replaced by crescent shaped contours with the same area and radius of the curvature (right panel in Fig. 1E). This resulted in four different visual stimuli, presented to the semi-intact preparations ( $n = 6$ ): Positive and negative contrast with the opening either in or against movement direction (to the left or to the right; see right panel in Fig. 1E). Due to the asymmetry of the contours, the stimuli were presented at constant velocity of  $10^\circ/\text{s}$  in counter-clockwise direction.

*Influence of contrast polarity-related biases of multi-unit optic nerve spike discharge.* To elucidate whether contrast polarity related biases of the OKR is a property of retinal motion detection or an emerging feature during further signal processing in central visual relay centers, a subset of the previously described stimuli was presented to isolated *Xenopus* eyes while recording multi-unit spike activity from the severed optic nerve.

*Optic nerve discharge in response to single moving edges.* To evaluate the spike discharge pattern in the optic nerve, induced by a moving edge, a single vertical edge (height = 2.5 mm,  $1.8^\circ$  visual angle) was moved through the isolated eye's field of view at a constant stimulus velocity of  $10^\circ/\text{s}$  in temporo-nasal direction (Fig. 1F). The edge had one of three shapes (concave, CV; convex, CX; straight, ST), was shown either in front of a dark (+) or bright (-) background, and was either a local change of light intensity from dark to bright (ON) or from bright to dark (OFF; see Fig. 1F).

*Data analysis and statistics.* The critical level of significance for all statistical comparisons was chosen as  $\alpha < 0.05$  unless otherwise stated. The influence of contrast intensity and contrast polarity was tested by a 2-way repeated measures ANOVA, with factors *contrast intensity* and *contrast polarity*. The correlation between total texture luminance and normalized OKR amplitude was analyzed by performing a linear regression analysis, using the model:

$$A = \beta_1 + \beta_2 * L$$

individually for both contrast polarities with  $A$  as the relative OKR amplitude and  $L$  as the relative normalized total luminance;  $\beta_2$  is the slope of the regression curve and indicates the sensitivity of the OKR amplitude to total luminance changes, and  $\beta_1$  is the offset of the regression line.

Corresponding 40 data points of the four pairs of overlapping luminance conditions (\* in middle panel of Fig. 1D) were used to allow for unbiased comparison of positive and negative contrast stimuli. The slope of the regression was then compared between the responses to positive and negative contrast stimuli, using a bootstrap approach: In 100,000 permutations, 10 values were randomly drawn from the OKR amplitudes obtained from the four pairs of overlapping luminance conditions each, resulting in 40 data points in total. The model was then fitted as described above to each randomly drawn dataset to generate a distribution for the  $\beta_2$  parameter, centered on its mean  $\mu_2$ . Significance was then assessed by counting the relative amount of fits to random permutations, which had  $|\beta_{2,\text{perm}} - \mu_2| > |\beta_{2,\text{data}} - \mu_2|$  and comparing to the critical value of significance. OKR amplitude differences between the two contrast polarities in the 50% fill rate textures were tested using a paired  $t$ -test.

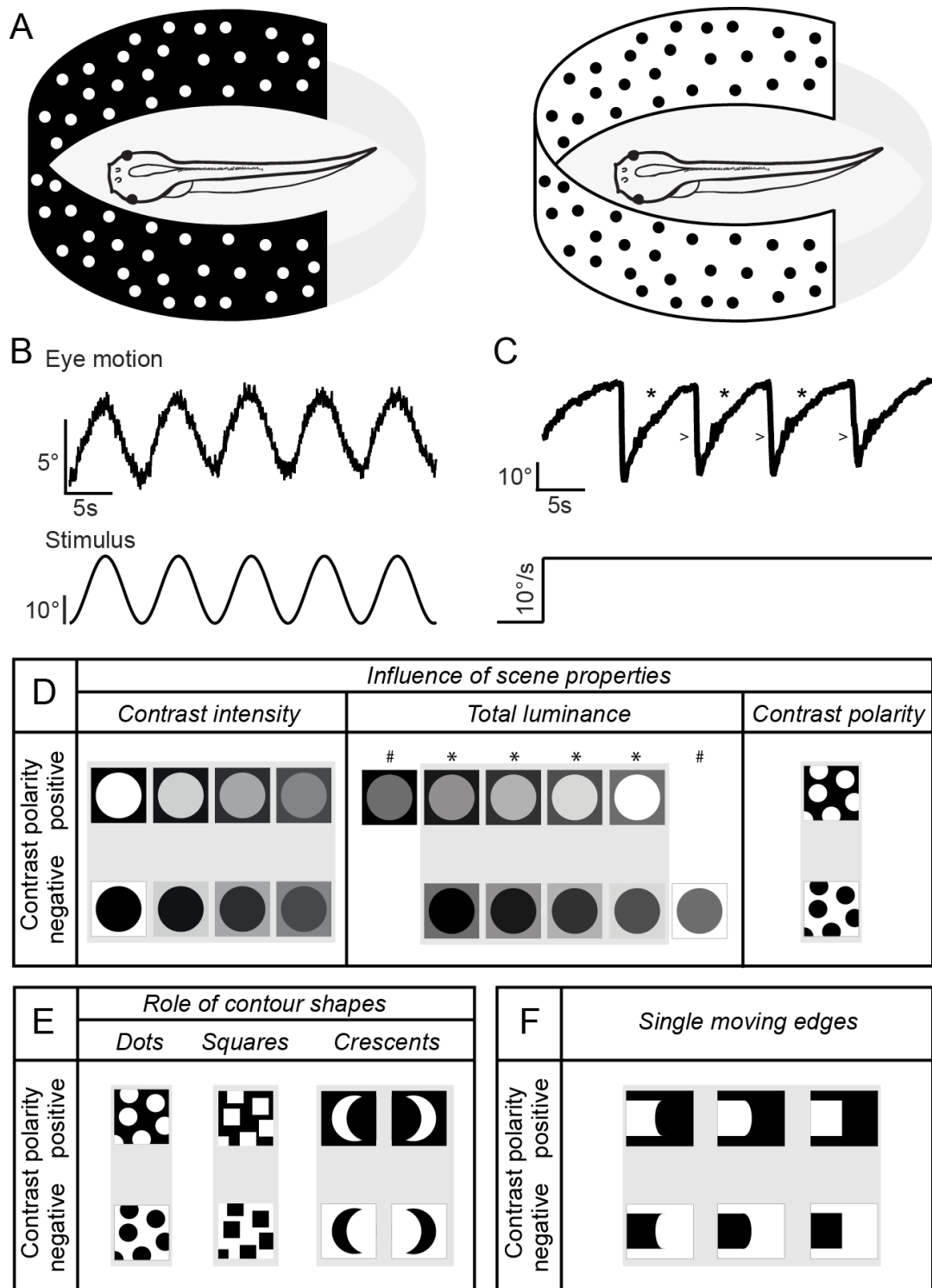


**Figure 1: Stimulation and recording paradigms of the horizontal OKR in *Xenopus* tadpoles.**

(A) Schematics, illustrating the experimental setting with a central recording chamber for semi-intact larval *Xenopus* preparations (adapted from Hänzi and Straka, 2016), surrounded by a cylindrical screen onto which a rotating large-field random-dot pattern with positive (white dots on black background, left) or negative (black dots on white background, right) contrast polarity

is projected. (B,C) Representative examples of movements of the left eye (upper traces) evoked by sinusoidal (frequency: 0.125 Hz, peak velocity:  $\pm 10^\circ/\text{s}$ ; B) or temporo-nasal constant velocity ( $10^\circ/\text{s}$ ; C) visual motion stimuli (lower traces); the evoked nystagmic eye movement in C consists of slow following-phases (\*) interrupted by resetting fast-phases (>). (D-F) Graphical illustration of variations in visual scene properties such as contrast intensity, total luminance, contrast polarity (left, middle and right panel in D, respectively), contour shapes (E) and shape of single moving edges (F). In the middle panel of D, \* indicates pairs of stimuli with different contrast polarity but same total luminance; # indicates those stimuli that had no match with stimuli of opposite contrast polarity.

## Results

### *Activation of horizontal optokinetic responses in Xenopus tadpoles*

Large-field sinusoidal image motion provokes phase-coupled following movements of both eyes in semi-intact *in vitro* preparations of *Xenopus laevis* tadpoles (Schuller et al., 2014). This reflexive eye motion is termed optokinetic reflex and represents the sensory feedback component of gaze stabilization during head/body motion (Collewijn, 1969; Straka and Dieringer, 2004). Pilot experiments in semi-intact *Xenopus* preparations using a sinusoidally oscillating large-field random-dot pattern in the framework of the current study evoked respective responses. Accordingly, stimulus frequencies of 0.1 - 0.2 Hz and peak velocities of  $\pm 10^\circ/\text{s}$  elicited robust eye movements at mid-larval stages of this amphibian species (e.g. red trace in Fig. 2A). The pilot experiments also revealed that the magnitudes of the evoked optokinetic responses were not only correlated with the frequency and amplitude of the motion stimulus, but also depended on contrast polarity, i.e. bright dots on dark background or *vice versa* (compare red and blue traces in Fig. 2A, B). This result suggests that the contrast of a moving visual scene plays an important role for the reflex performance. Thus, the first set of experiments systematically explored the influence of contrast polarity on the amplitude of the OKR.

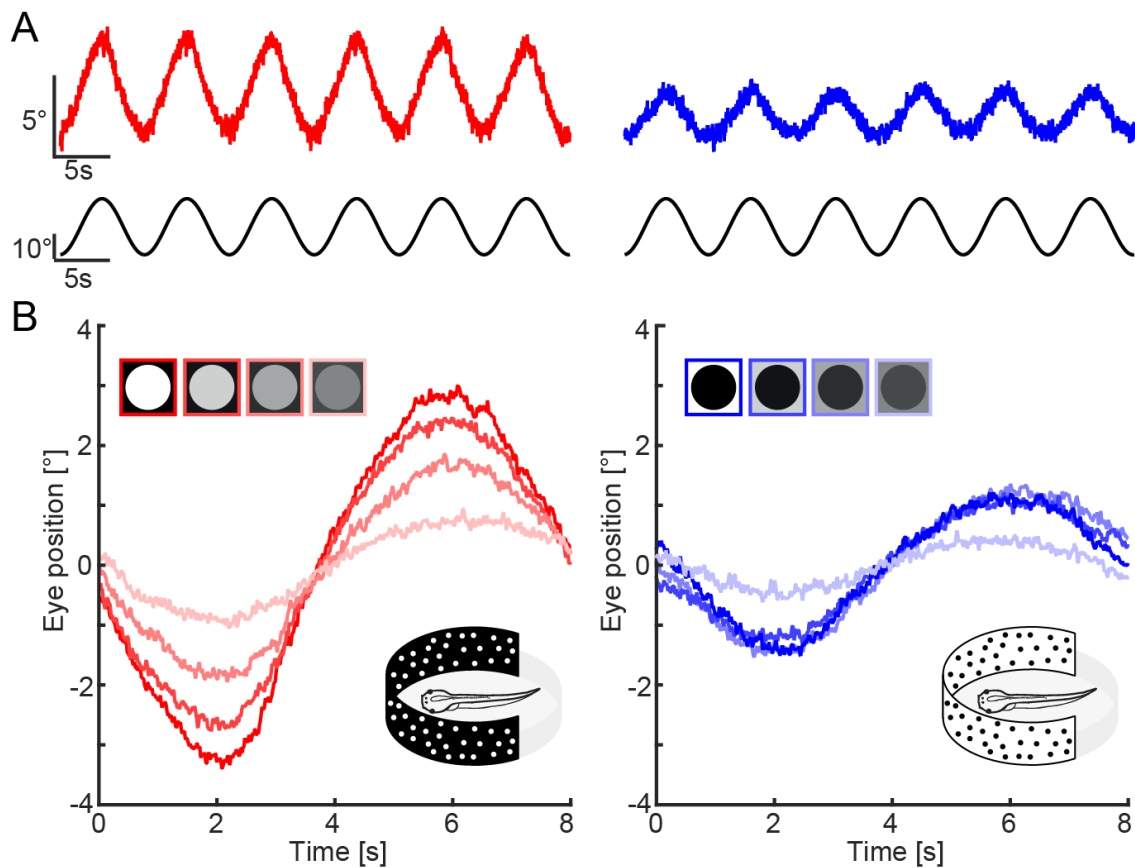


**Figure 2: Dependency of horizontal OKR amplitude on contrast polarity and intensity.**

(A) Representative examples of horizontal positional oscillations of the left eye (upper red and blue traces) extracted from video sequences during sinusoidal large-field image motion (frequency: 0.125 Hz, peak velocity:  $\pm 10^\circ/\text{s}$ ; lower traces) of a random-dot pattern with positive (left) and negative contrast (right); calibration bars on the left also apply to the traces on the right, respectively. (B) Averaged responses over a single cycle (from 20 cycles each) during visual motion stimulation with four textures of decreasing contrast intensity (color-coded in red and blue, respectively) for positive (left) and negative (right) contrast polarity; icons in the upper left corner depict the different contrast intensities, respectively.

### *Influence of visual stimulus parameters on OKR performance*

The effect of contrast polarity on the OKR of *Xenopus* tadpoles was investigated by presenting four different contrast magnitudes of dots vs background ( $n = 8$  preparations). The random-dot stimuli had either a positive (dots were brighter than the background; see left scheme in Fig. 1A) or a negative contrast (dots were darker than the background; see right scheme in Fig. 1A). The systematic variation of this parameter

revealed a gradual diminution of the OKR response amplitude with decreasing stimulus contrast, for both contrast polarities ( $F(3,52) = 24.17$ ,  $p < 0.001$ ,  $\eta = 0.30$ ; see red and blue colored traces in Fig. 2B, respectively; Fig. 3A). This decrease in OKR performance with decreasing contrast magnitude was very similar between different preparations as indicated by the relatively small variability across different experiments (Fig. 3A). In addition, a pronounced asymmetry was observed when varying contrast polarity (Fig. 3A). Response amplitudes were significantly larger for random-dot patterns with a positive than with a negative contrast ( $F(1,52) = 57.62$ ,  $p < 0.001$ ,  $\eta = 0.24$ ). In fact, at the same contrast intensity, the average OKR response to stimuli with a positive contrast out-sized the responses that were evoked by stimuli with a negative contrast by a factor of  $2.24 \pm 1.01$  ( $n = 8$ ). This indicates that OKR performance depends on both contrast magnitude as well as contrast polarity.

The effect of contrast polarity on OKR performance under different total luminance conditions was tested in another group of semi-intact *Xenopus* tadpole preparations ( $n = 10$  preparations) by presenting motion stimuli with different textures (fill rate 35%). These stimuli had the same magnitude of contrast, respectively, but different total luminance levels and either positive or negative contrast polarity, resulting in a total of 10 different stimuli (see middle panel in Fig. 1D). To compare the effect of stimuli with opposite contrast polarity, the luminance for dots and background was chosen such that the total luminance was matched in 4 pairs of stimuli with positive and negative contrast (marked by \* in Fig. 3B). Even though the obtained results were somewhat variable between different preparations (see individual lines in Fig. 3B), OKR amplitude nonetheless exhibited a clear and highly significant negative correlation with the total luminance of the visual scene ( $\rho(99) = -0.691$ ,  $p < 0.001$ ,  $df = 99$ ). The two individual regression fits resulted in slopes of  $\beta_2 = -2.65$  for bright dots on a dark background and of  $\beta_2 = -1.44$  for dark dots on a bright background. The two slope values were significantly different (positive contrast:  $p = 0.021$ ; negative contrast:  $p = 0.022$ ) compared to the mean slope of the bootstrap permutations. Accordingly, at lower overall brightness, the effect of contrast polarity is more pronounced, but vanishes for stimuli with higher total luminance (Fig. 3B). This indicates that contrast polarity differentially influences the OKR of *Xenopus* tadpoles depending on the total luminance of the optokinetic stimulus pattern.

Thirdly, a potential impact of variations in contrast intensity and total image luminance was tested by presenting a moving scene in which 50% of the screen area was filled with dots, while the other half was a uniform background ( $n = 12$ ; right panel in Fig. 1D). Thereby, the presented stimuli with inverse contrast polarity differed only by either having a positive or a negative contrast, but neither in total luminance nor in contrast magnitude. This experimental approach confirmed the asymmetry of OKR response amplitudes for motion stimuli with different contrast polarities (Fig. 3C). Accordingly, the OKR amplitude was significantly larger ( $t(11) = 2.97, p = 0.0126, d = 0.64$ ; Fig. 3C) with bright dots on dark background than with dark dots on bright background. Again, responses evoked by stimuli with positive contrast out-sized those that were elicited with negative contrast stimuli by a factor of  $1.49 \pm 0.49$  ( $n = 12$ ). The smaller relative difference between the responses to the presented textures compared to the previous result (Fig. 3B), however, suggests that the effect of contrast polarity inversion is complemented by concurrent changes in image brightness. This difference can be attributed to two structural variations in the image pattern that were caused by changing contrast polarity: Either the signal processing within the OKR circuitry is able to dissociate between foreground (dots) and background (one large connected area between the dots) and adjust its response based on this distinction, or it responds differently as a result of changing the curvature of contours from convex to concave and *vice versa*.

A potential impact of contour shape (convex vs concave curvature) on OKR performance was tested by presenting a set of stimuli in which 50% of the area was filled with squares with either positive or negative contrast polarity (left panel in Fig. 1E, Fig. 3D). Compatible with the dependency of the OKR magnitude on contrast polarity, the optokinetic response amplitude was significantly higher for stimuli with a positive, compared to a negative contrast by a factor of  $1.29 \pm 0.24$  ( $t(6) = 3.48, p = 0.013, d = 2.63$ ). This therefore suggests that contour curvature is not the main cause for the observed differences related to contrast polarity.

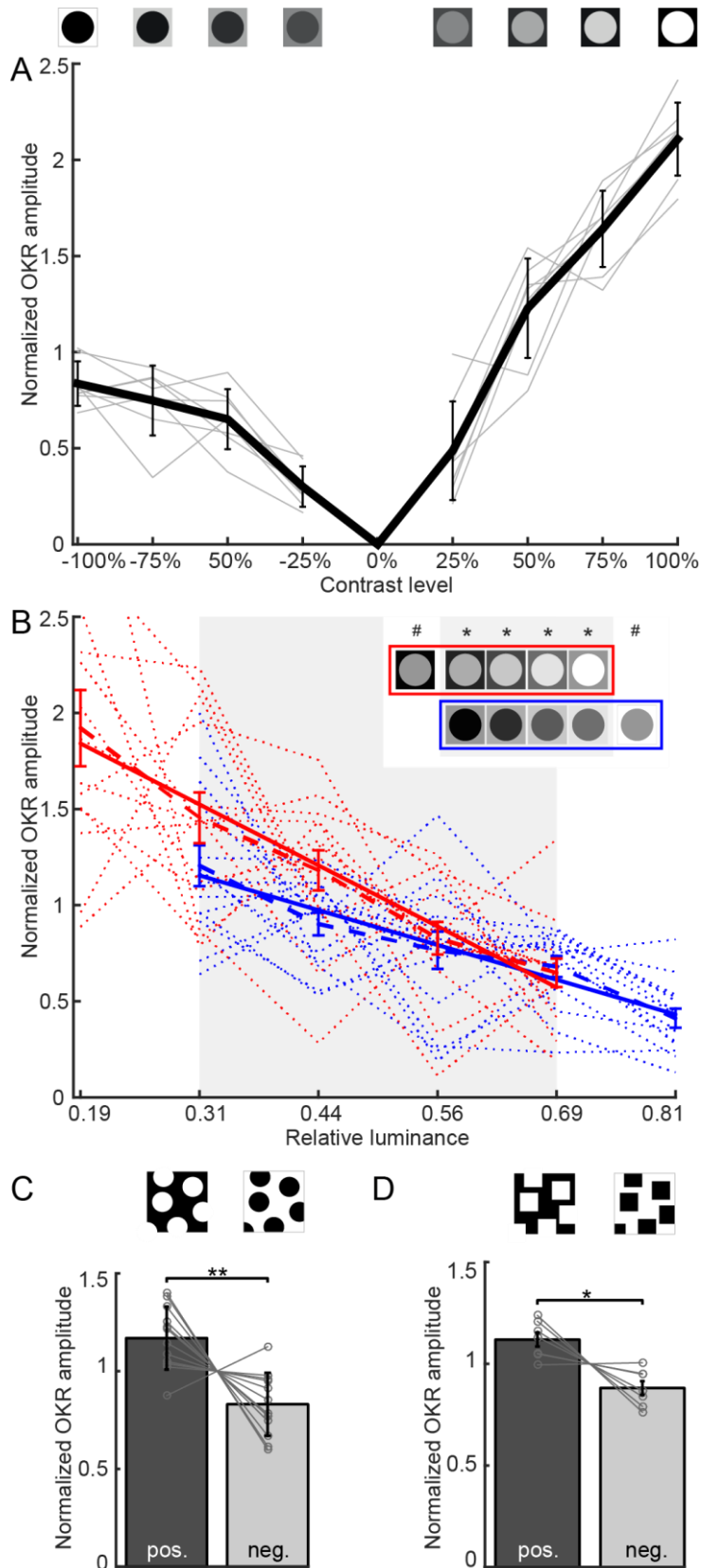


**Figure 3: Influence of large-field visual image properties on OKR performance.** (A) Dependency of OKR amplitudes on the contrast intensity of the random-dot pattern with positive (+) and negative contrast (-); note the asymmetry of responses to different contrast polarity; light grey

lines represent data from individual experiments; the black line indicates the mean ( $\pm$ SD). (B) Dependency of the normalized OKR amplitude on relative luminance; dotted lines represent data from individual preparations, dashed lines indicate the mean ( $\pm$ SD) and solid lines the linear regression for positive (red; slope = -2.65,  $r^2 = 0.49$ ) and negative contrast polarities (blue; slope = -1.44,  $r^2 = 0.45$ ). \*,  $p < 0.05$ . (C,D) Bar plots, depicting normalized OKR amplitudes under equi-luminant conditions of the motion stimuli with circular (C) and square contours (D) and positive (dark grey) and negative contrast polarity (light grey), respectively. Icons above the plots in A-D depict the image properties of the different visual stimuli, respectively. Amplitudes in A-D were normalized to the mean amplitude for each preparation in the corresponding experimental conditions.

This conclusion was supported by another set of experiments that directly tested the impact of contour curvature on OKR performance. In these experiments, the presented images consisted of randomly scattered crescent shaped contours (13% fill rate) with the opening either in or against the motion direction (Figs. 1F, 4). These direction-specific stimulus shapes with a positive or a negative contrast (left and right schemes in Fig. 4A) were presented at a constant velocity in one direction. In contrast to responses evoked by sinusoidal motion stimuli (e.g. Fig. 2A), constant velocity visual motion elicited nystagmic eye movements that consisted of slow following movements in stimulus motion direction interrupted by resetting fast-phase in the opposite direction (Fig. 4B). This allowed quantifying two parameters of the OKR: slow-phase velocity, which was calculated as the average slope of the slow following movement (Fig. 4B) and the number of resetting fast-phases.

Systematic variations of contrast polarity revealed consistent differences with respect to both parameters. Positive contrast stimuli (white crescent shapes on black background; red traces in Fig. 4C) evoked an OKR with a significantly higher slow-phase velocity and more fast-phases independent of the orientation of the crescent shaped pattern relative to the stimulus direction (compare red and blue traces in Fig. 4C). This is illustrated by the highly significant main effect of contrast polarity on the velocity of the slow following movements (compare red and blue bars in Fig. 4D<sub>1</sub>; repeated measures ANOVA;  $F(1, 19) = 138.4$ ,  $\eta^2 = 0.71$ ) and the number of fast-phases (compare red and blue bars in Fig. 4D<sub>2</sub>; repeated measures ANOVA;  $F(1, 19) = 26.01$ ,  $\eta^2 = 0.44$ ).

At variance with this result, the curvature of the crescent shaped pattern with respect to the motion direction elicited an OKR with similar slow-phase velocities and number of fast-phases independent of the contrast polarity as indicated by the representative example in Fig. 4C (compare CV with CX traces, respectively). Accordingly, no significant main effect of the crescent curvature nor a significant interaction between curvature and contrast polarity was encountered for the slow-phase eye velocity (main effect:  $F(1, 19) = 0.49$ ,  $p = n.s.$ , interaction:  $F(1, 18) = 0.19$ ,  $p = n.s.$ ) and number of fast-phases (main effect:  $F(1, 19) = 0.71$ ,  $p = n.s.$ , interaction:  $F(1, 18) = 0.09$ ,  $p = n.s.$ ; Fig. 4D<sub>1</sub>, D<sub>2</sub>). The tight link between slow-phase optokinetic eye velocity and number of induced fast-phases is further indicated by the close correlation between both parameters (Fig. 4D<sub>3</sub>;  $\rho = 0.82$ ,  $n = 28$ ,  $p < 0.001$ ). This is likely due to the fact that the neuronal correlate responsible for generating higher eye velocities during an OKR also causes fast-phase generating neuronal substrates to reach the activation threshold in a shorter time and thereby triggers fast-phases more often. In contrast, the higher slow-phase velocity during visual motion stimulation with a positive contrast might derive from a differential activation of motion detection circuits already within the retina.

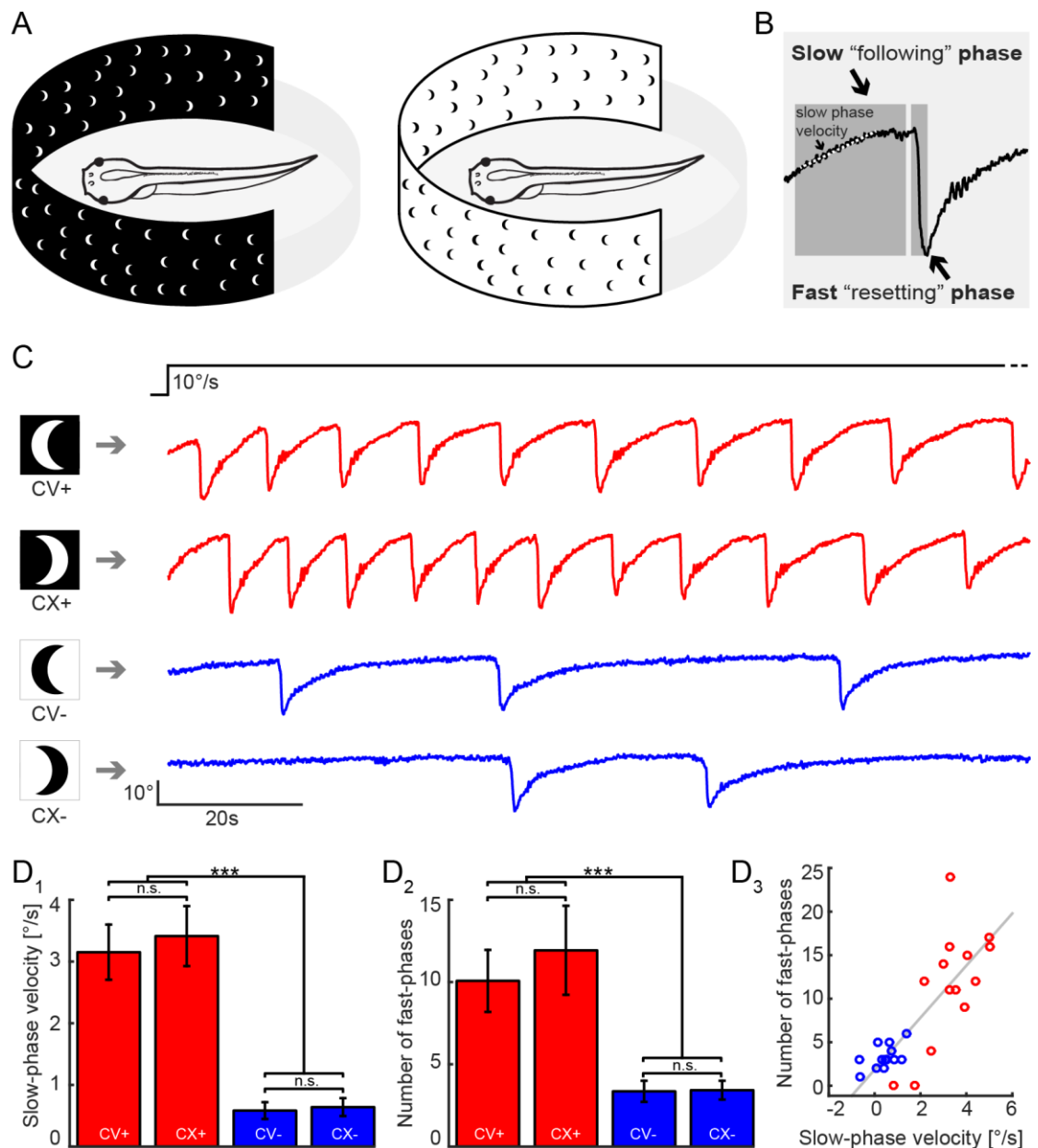


**Figure 4: Influence of contour shape on OKR performance.** (A) Schematics, illustrating the cylindrical large-field visual projection of crescent-shaped contours with positive (left) and negative (right) contrast polarity rotating at a constant velocity of  $10^\circ/\text{s}$ . (B) Typical nystagmic eye movement during unidirectional constant velocity image motion, consisting of slow following-phases (dotted line) interrupted by resetting fast-phases. (C) Representative examples of nystagmic movements of the left eye during constant velocity image motion of crescent-shaped contours in temporo-nasal direction with positive (+, red traces) and negative contrast polarity (-, blue traces) and different orientations of the curvature (concave, CV vs. convex, CX). (D) Bar plots comparing average slow-phase velocity ( $D_1$ ) and number of fast phases ( $D_2$ ) of eye movements evoked by constant velocity large-field image motion of crescent-shaped contours with positive (CV+, CX+, red) and negative contrast (CV-, CX-, blue); dependency of the number

of fast phases on slow phase eye velocity ( $D_3$ ) for constant velocity crescent-shaped contour images with positive (red;  $n = 14$ ) and negative contrast (blue;  $n = 14$ ); \*\*\*,  $p < 0.001$  in  $D_1$  and  $D_2$  (Wilcoxon signed-rank test;  $n = 14$ , respectively); *n.s.*, not significant.

### *Optic nerve activation during large-field visual motion stimulation*

The implementation of a contrast polarity-biased motion detection system already at the retinal level was tested by extracellular recordings of retinal ganglion cell activity as multi-unit spike discharge from the severed optic nerve in isolated *Xenopus* eye preparations (Fig. 5A). During sinusoidal horizontal large-field image motion, the multi-unit optic nerve discharge was cyclically modulated for both contrast polarities, i.e. white dots on background or black dots on white background (Fig. 5B). However, motion stimuli with a positive contrast consistently yielded a more pronounced and robust discharge modulation (compare red and blue traces in Fig. 5B). Since the multi-unit recordings likely included units with a motion-sensitivity for either of the two stimulus directions, the population activity in the optic nerve could not be specified for naso-temporal or temporo-nasal motion. Accordingly, the multi-unit optic nerve firing rate was quantified by the bidirectional maximal discharge for further analysis. Despite the likely presence of different motion-sensitive retinal ganglion cells in the recordings with sensitivities to one or the other stimulus direction, the multi-unit discharge of the optic nerve proved to be a reliable estimate for the efficacy of large-field motion stimulus velocity. Thus, based on these results, a differential processing in the retina is the likely origin of the contrast sign-dependent differential OKR performance described above (Fig. 3A).

The influence of contrast polarity and total luminance of the visual scene on retinal ganglion cell activity during large-field image motion was further tested with the same protocol that was used above for determining OKR performance (see left and middle panel in Fig. 1D). Accordingly, the effect of contrast polarity on modulated optic nerve activity was evaluated by presenting four different contrast magnitudes of dots vs background ( $n = 6$  preparations, red and blue dotted lines in Fig. 5C). The differential influence of contrast polarity on the discharge modulation magnitude was more pronounced at low total luminance levels, and gradually decreased with higher light

intensities (solid red and blue lines in Fig. 5C), similar to the impact of this parameter on the dependency of the OKR (dashed red and blue lines in Fig. 5C). In addition, the changes in modulation depth during both 50% fill rate stimulus conditions indicated that the modulation depth was significantly larger in response to positive than to negative contrast stimuli (dots:  $t(6) = 3.10$ ,  $p = 0.021$ ,  $d = 2.35$ ; squares:  $t(6) = 2.95$ ,  $p = 0.26$ ,  $d = 2.23$ ), compatible with the representative example shown in Fig. 5B. Moreover, the effect of contrast polarity was very similar for dots and squares, respectively, suggesting that contour shape plays at most a minor role for retinal motion detection (left and right bar plot in Fig. 5D). These results indicate that the multi-unit optic nerve discharge during large-field image motion has a similar dependency from basic contrast and luminance parameters as the horizontal OKR behavior and thus suggests that the differential signal processing of contrast and luminance within the retina is at the origin of this effect.

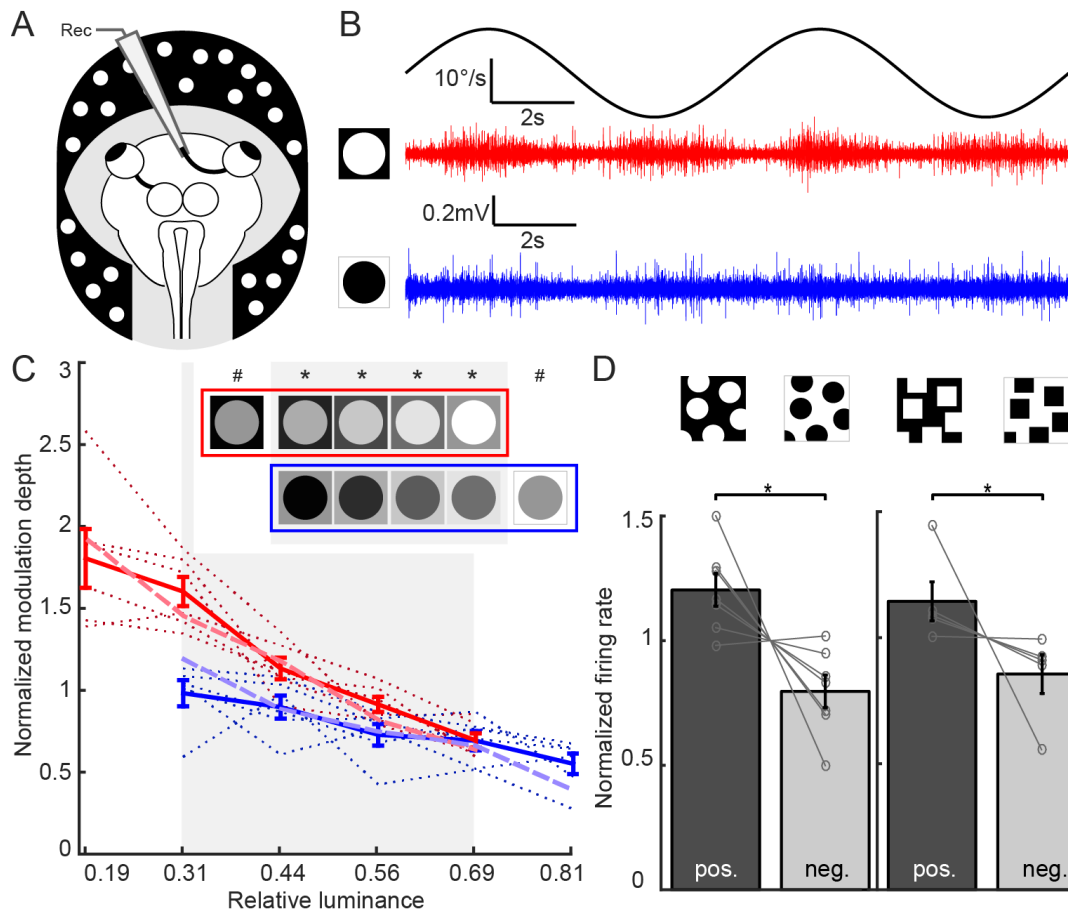


**Figure 5: Influence of large-field visual image properties on multi-unit optic nerve spike discharge.** (A) Schematic, illustrating the experimental setting for extracellular recordings of the severed right optic nerve with suction electrodes. (B) Representative example of modulated multi-unit optic nerve spike discharge during sinusoidal rotation (frequency: 0.125 Hz; peak velocity:  $\pm 10^\circ/\text{s}$ ) of a large-field image of circular contours with positive (red) and negative (blue) contrast. (C) Dependency of the normalized discharge modulation depth on relative luminance; dotted lines represent data from individual preparations for positive and negative contrast polarities and solid lines the mean ( $\pm$ SD), respectively; dashed red and blue lines indicate corresponding relative changes in OKR amplitude over the same range of relative luminance shown in Fig. 3B. (D) Bar plots, depicting the normalized firing rate of multi-unit optic nerve discharge under equi-luminant conditions of the motion stimuli with circular (left) and square contours (right) and positive (dark grey) and negative (light grey) contrast polarity, respectively. Icons above the plots in C,D depict the image properties of the different visual stimuli, respectively. Normalization in C,D was performed with respect to the mean firing rate for each preparation in the corresponding experimental conditions.

### *Optic nerve responses to individual moving edges*

All motion stimuli, employed so far consisted of different moving shapes (dots, squares, crescents) that were randomly scattered across the visual scene. The magnitude of the optic nerve discharge however might depend on the entirety of the large-field image properties (i.e. explicit distinction between fore- and background) or on the characteristics of individual moving edges that move through the visual field in any of the used stimulus patterns. In fact, every moving shape consisted of two relevant moving vertical edges: the leading edge, facing the motion direction and the trailing edge, facing the rear end. Depending on contrast polarity of the respective stimulus pattern, the two edges have different characteristics. For positive contrast stimuli, the leading edge presents a light intensity increment (ON edge), while the trailing edge presents a light decrement (OFF edge), and *vice versa* for negative contrast stimuli.

In order to elucidate the impact of moving edges, several sets of experiments were conducted that investigated the influence of single edges moving through the visual field under different conditions on the magnitude of the multi-unit optic nerve discharge (Fig. 6A). In a first set of experiments, a single moving edge with a height of 2.5 |mm (vertical visual angle 1.8°) was presented in front of a dark (+) or bright background (-) and with three different shapes (concave, CV; convex, CX; straight, ST), respectively. Multi-unit neuronal optic nerve activity evoked by the motion of the edge was independent of edge shape (repeated measures ANOVA,  $F(2, 89) = 0.05$ ,  $p = n.s.$ ), but showed a highly significant difference related to the background ( $F(1, 89) = 56.19$ ,  $p < 0.001$ ,  $\eta^2 = 0.36$ ; Fig. 6B). This indicated that for a given contrast polarity, the curvature of an edge was not a discriminating factor for motion detection.

Since edge shape was not a confounding factor, we next assessed a potential impact of edge type (ON edge or OFF edge) and contrast polarity (dark or bright background) on the multi-unit optic nerve discharge by using moving straight vertical edges (Fig. 6C). In agreement with the general definition, ON edges are characterized by a change in intensity of the horizontal moving bar from black to white, while OFF edges mark a change of the bar from white to black. Accordingly, stimuli were constructed such that stimuli of the same edge type (ON+/ON- or OFF+/OFF-) were identical in the horizontal

neighborhood of the moving edge (i.e. dark in front of the edge, bright behind the edge of ON edges, and *vice versa* for OFF edges; see Fig. 6C). Accordingly, these stimuli only differed in the vertical neighborhood under the two contrast polarity conditions (dark background for positive contrast and bright background for negative contrast), respectively. Recordings of multi-unit optic nerve activity during image motion revealed considerable differences in the firing rate magnitude during the four different stimulus conditions (spike discharge in Fig. 6C). In fact, OFF edges evoked on average significantly greater (compare white and grey bars in Fig. 6D, respectively) motion-related optic nerve discharge magnitudes (repeated measures ANOVA,  $F(1, 89) = 51.2$ ,  $p < 0.001$ ,  $\eta^2 = 0.19$ ). However, this difference was much less pronounced for negative compared to positive contrast edges (compare bottom with top traces in Fig. 6C and right and left bars in Fig. 6D). In fact, responses to light decrements (OFF edges) were on average 126% stronger than to light increments, suggesting that motion detection in the retina of larval *Xenopus* is predominantly performed by the OFF pathway. Moreover, the contrast polarity related bias observed in the previous experiments was also reproduced at the level of single moving edges. This was demonstrated by a significant main effect of contrast polarity ( $F(1, 89) = 94.84$ ,  $p < 0.001$ ,  $\eta^2 = 0.36$ ) as well as a significant interaction between edge type and contrast polarity ( $F(1, 89) = 10.2$ ,  $p = 0.002$ ,  $\eta^2 = 0.04$ ), suggesting that the stimulus velocity-related retinal ganglion cell discharge is influenced by the light intensity in the vertical neighborhood of the horizontally moving edge.

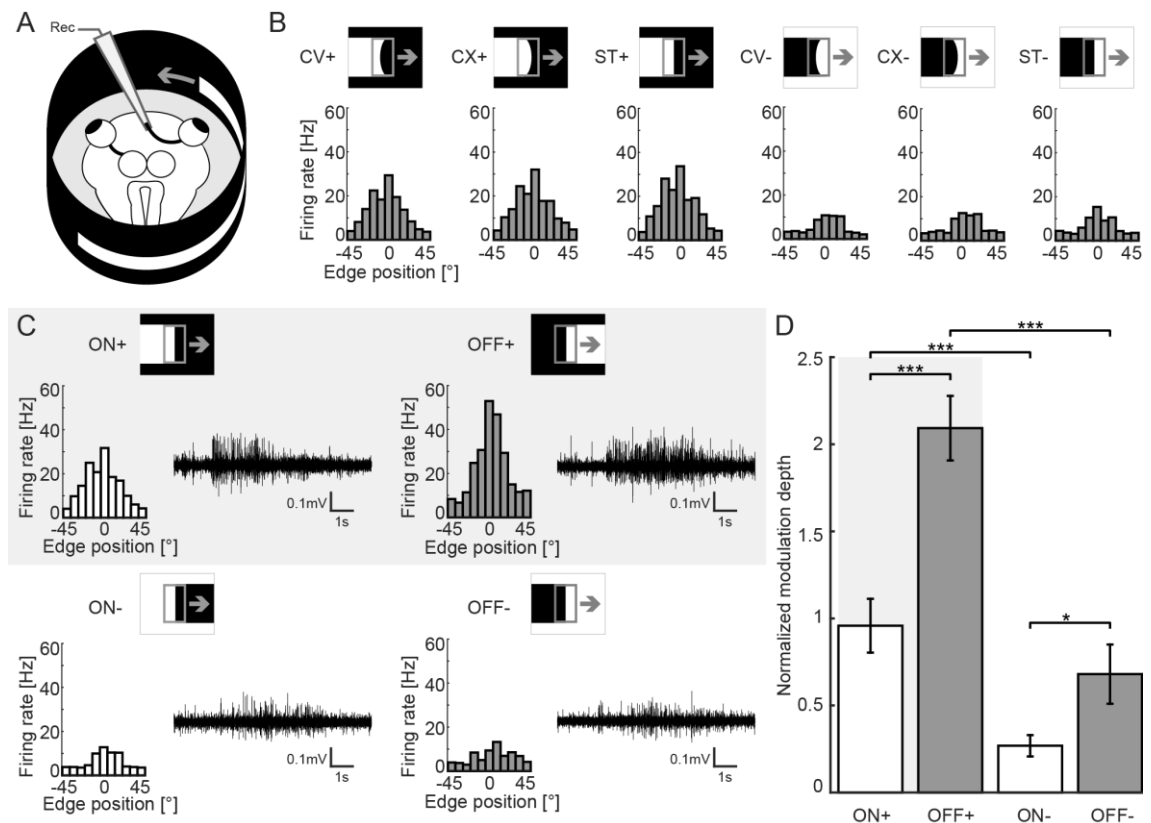


**Figure 6: Multi-unit optic nerve discharge pattern in response to moving single edges.** (A) Schematic, illustrating the experimental setting for extracellular recordings of the severed right optic nerve with suction electrodes; motion of a long horizontal bar ( $180^\circ$ ) with either positive or negative contrast polarity at constant velocity in temporo-nasal direction at  $10^\circ/\text{s}$  caused stimulation of the eye with a single moving vertical edge. (B) Comparison of multi-unit optic nerve discharge rates over a range of  $90^\circ$  centered on the right eye during motion of a horizontal bar with different edge shapes (concave, CV; convex, CX; straight, ST) and positive (+) or negative (-) contrast polarity; grey arrows indicate the motion direction. (C) Multi-unit optic nerve discharge (traces in black) and firing rates over a range of  $90^\circ$  centered on the right eye (open and solid bar plots) during motion of a horizontal bar with a straight moving vertical ON or OFF edge in front of a dark (+) or bright (-) background (icons above spike discharge traces); note that both ON edges (ON+, ON-) and both OFF edges (OFF+, OFF-) were identical in their respective horizontal neighborhoods and only differed in the vertical surroundings. (D) Bar plots depicting the average normalized modulation depth, (normalized to the mean modulation depth per preparation in all corresponding conditions) of multi-unit optic nerve discharge in response to moving bars with ON and OFF edges in front of a dark (ON+, OFF+) or bright background (ON-, OFF-). \*,  $p < 0.05$ ; \*\*,  $p < 0.01$ ; \*\*\*,  $p < 0.001$  (Wilcoxon signed-rank test;  $n = 14$ , respectively).

## Discussion

At low light intensities, OKR performance in *Xenopus* tadpoles is superior for positive (white dots on black background) compared to negative contrast large-field visual stimuli (black dots on white background). This effect is independent of contrast intensity, contour shape and motion stimulus pattern. Recordings of multi-unit optic nerve discharge during visual motion stimulation yielded similar results, thus indicating that the neuronal basis for this effect might originate from signal processing properties of the retinal circuitry.

### *OKR performance in semi-intact preparations*

Effective gaze stabilization of the residual retinal image slip during passive or self-motion in all vertebrates requires an estimate of the velocity of the large-field visual world motion (Collewijn, 1969). This image velocity directly determines the performance of the OKR with the purpose of minimizing the retinal slip, thereby ensuring high visual acuity (Cohen et al., 1977). In amphibians, the horizontal OKR is mediated by a short-latency, three-neuronal reflex arc that involves retinal ganglion cells, a set of accessory optic neurons in the pretectum and extraocular motoneurons that activate synergistic muscles of the two eyes (Cochran et al., 1984). The employment of semi-intact preparations of *Xenopus laevis* tadpoles offers a convenient approach to evoke and quantify this sensory-driven motor behavior (Straka and Simmers, 2012). Based on the presence of intact sensory (eyes), motor structures (eye muscles) and central circuits as well as the experimental accessibility, this preparation facilitates studying the dynamic range of visual motion processing at the brainstem level as well as the dependency of the behavioral performance on visual scene features.

The generally robust performance of the OKR in semi-intact *Xenopus* tadpole preparations in the current study is similar to previous results obtained in these animals (Schuller et al., 2014) and also complies with expectations from studies of adult frog optokinetic responses under *in vivo* conditions (Dieringer and Precht, 1982). Thus, the present *in vitro* approach represents a convenient method with high validity and accountability to decipher the influence of general visual scene properties on the performance of this visuo-motor behavior. Moreover, the anatomically very similar

basic layout of vertebrate eyes and subcortical visual circuits (Maximino, 2008; Masseck and Hoffmann, 2009) make the visual system of *Xenopus laevis* ideally suited to provide insight into basic mechanisms of image motion processing across vertebrate species.

*OKR performance is influenced by contrast polarity*

Experimental manipulations of visual scene parameters in the current behavioral experiments indicated that the OKR amplitudes varied strongly as a result of inverting contrast polarity of the visual scene. This dependency is remarkable, given that the stimulus texture with respect to number and intensity of contours is identical. Moreover, the influence of contrast polarity is clearly at variance with prior expectations based on e.g. spatiotemporal motion energy (Adelson and Bergen, 1985; Reichhart, 1987). According to the latter parameter, motion perception including visual stimulus velocity estimation should be unaffected by pure inversion of contrast polarity. However, this is not the case, even though this effect is limited to lower light levels. A uniform increase of the total luminance of the visual scene by a constant value caused a decrease in both the amplitude of the optokinetic response as well as in the influence of contrast polarity on OKR performance (Fig. 3B, red and blue lines). Interestingly, the slopes, intercept, and point at which the contrast polarity effect vanished (intersection of the two lines) were identical for the visuo-motor behavior and the spike discharge of the optic nerve. The general corresponding effects of these alterations in visual scene parameters on both OKR and optic nerve discharge suggests that the origin of the dependency of OKR performance on large-field visual scene properties is due to an influence of the latter directly on retinal signal processing (see below). Accordingly, pretectal and extraocular motor signal processing has a rather limited impact compared to the influence of retinal processing for the calculation of the motion velocity estimate.

The asymmetry in OKR performance that is related to contrast polarity and likely caused by retinal velocity computations is not only expressed in the magnitude of the slow-phase eye velocity during constant velocity stimulation but also by the number of evoked fast-phases during constant velocity stimulation (Fig. 4C, D<sub>2</sub>). In general, fast-phase generation is directly related to an internal estimate of the visual surround velocity (Anastasio, 1996), and thus influenced by those parameters that affect the

estimation of the image slip velocity at retinal/central nervous system levels. The strong correlation between fast-phase number and slow-phase eye movements supports this assumption. Accordingly, the motor commands for slow-phase following eye movements as well as the neural signals for fast-phases derive directly or indirectly from the same velocity estimate.

#### *Functional relevance of OKR asymmetry*

From a functional point of view, the OKR asymmetry appears counterintuitive at first. However, most animals, including *Xenopus* tadpoles, have to cope with a large range of visual scenarios. This requires a robust estimate of the motion velocity of the residual visual slip to generate appropriate eye movements for a constant maintenance of high visual acuity. Thus, in complex environments enriched by stationary and moving objects, distinctions based on contrast polarity would facilitate the adjustment of visuo-motor responses to relevant portions of the possibly incoherent large-field visual motion. The preference in response to small bright objects in front of a dark background as shown in the present study in *Xenopus* tadpoles might be considered as a low-level functional interpretation of image motion. This would thereby assist distinguishing self-motion from motion of external objects in the visual field. The more effective activation of an OKR by positive contrast stimuli is consistent with findings in zebrafish where large dark spots on a bright background were highly efficient in evoking a behavioral response in a virtual hunting assay (Bianco and Engert, 2015). This suggests that closed contours with negative contrast are likely interpreted as prey (Bianco and Engert, 2015) and not as background, compatible with the activation of specific visual pathways in predatory zebrafish (Semmelhack et al., 2014). Similar prey/non-prey distinctions were also found in adult frog (Lettvin, 1959; Barlow and Hill, 1963). However, even though adult *Xenopus* are predators, the required circuitry for prey detection in visual pathways might not yet be in place in the herbivorous larval stages and potentially implemented only after metamorphosis.

#### *Optic nerve population activity encodes stimulus velocity*

The population activity of the optic nerve is modulated with the velocity of a moving large-field visual scene, however differentially in strength depending on contrast

polarity. This suggests that the information about this parameter is already encoded as population rate code at the level of the retinal ganglion cell axons in the optic nerve. The striking similarity between visual scene-related biases of oculomotor behavior and optic nerve discharge observed in this study (Figs. 3, 5) suggests that the latter population activity is interpreted as a velocity signal by the OKR circuitry and directly forms the basis for the performance of this visuo-motor behavior. However, the rate code of the entire retinal ganglion cell population does not provide information about the direction of motion. The information for both motion directions, i.e. temporo-nasal and naso-temporal is likely processed in separate channels, which begin with motion-sensitive retinal ganglion cells and project to different premotor nuclei in the pretectum (Fite et al., 2008).

*Retinal motion velocity signals in retinal circuits are influenced by contrast polarity*

Directionally sensitive signals in neurons of the peripheral visual circuitry have been reported in numerous vertebrate (Barlow and Hill, 1963; Oyster et al., 1993; Pinsky et al., 2015) and invertebrate (Haag et al., 2016) species and appear to be a common feature in the processing of visual motion. The neuronal substrate is known to be organized in different information streams, which operate as edge detectors and respond either to light increments (ON), light decrements (OFF) or both (ON/OFF; Borst and Euler, 2011). These cells in the vertebrate retina extract motion information but also perform an advanced processing of the incident image (Lettvin et al., 1959; Clifford and Ibbotson, 2002; Gollisch and Meister, 2010). In particular, neuronal computation in retinal ganglion cells allows toads to perceptually discriminate between prey- and non-prey objects simply based on the sign of contrast (Ewert and Siefert, 1974). This notion is supported by a pattern analysis based on image contrast in tectal and thalamic areas (Ewert and von Wietersheim, 1974). The organization of the visual scene, however, strongly influences the extraction of motion information. Even when presented with an identical velocity profile, retinal ganglion cell population activity modulates differently depending on whether the image was presented with positive or negative contrast. One possible mechanism would be different temporal characteristics in the interaction between ON and OFF edge detectors. Another cause of the contrast polarity-related asymmetry could be the change in curvature of ON and OFF edges. For positive contrast,

a moving closed contour consists of a convex leading ON and a concave trailing OFF edge and *vice versa* for stimuli with negative contrast.

Differential modulation of responses to ON or OFF edges depending on contour curvature was however not observed in the present study, excluding the latter possibility as relevant mechanism for the observed contrast polarity effects. Instead, our study suggests another mechanism as the cause for a differential activation of retinal ganglion cells that depends on the light intensity in the vertical neighborhood of horizontally moving edges (Fig. 6). Optic nerve population responses to a single moving vertical edge showed different activation patterns depending on whether the moving edge was presented on a bright or a dark background. This could be due to the size of receptive field properties of retinal ganglion cells extending across the dimensions of the edge into the background area. High uniform light intensities illuminating the receptive field appear to suppress/inhibit responses of these neurons to moving contours compatible with the weaker optic nerve discharge modulation during motion of random particle scenes with bright backgrounds. This is also consistent with our observation that the overall modulation depth as well as the difference related to inversion of contrast polarity decreases with higher overall luminance (Fig. 5C, red and blue line). Accordingly, at high light intensities, the background brightness appears to be intense enough to attenuate retinal ganglion cell discharge even for objects with a positive contrast (i.e. brighter than the background). In zebrafish, the OKR is activated by the retinal ON but not the OFF pathway (Emran et al., 2007). Whether this is also the case for *Xenopus laevis* is unknown so far. However, since the relative decrease of retinal ganglion cell discharge modulation by a bright background was similar for responses to ON and to OFF edges (Fig. 6D), a direct correlate of retinal biases can be observed in the OKR, independent of which channel(s) drive the OKR.

## Conclusion

Visuo-motor behavior and motion stimulus-related retinal output signal amplitudes are highly influenced by contrast polarity in otherwise identical visual scenes. This is due to retinal signal processing of moving edges that depends on the local context of the stimulus environment. For horizontal moving vertical edges, the light intensity in the

area beyond the edges has a large impact on the computations underlying retinal motion processing. This directly translates into OKR performance, which scales in magnitude with population discharge activity of retinal ganglion cells.

## References

- Adelson, E. H., & Bergen, J. R. (1985). Spatiotemporal energy models for the perception of motion. *Journal of the Optical Society of America A, Optics and Image Science*, 2(2), 284–299. <https://doi.org/10.1364/JOSAA.2.000284>
- Anastasio, T. J., & Anastasio, T. J. (1996). A random walk model of fast-phase timing during optokinetic nystagmus. *Biol. Cybern*, 75(19), 1–9. <https://doi.org/10.1007/BF00238734>
- Barlow, H. B., & Hill, R. M. (1963). Selective sensitivity to direction of movement in ganglion cells of the rabbit retina. *Science (New York, N.Y.)*, 139(3553), 412–414. <https://doi.org/10.1126/science.139.3553.412>
- Barlow, H. B. (1953). Summation and inhibition in the frog's retina. *Journal of Physiology*, 119(1), 69–88. <https://doi.org/10.1113/jphysiol.1953.sp004829>
- Beck, J. C., Gilland, E., Baker, R., & Tank, D. W. (2004). Instrumentation for Measuring Oculomotor Performance and Plasticity in Larval Organisms. *Methods in Cell Biology*, 76, 385–413. [https://doi.org/10.1016/S0091-679X\(04\)76017-3](https://doi.org/10.1016/S0091-679X(04)76017-3)
- Bianco, I. H., & Engert, F. (2015). Visuomotor Transformations Underlying Hunting Behavior in Zebrafish. *Current Biology*, 25(7), 831–846. <https://doi.org/10.1016/j.cub.2015.01.042>
- Borst, A., & Euler, T. (2011). Seeing Things in Motion: Models, Circuits, and Mechanisms. *Neuron*, 71(6), 974–994. <https://doi.org/10.1016/j.neuron.2011.08.031>
- Clifford, C. W. G., & Ibbotson, M. R. (2002). Fundamental mechanisms of visual motion detection: Models, cells and functions. *Progress in Neurobiology*, 68(6), 409–437. [https://doi.org/10.1016/S0301-0082\(02\)00154-5](https://doi.org/10.1016/S0301-0082(02)00154-5)
- Cochran, S. L., Dieringer, N., & Precht, W. (1984). Basic optokinetic-ocular reflex pathways in the frog. *The Journal of Neuroscience: The Official Journal of the*

- Society for Neuroscience*, 4(1), 43–57. Retrieved from <http://www.ncbi.nlm.nih.gov/pubmed/6198496>
- Cohen, B., Matsuo, V., & Raphan, T. (1977). Quantitative analysis of the velocity characteristics of optokinetic nystagmus and optokinetic after-nystagmus. *The Journal of Physiology*, 270(2), 321–44. <https://doi.org/10.1113/jphysiol.1977.sp011955>
- Collewijn, H. (1969). Optokinetic eye movements in the rabbit: Input-output relations. *Vision Research*, 9(1), 117–132. [https://doi.org/10.1016/0042-6989\(69\)90035-2](https://doi.org/10.1016/0042-6989(69)90035-2)
- Dieringer, N., & Precht, W. (1982). Compensatory head and eye movements in the frog and their contribution to stabilization of gaze. *Experimental Brain Research*, 47(3), 394–406. <https://doi.org/10.1007/BF00239357>
- Donaghy, M. (1980). The contrast sensitivity, spatial resolution and velocity tuning of the cat's optokinetic reflex. *The Journal of Physiology*, 300(1), 353–65. <https://doi.org/10.1113/jphysiol.1980.sp013166>
- Dvorak, D., Srinivasan, M. V., & French, A. S. (1980). The contrast sensitivity of fly movement-detecting neurons. *Vision Research*, 20(5), 397–407. [https://doi.org/10.1016/0042-6989\(80\)90030-9](https://doi.org/10.1016/0042-6989(80)90030-9)
- Emran, F., Rihel, J., Adolph, A. R., Wong, K. Y., Kraves, S., & Dowling, J. E. (2007). OFF ganglion cells cannot drive the optokinetic reflex in zebrafish. *Proceedings of the National Academy of Sciences of the United States of America*, 104(48), 19126–31. <https://doi.org/10.1073/pnas.0709337104>
- Enroth-Cugell, C., & Robson, J. G. (1966). The contrast sensitivity of retinal ganglion cells of the cat. *Journal of Physiology*, 187(3), 517–552. <https://doi.org/10.1113/jphysiol.1966.sp008107>
- Ewert, J. P., & Siefert, G. (1974). Neuronal correlates of seasonal changes in contrast-detection of prey catching behaviour in toads (*bufo bufo* L.). *Vision Research*, 14(6), 431–432. [https://doi.org/10.1016/0042-6989\(74\)90241-7](https://doi.org/10.1016/0042-6989(74)90241-7)

- Ewert, J.-P., & von Wietersheim, A. (1974). Musterauswertung durch Tectum- und Thalamus/Praetectum-Neurone im visuellen System der Kröte *Bufo bufo* (L.). *Journal of Comparative Physiology*, *92*(2), 131–148.  
<https://doi.org/10.1007/BF00694502>
- Faul, F., Erdfelder, E., Lang, A., & Buchner, A. (2007). G \* Power 3: A flexible statistical power analysis program for the social, behavioral, and biomedical sciences. *Behavior Research Methods*, *39*(2), 175–191.  
<https://doi.org/10.3758/BF03193146>
- Faul, F., Erdfelder, E., Buchner, A., & Lang, A.-G. (2009). Statistical power analyses using G\*Power 3.1: tests for correlation and regression analyses. *Behavior Research Methods*, *41*(4), 1149–60. <https://doi.org/10.3758/BRM.41.4.1149>
- Fite, K. V, Kwei-Levy, C., & Bengston, L. (1989). Neurophysiological investigation of the pretectal nucleus lentiformis mesencephali in *Rana pipiens*. *Brain, Behavior and Evolution*, *34*(3), 164–170. <https://doi.org/10.1159/000116502>
- Gollisch, T., & Meister, M. (2010). Eye Smarter than Scientists Believed: Neural Computations in Circuits of the Retina. *Neuron*, *65*(2), 150–164.  
<https://doi.org/10.1016/j.neuron.2009.12.009>
- Haag, J., Arenz, A., Serbe, E., Gabbiani, F., & Borst, A. (2016). Complementary mechanisms create direction selectivity in the fly. *eLife*, *5*(AUGUST), 175–181.  
<https://doi.org/10.7554/eLife.17421.001>
- Hänzi, S., & Straka, H. (2016). Schemes of *Xenopus laevis* tadpoles. *Figshare*. Retrieved from  
[https://figshare.com/articles/Schemes\\_of\\_Xenopus\\_laevis\\_tadpoles/3841173](https://figshare.com/articles/Schemes_of_Xenopus_laevis_tadpoles/3841173)
- Lambert, F. M., Combes, D., Simmers, J., & Straka, H. (2012). Gaze stabilization by efference copy signaling without sensory feedback during vertebrate locomotion. *Current Biology*, *22*(18), 1649–1658. <https://doi.org/10.1016/j.cub.2012.07.019>

- Lettvin, J. Y., Maturana, H. R., Maturana, H. R., McCulloch, W. S., & Pitts, W. H. (1959). What the Frog's Eye Tells the Frog's Brain. *Proceedings of the IRE*, 47(11), 1940–1951. <https://doi.org/10.1109/JRPROC.1959.287207>
- Lisberger, S. G., & Westbrook, L. E. (1985). Properties of visual inputs that initiate horizontal smooth pursuit eye movements in monkeys. *The Journal of Neuroscience: The Official Journal of the Society for Neuroscience*, 5(6), 1662–1673. Retrieved from <http://www.jneurosci.org/content/5/6/1662>
- Masseck, O. A., & Hoffmann, K. P. (2009). Comparative neurobiology of the optokinetic reflex. *Annals of the New York Academy of Sciences*, 1164(1), 430–439. <https://doi.org/10.1111/j.1749-6632.2009.03854.x>
- Maximino, C. (2008). Evolutionary changes in the complexity of the tectum of nontetrapods: A cladistic approach. *PLoS ONE*, 3(10), e3582. <https://doi.org/10.1371/journal.pone.0003582>
- Nieuwkoop PD, Faber J. (1994). *Normal table of Xenopus laevis (Daudin): A systematical and chronological survey of the development from the fertilized egg till the end of metamorphosis*. New York: Garland.
- Nityananda, V., Tarawneh, G., Jones, L., Busby, N., Herbert, W., Davies, R., & Read, J. C. A. (2015). The contrast sensitivity function of the praying mantis *Sphodromantis lineola*. *Journal of Comparative Physiology A: Neuroethology, Sensory, Neural, and Behavioral Physiology*, 201(8), 741–750. <https://doi.org/10.1007/s00359-015-1008-5>
- Oyster, C. W., Amthor, F. R., & Takahashi, E. S. (1993). Dendritic architecture of ON-OFF direction-selective ganglion cells in the rabbit retina. *Vision Research*, 33(5–6), 579–608. [https://doi.org/10.1016/0042-6989\(93\)90181-U](https://doi.org/10.1016/0042-6989(93)90181-U)
- Packer, O., Diller, L. C., Verweij, J., Lee, B. B., Pokorny, J., Williams, D. R., ... Brainard, D. H. (2001). Characterization and use of a digital light projector for vision research. *Vision Research*, 41(4), 427–439. [https://doi.org/10.1016/S0042-6989\(00\)00271-6](https://doi.org/10.1016/S0042-6989(00)00271-6)

- Pinsky, E., Donchin, O., & Segev, R. (2015). Pharmacological study of direction selectivity in the archer fish retina. *Journal of Integrative Neuroscience*, *14*(4), 473–490. <https://doi.org/10.1142/S0219635215500247>
- Ramlochansingh, C., Branoner, F., Chagnaud, B. P., & Straka, H. (2014). Efficacy of tricaine methanesulfonate (MS-222) as an anesthetic agent for blocking sensory-motor responses in *Xenopus laevis* tadpoles. *PLoS ONE*, *9*(7), e101606. <https://doi.org/10.1371/journal.pone.0101606>
- Reichardt, W. (1987). Evaluation of optical motion information by movement detectors. *Journal of Comparative Physiology A*, *161*(4), 533–547. <https://doi.org/10.1007/BF00603660>
- Schuller, J. M., Knorr, A. G., Glasauer, S., & Straka, H. (2014). Task-specific activation of extraocular motoneurons in *Xenopus laevis*. In *Society for Neuroscience Abstracts*, *40*, 247.06.
- Semmelhack, J. L., Donovan, J. C., Thiele, T. R., Kuehn, E., Laurell, E., & Baier, H. (2014). A dedicated visual pathway for prey detection in larval zebrafish. *eLife*, *3*, E2391–E2398. <https://doi.org/10.7554/eLife.04878>
- Straka, H., & Dieringer, N. (2004). Basic organization principles of the VOR: Lessons from frogs. *Progress in Neurobiology*, *73*(4), 259–309. <https://doi.org/10.1016/j.pneurobio.2004.05.003>
- Straka, H., & Simmers, J. (2012). *Xenopus laevis*: An ideal experimental model for studying the developmental dynamics of neural network assembly and sensory-motor computations. *Developmental Neurobiology*, *72*(4), 649–663. <https://doi.org/10.1002/dneu.20965>
- Straw, A. D., Rainsford, T., & O'Carroll, D. C. (2008). Contrast sensitivity of insect motion detectors to natural images. *Journal of Vision*, *8*(3), 32.1-9. <https://doi.org/10.1167/8.3.3>

### 3 Manuscript 2

Add a splash of color: Interaction of luminance and color information in the optokinetic reflex system of *Xenopus laevis* tadpoles

Alexander G. Knorr<sup>1,2,\*</sup>, Céline M. Gravot<sup>3,4,\*</sup>, Stefan Glasauer<sup>1</sup> and Hans Straka<sup>3</sup>

<sup>1</sup> Center for Sensorimotor Research, University Hospital Großhadern, Feodor-Lynen-Str. 19, 81377 Munich

<sup>2</sup> Institute for Cognitive Systems, TUM Department of Electrical and Computer Engineering, Technical University of Munich, Karlstraße 45/II, 80333 München

<sup>3</sup> Department Biology II, Ludwig-Maximilians-University Munich, Großhaderner Str. 2, 82152 Planegg

<sup>4</sup> Graduate School of Systemic Neurosciences, Ludwig-Maximilians-University Munich, Großhaderner Str. 2, 82152 Planegg

\* A.G.K and C.M.G. contributed equally to this work

**Acknowledgments:** The authors further acknowledge financial support from the German Science Foundation (CRC 870; STR 478/3-1 and GL 342/2-1), the German Federal Ministry of Education and Research under the Grant code 01 EO 0901 and the Bernstein Center for Computational Neuroscience Munich (BT-1).

**Abstract**

While moving through dynamic environments, vertebrates ensure gaze stability through compensatory reflexes, such as the optokinetic reflex (OKR) that responds to large-field image motion and drives eye movements that follow the motion of a visual scene. Information of these visual scenes, such as luminance or color contrasts, can be used to detect and estimate motion. However, the role and contribution of color to motion perception has been a matter of controversy in the literature of the last decades. Using the animal model *Xenopus laevis* tadpoles, we investigated how luminance and color information interact on the optokinetic reflex.

To test color motion perception of *Xenopus* tadpoles, characteristic slow following eye movements of the OKR were monitored during stimulation with rotatory large-field images, consisting of chromatic and luminance contrasts. The brightness ratio of the two colors (red and blue), at which the OKR response was minimal, was determined. The results showed that, at this point of equiluminance (POE), color contrast is able to evoke a minor following OKR response and is therefore sufficient to elicit motion vision. To assess the interaction of color and luminance at high luminance contrast levels, visual motion stimuli were presented at high intensity levels. The results showed that the OKR of *Xenopus* tadpoles responds differentially to motion stimuli presented in different colors, advising an influence of color on the OKR. Further, electrophysiological recordings of the optic nerve revealed that the behavioral observations were not mirrored at a population activity level. However, single units of the optic nerve showed a clear color preference, suggesting that these units may be differentially coupled to the optokinetic circuitry in the midbrain.

Taken together, this study shows that color influences the optokinetic reflex in *Xenopus* tadpoles and may be behaviorally relevant to distinguish between self-motion patterns and movements of other objects in dynamic environments.

## Introduction

Most vertebrates possess mechanisms to ensure a stable image on the retina while moving through dynamic environments. While the vestibulo-ocular reflex (VOR) compensates for self-motion-induced retinal slip by means of the vestibular signal (Straka and Dieringer, 2004), the brainstem-mediated optokinetic reflex (OKR) responds to large-field image motion and drives eye movements that follow the visual surround's motion (Collewijn, 1969; Dieringer and Precht, 1982). This latter reflex relies on an internal estimate of the velocity of the visual scenery (Raphan et al., 1977) and is strongly influenced by the image characteristics of the visual motion stimulus (Rinner et al., 2005; see chapter 2, manuscript 1). Natural environments present various different forms of visual information that can be used to detect and estimate motion: In particular, the visual scene can be structured by luminance and color cues, both of which can provide information for motion vision. While most images are well-defined only by local changes in light intensity, adjacent image components need not vary in brightness, but could also vary only in color, such that also color could provide relevant information for motion vision.

The role of color information in motion perception has been a matter of debate for over 20 years (Gegenfurtner and Hawken, 1996). Early studies purported that color and motion are perceived in strict separation based on neurophysiological and lesion studies (Livingstone and Hubel, 1987). At the same time, other studies argued in favor of a contribution of color information to motion perception (Cavanagh and Anstis, 1991; Dobkins and Albright, 1994), observing that motion of patterns of two equiluminant colors could still be detected in human psychophysical experiments (Cavanagh et al., 1984). In the meantime, the bulk of evidence supports the idea that motion vision does not operate totally independent of color.

This study uses an amphibian species, *Xenopus laevis* tadpoles, to study how luminance and color information interact on a brainstem-level visuomotor reflex (OKR). The use of such simpler model species (Zoccolan et al., 2015) enables researchers to investigate and understand neuronal computations underlying visual processing. *Xenopus* tadpoles show a large range of advantages, such as the relative simplicity of its central nervous

system as well as an easy experimental accessibility of the visual circuitry. Like in various other vertebrates, including humans, the *Xenopus* eye has different types of cones with three distinct absorption spectra (Witkovsky, 2000) making it a model of choice for investigating the principles underlying low-level vision processes.

So far, different studies investigating color motion vision found conflicting results in different species. Yamaguchi et al. (2008) found that in the fly *Drosophila* color is strictly excluded from motion information processing, suggesting two separate functional pathways. On the other hand, a study performed by Matsuura et al. (2016) in monkeys suggest that, although color cues play a subordinate role compared to luminance cues, color information contributes not only to the sensation of motion but also to the generation of visuomotor responses (here ocular following responses, OFR) and thereby provide evidence that color and luminance information are processed together to activate motor responses.

Already the retina performs advanced image processing and is able to extract motion information from a moving image (Lettvin et al., 1959). This raises the question of whether the retina already exploits color contrast for motion vision or whether motion detection based on color contrast occurs further downstream.

Based on behavioral observations of the OKR and extracellular recordings of signals transmitted from the retina to the oculomotor system via the optic nerve, this study investigated whether and how luminance and color information interact on a brainstem-mediated reflex and to what extent these interactions are already present at the level of the optic nerve.

## Methods

*Animal Experiments.* Experiments were performed *in-vitro* on isolated, semi-intact preparations of *Xenopus laevis* tadpoles and comply with the National Institute of Health publication entitled "Principles of animal care", No. 86-23, revised 1985. Permission for these experiments was granted by the governmental institution at the Regierung von Oberbayern/Government of Upper Bavaria (55.2-1-54-2532.3-59-12). Animals were obtained from the in-house animal breeding facility at the Biocenter-Martinsried of the Ludwig-Maximilians-University Munich. A total of 46 *Xenopus laevis* tadpoles of developmental larval stages 50-55 (Nieuwkoop and Faber, 1994) were used for experimentation. For preparation, tadpoles were anesthetized in 0.05% 3-aminobenzoic acid ethyl ester (MS-222; Pharmaq) in frog Ringer solution (in mM: 75NaCl, 25NaHCO<sub>3</sub>, 2CaCl<sub>2</sub>, 2KCL, 0.5MgCl<sub>2</sub> and 11glucose, pH7.4). The telencephalon was removed according to the preparation procedure described by Lambert et al. (2012).

For behavioral experiments, the skin covering the dorsal head was removed, the soft skull tissue opened and the forebrain disconnected. This surgical procedure anatomically preserved the remaining CNS and the eyes including the optic nerve, extraocular motor innervation and eye muscles. Such preparations allowed prolonged experimentation and *in vivo*-like activation of the OKR by horizontal large-field image motion under controlled *in-vitro* conditions.

For electrophysiological recordings of the optic nerve, in addition to the procedure described above, the optic nerve of the right eye was freed of surrounding tissue and transected at the level of the optic chiasma. All eye muscles connected to the right eye were then transected at their medial end to immobilize the eye while retaining it in its natural position within the body and thus prevent retinal image motion evoked by optokinetic eye movements. Preparations were kept at 14°C for 3 hours after the preparation, allowing their central nervous system to recover (Ramlochansingh et al., 2014).

*Setup.* Semi-intact preparations were fixed with insect pins to the Sylgard floor of a Petri dish (5 cm diameter). The chamber, which was constantly perfused with oxygenated frog Ringer solution at a rate of 3.0 - 5.0 ml/min, was mechanically secured in the center of

an open cylindrical screen with a height of 5 cm and a diameter of 8 cm, encompassing 275°. Three digital light processing (DLP) video projectors (Aiptek V60), installed in 90° angles to each other, projected visual motion stimuli onto the screen (Packer et al., 2001) at a refresh rate of 60 Hz. A CCD camera (Grasshopper 0.3 MP Mono FireWire 1394b, PointGrey), mounted onto the table, permitted on-line tracking of horizontal eye movements by custom-written software (Beck et al., 2004). The chamber was illuminated from above using an 840 nm infrared light source. An infrared long-pass filter in the camera ensured selective transmission of infrared light and a high contrast of the eyes for online analysis of induced movements. The visual motion stimulus, the extracellular signals and the position of both eyes were digitized and read out into the data acquisition program (Spike2, Version 7.04, Cambridge Electronic Design Ltd., United Kingdom).

Electrophysiological recordings were performed in the same setup. Spike discharge of the optic nerve was recorded extracellularly (EXT 10-2F, mpi electrodes, Tamm, Germany) with individually adjusted electrodes and digitized at a sampling rate of 28.6kHz (CED Micro1401-3, Cambridge Electronic Design, UK). Glass microelectrodes for extracellular recordings were produced with a horizontal puller (P-87 Brown/Flaming, Sutter Instruments Company, USA) and the tips were individually adjusted to fit the respective optic nerve diameter.

*Experimental paradigm.* A convenient method to test for color motion perception in animal models is to monitor the optomotor response to moving chromatic and luminance contrast stimuli and determine the brightness ratio of the two colors, at which the optomotor response is minimal (Schaerer and Neumeyer, 1996, Yamaguchi et al., 2008). At this point of equiluminance (POE), the subjective brightness of the scene is homogeneous, such that the scene is only structured by color changes. At the POE, the optomotor response can either be absent, arguing in favor of a color-blind motion perception system or show a residual response, indicating that color information does provide motion cues.

The optokinetic reflex was assessed by a rotatory large-field visual motion stimulus moving with a rectangular velocity profile with a speed of  $\pm 10^\circ/\text{s}$  and a frequency of 0.2 Hz (i.e. alternating directions ever 2.5 s).

*Condition 1: Point of equiluminance.* To determine the point of equiluminance (POE), the presented visual stimulus consisted of alternating red and blue vertical chromatic stripes. The radiance of the red stripes was manipulated in a range of 0.29 to  $3.18 \text{ W}^*\text{sr}^{-1}\text{m}^{-2}$ , while the intensity of the blue stripes was maintained at a constant value of  $4.66 \text{ W}^*\text{sr}^{-1}\text{m}^{-2}$ . As a control condition, the optokinetic response to rotation of a uniformly grey screen was measured to obtain the reference level for comparison of the minimum OKR amplitude (*Grey condition*).

*Condition 2: Interaction of color and motion at high intensities.* In another experimental condition, three additional visual motion stimuli were presented at high intensity levels in randomized order to assess the interaction of color and luminance motion at high luminance contrast levels. Stripes were either white ( $18.7 \text{ W}^*\text{sr}^{-1}\text{m}^{-2}$ ), red ( $3.39 \text{ W}^*\text{sr}^{-1}\text{m}^{-2}$ ), blue ( $4.66 \text{ W}^*\text{sr}^{-1}\text{m}^{-2}$ ) or black ( $0.187 \text{ W}^*\text{sr}^{-1}\text{m}^{-2}$ ) and were presented in alternating White/Black, Red/Black, Blue/Black, and Red/Blue stripes arrangement.

*Condition 3: Optic nerve activity at high intensities.* To investigate how colored motion stimuli at high intensities are represented on the population activity of the optic nerve, electrophysiological recordings from the optic nerve were performed during stimulation with rotatory large-field image motion. To identify optic nerve responses modulating with stimulus velocity, a sinusoidal velocity profile with a peak velocity of  $\pm 10^\circ/\text{s}$  and a frequency of 0.125 Hz was used, resulting in a similar position amplitude to the behavioral conditions. Otherwise, the stimuli were identical to those presented in *Condition 2*.

*Condition 4: Optic nerve activity near the POE.* To determine whether velocity modulated activity at the level of the optic nerve is exclusively driven by luminance contrasts, or whether some units respond also to pure color contrast, optic nerve activity was measured in response to red and blue stripes at three red light intensities (1.14, 1.19 and  $1.25 \text{ W}^*\text{sr}^{-1}\text{m}^{-2}$ ), while the intensity of the blue stripes was held constant ( $4.66 \text{ W}^*\text{sr}^{-1}\text{m}^{-2}$ ).

*Spectral distribution of color stimuli.* The individual red and blue colors were generated using the red and blue channels of the image projectors, the white bars were generated using all three color channels (for spectra see Appendix 1). The spectra and radiance values were measured using a spectrometer (PhotoResearch SpectraScan PR655).

*Data Analysis.* To obtain a robust measure of the strength of the optokinetic response, the amplitude of the OKR was then computed by fitting a triangular position profile to the recorded eye position trace and evaluating the amplitude of the fit.

To account for the fact that the “true” value of the point of equiluminance (POE) might lie between the sampled intensities, we fitted the resulting intensity-amplitude curve with a function for the normalized OKR amplitude  $A$  defined by

$$A = m * \frac{|b_{Red} - b_{Blue}|}{|b_{Red} - b_{Blue}| + c} + A_{CR},$$

with the subjective brightness for red or blue:

$$b_{Red,Blue} = \log(L_{Red,Blue} + 1) * c_{Red,Blue}.$$

and  $c_{Red}$  and  $c_{Blue}$  as the relative sensitivities to red and blue, respectively. The parameters  $m$  and  $c$  were required to model the sensitivity of each preparation’s optokinetic reflex to changes in subjective contrast. This model was able to fit the observed data well, especially near the point of equiluminance.

The POE was identified as the radiance value of the red stripes at which the fitted optokinetic response amplitude function became minimal ( $A_{CR}$ ) in each preparation. The OKR amplitude at this point was then defined as the isolated chromatic response (CR) component of the optokinetic response.

For electrophysiological recordings, optic nerve activity was quantified by the total count of action potentials during each trial. Since all trials had the same length and surround velocity profile, this gave a robust estimate of nerve activity during stimulation with differently colored optokinetic stimuli.

*Spike sorting.* To distinguish the response properties of individual retinal ganglion cells at the level of the optic nerve, spike sorting was performed in MATLAB (R2016a) on the recorded extracellular signals from the optic nerve.

For each preparation, all trials were pooled, action potentials were detected using a non-linear energy operator threshold (Malik et al., 2016). Artifacts were identified as all segments of the dataset in which the electrical signal was greater than 1000mV and subsequently removed by replacing the respective values with zeroes. Spikes were then extracted in a 7 ms window around their respective peaks. The collected spike shapes were then subjected to a singular value decomposition. The three largest singular values were then used for spike sorting. The values were clustered using k-means clustering (MATLAB 2016a). The number of clusters was determined by visual inspection of the 3D scatter plot of singular values. The success of clustering was verified by visual inspection of the 3D-plot.

*Statistical Procedures.* The critical value of significance was chosen as  $\alpha = 0.05$  for all statistical tests. The optokinetic response amplitudes at the POE were compared to the reference values obtained from the *Grey condition* using a two-sample t-test. The OKR amplitudes in response to White/Black, Blue/Black, Red/Black and Red/Blue visual motion stimuli were compared using a repeated measures ANOVA. Post-hoc-tests were performed using pairwise paired t-tests between all conditions, using the Bonferroni method to compensate for multiple comparisons.

To reveal a possible linear interaction between color and luminance motion information, the correlation between the chromatic component of the OKR and the differences between the responses to Red/Blue – Black and White-Black stimuli was computed.

To determine the strength of single units' neuronal responses to colored compared to pure luminance stimuli, color preference ( $g_{Red, Blue}$ ), as the relative increase or decrease of activity in response to colored vs white stimuli was measured by computing the log of the ratio of spike counts (SC) in either the red or blue color conditions over the spike count in the white condition:

$$g_{Red,Blue} = \log\left(\frac{SC_{Red,Blue}}{SC_{White}}\right).$$

## Results

### *Point of equiluminance*

The point of equiluminance (POE) at which the luminance contrast with respect to blue stripes with a radiance of  $4.66 \text{ W}^* \text{sr}^{-1} \text{m}^{-2}$  vanished was robust across animals and was at a value of  $1.22 \pm 0.09 \text{ W}^* \text{sr}^{-1} \text{m}^{-2}$ . The normalized amplitude of the OKR at the POE was  $0.22 \pm 0.15$  times the mean amplitude over all conditions (Fig. 1B). This residual optokinetic response, albeit small, was still significantly greater than the baseline (Two-sampled t-test:  $t(57) = 3.02$ ,  $p = 0.004$ ,  $d = 0.86$ ; Fig. 1C), indicating that pure color contrast is sufficient to elicit motion vision and thereby evoke a minor ocular following response.

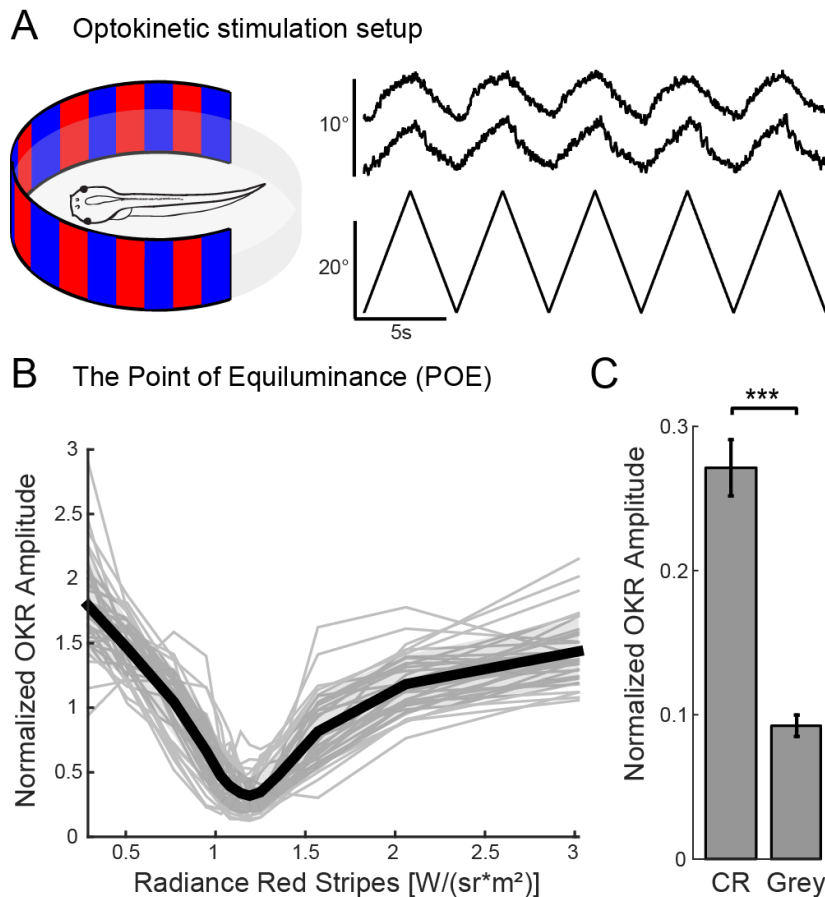


**Figure 1: Experimental setting for recording optokinetic reflexes (OKR) in *Xenopus* tadpoles.**

(A) Schematic, illustrating the experimental setup with a central recording chamber for semi-intact larval *Xenopus* preparations (adapted from Hänzli and Straka, 2016), surrounded by a cylindrical screen onto which a rotating large-field striped pattern with alternating vertical stripes and different colors and intensities was projected. Representative eye position and stimulus traces for constant velocity stimulation ( $\pm 10^\circ/\text{s}$ , alternating every 2.5s). (B) Optokinetic response amplitudes for alternating red and blue stripes at different radiances of the red stripes. At the point of equiluminance (POE), the OKR amplitude became minimal. (C) Bar plot indicating that the chromatic response (CR) i.e. the OKR amplitude at the POE is significantly higher than baseline amplitude in the control condition (*Grey condition*).

*Interaction of color and luminance on the OKR at high intensities*

In addition to the optokinetic response evoked by pure color contrast stimuli, also at high intensities colored motion stimuli led to higher OKR amplitudes compared to White/Black stimuli, indicated by a significant main effect of stimulus color (Repeated measures ANOVA:  $F(3, 102) = 46.62, p < 0.001, \eta^2 = 0.26$ ; Fig. 2A) and the successive post-hoc tests. This was surprising as the radiance of white bars was approximately four-fold that of blue and more than five-fold that of red stripes ( $18.7 \text{ W} \cdot \text{sr}^{-1} \cdot \text{m}^{-2}$  compared to  $4.66 \text{ W} \cdot \text{sr}^{-1} \cdot \text{m}^{-2}$  or  $3.39 \text{ W} \cdot \text{sr}^{-1} \cdot \text{m}^{-2}$ , respectively), while the black bars always had the same intensity. The effect was still present when matching the radiance of the white stripes to the colored stripes (Two-sampled t-test for blue:  $t(5) = -2.90, p = 0.034, d = -0.377$ ). Interestingly, these additional color-related components were not correlated with the isolated chromatic OKR response (blue:  $\rho = 0.04, p > 0.05$ ; red:  $\rho = 0.05, p > 0.05$ ; Fig. 2C). Nevertheless, the additional color-related components in the red and blue conditions were strongly correlated ( $\rho = 0.71, p < 0.001$ ), suggesting that some preparations are more sensitive to color motion stimuli than others (Fig. 2B).

Furthermore, even comparisons between colored stimuli revealed a significantly larger optokinetic response to Blue/Black, than to Red/Black stimulus patterns, indicating that the optokinetic reflex in *Xenopus* tadpoles responds differentially to motion stimuli presented in different colors.

Varying pure luminance contrast in achromatic stimuli in a previous study (see chapter 2, manuscript 1) indicated that upon reaching a certain contrast level, the optokinetic response becomes maximal and does not increase at higher contrast levels. Therefore, increasing the luminance contrast of either of these stimuli would likely not change the optokinetic response amplitude, since all stimuli are bright enough to elicit the maximal response. Nevertheless, the increases in OKR amplitude in colored stimuli at distinctly lower luminance contrasts than black and white suggests that there is an additional color-related component that plays a role in driving the OKR of *Xenopus* tadpoles.

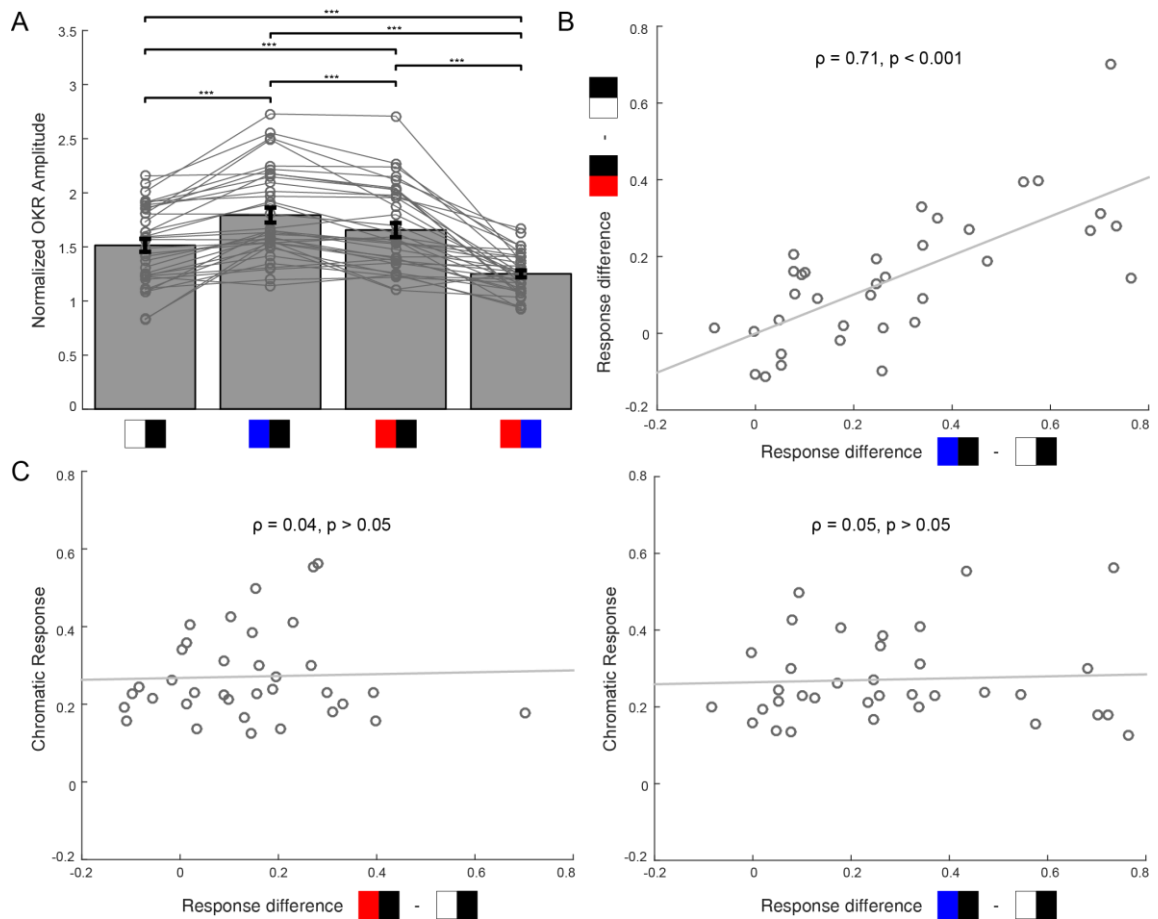


**Figure 2: Optokinetic reflex response to high intensity colored stimulation.**

(A) Bar plot indicating the relative optokinetic response amplitude to large-field visual motion stimuli presented with different colors. Surprisingly, responses were larger when black stripes were presented together with colored than with white stripes, suggesting an influence of color on the OKR. The smaller response to alternating red and blue stripes is likely due to the smaller luminance contrast in this condition. (B) Scatter plot showing the difference in response between blue and white (x-axis) and red and white (y-axis) for each preparation. The differences were strongly correlated across preparations. (C) Scatter plots showing the chromatic response over the difference in response between red and white (left) and blue and white (right). The differences were not correlated with the chromatic response.

### *Optic nerve population responses to colored moving stimuli*

Pilot experiments showed that for luminance motion stimuli, there is a close association between population activity on the level of the optic nerve, indicating that optic nerve population activity can be interpreted as surround velocity estimate. Whether this also applies when comparing the responses to stimuli which have distinct wavelength components – and therefore likely excite different retinal photoreceptors – was investigated by recording extracellularly from the optic nerve of *Xenopus* eye preparations. Surprisingly, at a population level, the relative neuronal response magnitude (spike count) appeared not to mirror the behavioral observations (Fig. 3B). Although the neuronal response to high intensity Red/Blue striped patterns was smaller than the response to the three other patterns (likely due to the smaller contrast in this condition), the response magnitudes in the other three conditions showed a different activation pattern than in the behavioral experiments.

This suggests that the mechanism causing the different optokinetic response amplitudes for different colors at high light intensities is qualitatively different from the mechanism responsible for adjusting the optokinetic response based on luminance contrast, which would also be expressed in the relative size of the retinal responses.

### *Optic nerve single unit responses to colored moving stimuli*

Rather, it suggests an alternative possible mechanism for the *partially* color-specific optokinetic response amplitude: Separate subgroups of retinal motion detectors, which respond preferentially to certain wavelengths differ in how strongly they are coupled to the optokinetic circuitry in the midbrain.

To test this hypothesis, single unit responses were isolated from the extracellular recordings using SVD-based spike sorting (Matlab2015a), resulting in a total of  $n = 25$  discernable spike waveforms which modulated their activity with stimulus velocity. Single units' color preference was then identified by evaluating the magnitude of their response to the four high intensity color stimuli (Fig. 3A). While the total spike count varied strongly between individual units, there were clear differences between the color-preference of different units. Units that responded preferentially to either white,

red or blue stripes were found. The distinction between units with color-sensitive and color-insensitive response characteristics was relatively clear-cut (indicated by the gap between squares and plusses in Fig. 3C). Among the color-sensitive units, however, there was no clear distinction based on the response preference to either red or blue color. Instead, units which responded strongly to one color also responded more strongly to the other, as demonstrated by the strong correlation between red and blue preference ( $g_{\text{Red}}$  and  $g_{\text{Blue}}$ ) in Fig. 3C ( $\rho = 0.67$ ,  $n = 25$ ,  $p < 0.001$ ). This, again, is in line with the behavioral findings that animals with a strong preference for one color (expressed by their relative OKR amplitude) also show a strong response to the other color stimulus.

#### *Retinal response at equiluminance*

While most of the measured units were inactive during stimulation near the point of equiluminance, a small number of single units still clearly modulated their activity along with stimulus velocity.

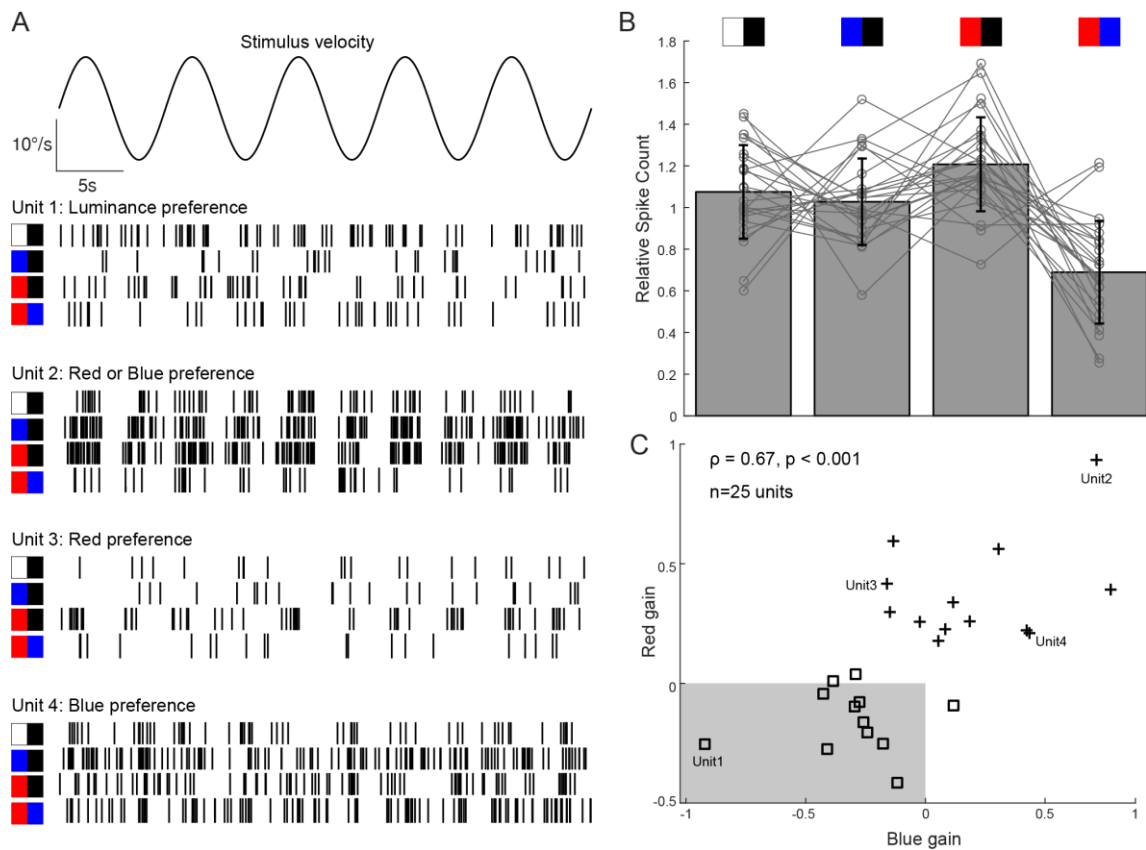


**Figure 3: Optic nerve activity to high intensity colored stimulation.** (A) Exemplary spike trains for four different single units of the optic nerve with different luminance or color preferences. Unit 1 responded more strongly to high luminance contrast, Unit 2 responded more strongly to blue or red vs. black, Unit 3 and 4 responded more to red or blue stimulation, respectively. (B) Bar plot showing the relative spike count of all recorded units to visual motion stimulation with different colors. On average, the significantly stronger response to colored stimuli was not mirrored in the optic nerve activity. The smaller response to the alternating red and blue stripes is also present on the level of the optic nerve. (C) Scatter plot, showing the relative preference for red and blue color motion stimuli for all units recorded. Units in the grey box respond more strongly to pure luminance stimuli, whereas the other units respond more strongly to at least one chromatic stimulus. Units appear to fall in two clusters with either luminance (squares) or color (plusses) preference.

## Discussion

The color of a moving visual scene systematically influences the optokinetic reflex in *Xenopus laevis* tadpoles. Firstly, while the optokinetic response decreased in amplitude with decreasing luminance contrast, preparations showed a residual optokinetic response at the point of equiluminance, i.e. even in the absence of luminance contrasts, an oculomotor response was present. Furthermore, at high intensity stimuli, responses were larger when black stripes were presented together with colored than with white stripes, suggesting an influence of color on the OKR. Finally, on the optic nerve these differences of response magnitudes are not mirrored on a population level but single units show clear color preferences.

The residual response at the POE (*Condition 1*) shows that pure color contrasts cannot be excluded to play a role in the visual motion detection mechanism which forms the basis of the optokinetic reflex. Anatomically, the necessary requirements for color vision have been shown to be present in adult *Xenopus*, who possess principal (red-sensitive) and thin (blue-sensitive) rods as well as four types of cones exhibiting red, blue and ultraviolet-sensitive opsins (Röhlich and Szél, 2000). This study provides further evidence that *Xenopus* tadpoles possess and employ the required anatomical structures to be able to see and distinguish different colors and adjust their behavior accordingly. In larval *Xenopus*, an influence of color on navigation and evasion behavior were reported by Rothman et al. (2016), who found that larval *Xenopus* could be trained to avoid a specifically-colored segment of their environment, concluding that color vision was behaviorally relevant for *Xenopus* tadpoles.

Recording visual motion induced behavior at the point of equiluminance is an advantageous method to investigate how visual motion perception depends on color (Cavanagh, 1991) and can be applied especially in simple animal models. In both fly (Yamaguchi et al., 2005) and zebrafish (Krauss and Neumeier, 2003), recording optomotor locomotion responses led to the conclusion that motion vision is "color-blind". However, in comparison to locomotor behavior, the well-known system characteristics of the optokinetic reflex and its approximately linear input-output relationship (Robinson, 1981) advocate the use of this reflex as a more sensitive

behavioral assay, since it is possible to isolate even small responses based on their frequency characteristics and robustly distinguish them from spontaneous motor activity.

This paradigm revealed a non-zero optokinetic response at the POE in the clear majority of animals (26 out of 35), suggesting that color information does indeed play a role in low-level motion vision. Also in higher-order motion vision, such as human subjective speed estimation, color has been shown to play a role (Gegenfurtner and Hawken, 1996): While the speed of an equiluminant chromatic grating is only perceived to be moving at about half the speed of a corresponding luminance grating, a motion percept is still evoked in the absence of luminance contrast (Cavanagh et al., 1984). Since all animals used in this study were reared under identical artificial lighting conditions, it could reasonably be anticipated that the location of the POE is similar across animals (Kröger et al., 2003), which is indeed the case.

An influence of color on the optokinetic reflex was also observed at high light intensities, in which alternating White/Black, Red/Black and Blue/Black stripes were presented. Surprisingly, *Xenopus* preparations showed a larger response to stimuli with either blue or red bars, compared to White/Black stimuli, even though the luminance contrast of white vs black stripes was the highest, independent of which measure was used (candela, radiance, photon radiance, see Table 1). Likely, all stimuli have sufficient luminance contrast to evoke the maximal optokinetic response, while the colored stimuli recruit additional sensorimotor pathways and thus lead to an increase in OKR amplitude.

Variations in luminance characteristics of a large-field motion stimulus lead to strongly correlated changes in both the optokinetic reflex amplitude as well as the population activity of the optic nerve (see chapter 2, manuscript 1). However, varying stimulus color above the saturation level for luminance contrast evoked no conjugate variations in optic nerve activity. This suggests that the observed differences in response amplitude are not caused by luminance contrast artifacts, such as reflections, but rather motivates a different explanation for the increase of OKR amplitude during chromatic stimulation: The differences can be explained by retinal motion detectors with preferences for

specific colors, which differ in how strongly they are coupled to the optokinetic reflex circuitry in the brainstem (Orger and Baier, 2005). This hypothesis is supported by our observation of single units at the optic nerve level with varying preferences for large-field motion stimuli in red, blue or white color (Fig. 3). Evaluating individual units based on how their response changed between white and red or blue stimuli, respectively showed a relatively large separation between two types (see Fig. 3C): In about half of the recorded units, activity decreased when colored stimuli were presented, while in the other half activity increased. This increase was typically similar comparing red and blue stimuli, although units with a preference for either color were found. This demonstrates that the neuronal substrate for color-specific processing of motion information in the optokinetic reflex is also in place in *Xenopus* tadpoles.

Ecologically, including color information for optokinetic reflex performance appears advantageous: Color provides many additional cues about the environment and visual motion within it. It increases the saliency of objects, and it seems intuitive that color might also facilitate motion perception (Dobkins and Albright, 1994). It also appears likely that certain environmental features have consistent colors and – based thereupon – can be more easily distinguished from other objects. Especially in the distinction between visual motion of the entire scene (which is most likely caused by self-motion and therefore should elicit an optokinetic response), and motion of outside objects (which should be ignored by the optokinetic system), these characteristics might play a role. For example, distinguishing between the blue sky and other animals or objects moving through the water.

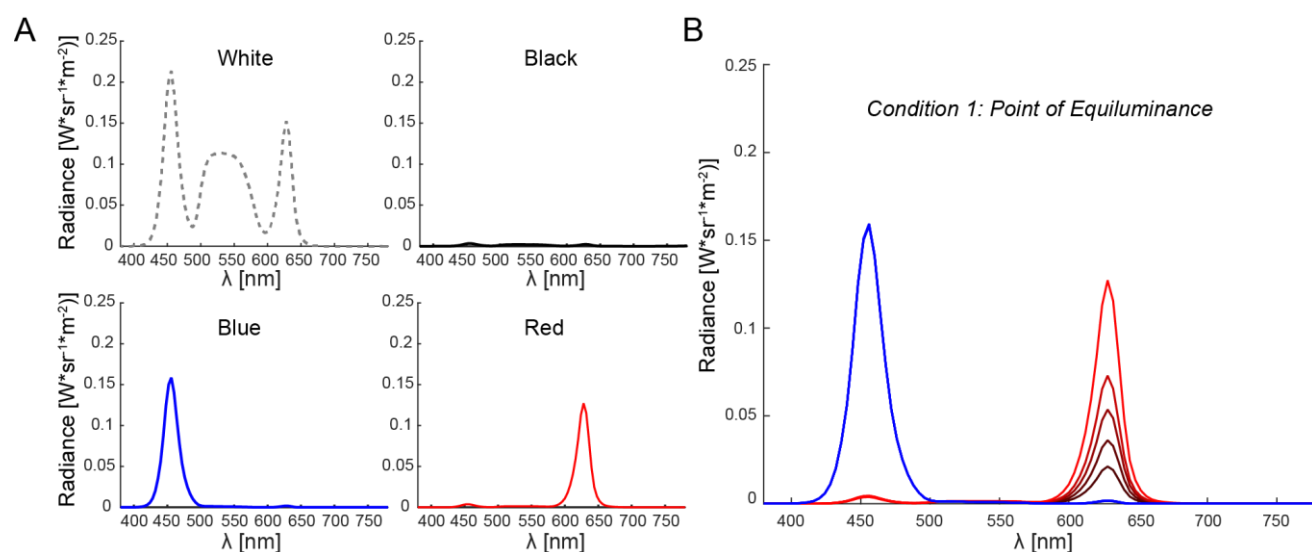
## **Conclusion**

This study shows that in larval *Xenopus*, the optokinetic reflex is systematically influenced by color information. The underlying mechanism is likely to be found in separate channels for motion detection which have different color preferences and differ in their projections to the premotor optokinetic nuclei in the brainstem.

	Candela [cd·m <sup>-2</sup> ]	Radiance [W·m <sup>-2</sup> ·sr <sup>-1</sup> ]	Photon Radiance [m <sup>-2</sup> ·sr <sup>-1</sup> ·s <sup>-1</sup> ]
White	5871	1.87·e <sup>+1</sup>	5.0·10 <sup>19</sup>
Black	101.7	3.21·e <sup>-1</sup>	8.6·10 <sup>17</sup>
Red	751.8	3.39·e <sup>+0</sup>	1.06·10 <sup>19</sup>
Blue	224.7	4.66·e <sup>+0</sup>	1.07·10 <sup>19</sup>

**Table 1: Different photometric and radiometric measures.**

Different measures can be used to quantify the intensity of light with different colors. Note that while white has the largest intensity regardless of the used measure, whether red or blue are construed as more intense depends on the measure used.



**Appendix 1: Wavelength spectrum of the different stimuli produced by the used video projectors.**

(A) Graph, showing the spectra of white, black, blue and red light emitted by the projectors at their relative maximal intensities. (B) Graph illustrating how the intensity of the red stripes was modulated to identify the point of equiluminance in *Condition 1*. The intensity of the blue stripes was held constant, whereas the intensity of the red stripes was scaled without changing the wavelength.

## References

- Beck, J. C., Gilland, E., Baker, R., & Tank, D. W. (2004). Instrumentation for measuring oculomotor performance and plasticity in larval organisms. *Methods in Cell Biology*, *76*, 385–413. [https://doi.org/10.1016/S0091-679X\(04\)76017-3](https://doi.org/10.1016/S0091-679X(04)76017-3)
- Cavanagh, P., & Anstis, S. (1991). The contribution of color to motion in normal and color-deficient observers. *Vision Research*, *31*(12), 2109–2148. [https://doi.org/10.1016/0042-6989\(91\)90169-6](https://doi.org/10.1016/0042-6989(91)90169-6)
- Cavanagh, P. (1991). Vision at equiluminance. In J. J. Kulikowski, I. J. Murray, & V. Walsh (Eds.), *Vision and Visual Dysfunction: Limits of Vision* (Vol. 5, pp. 234–250). Boca Raton, FL: CRC Press.
- Cavanagh, P., Tyler, C. W., & Favreau, O. E. (1984). Perceived velocity of moving chromatic gratings. *Journal of the Optical Society of America. A, Optics and Image Science*, *1*(8), 893–9. <https://doi.org/10.1364/JOSAA.1.000893>
- Collewijn, H. (1969). Optokinetic eye movements in the rabbit: Input-output relations. *Vision Research*, *9*(1), 117–132. [https://doi.org/10.1016/0042-6989\(69\)90035-2](https://doi.org/10.1016/0042-6989(69)90035-2)
- Dieringer, N., & Precht, W. (1982). Compensatory head and eye movements in the frog and their contribution to stabilization of gaze. *Experimental Brain Research*, *47*(3), 394–406. <https://doi.org/10.1007/BF00239357>
- Dobkins, K. R., & Albright, T. D. (1994). What happens if it changes color when it moves? the nature of chromatic input to macaque visual area MT. *The Journal of Neuroscience: The Official Journal of the Society for Neuroscience*, *14*(8), 4854–70.
- Gegenfurtner, K. R., & Hawken, M. J. (1996). Interaction of motion and color in the visual pathways. *Trends in Neurosciences*, *19*(9), 394–401. [https://doi.org/10.1016/S0166-2236\(96\)10036-9](https://doi.org/10.1016/S0166-2236(96)10036-9)
- Hänzi, S., & Straka, H. (2016). Schemes of *Xenopus laevis* tadpoles. *Figshare*. Retrieved from [https://figshare.com/articles/Schemes\\_of\\_Xenopus\\_laevis\\_tadpoles/3841173](https://figshare.com/articles/Schemes_of_Xenopus_laevis_tadpoles/3841173)

- Krauss, A., & Neumeier, C. (2003). Wavelength dependence of the optomotor response in zebrafish (*Danio rerio*). *Vision Research*, *43*(11), 1273–1282. [https://doi.org/10.1016/S0042-6989\(03\)00090-7](https://doi.org/10.1016/S0042-6989(03)00090-7)
- Kröger, R. H. H., Knoblauch, B., & Wagner, H.-J. (2003). Rearing in different photic and spectral environments changes the optomotor response to chromatic stimuli in the cichlid fish *Aequidens pulcher*. *Journal of Experimental Biology*, *206*(10), 1643–1648. <https://doi.org/10.1242/jeb.00337>
- Lambert, F. M., Combes, D., Simmers, J., & Straka, H. (2012). Gaze stabilization by efference copy signaling without sensory feedback during vertebrate locomotion. *Current Biology*, *22*(18), 1649–1658. <https://doi.org/10.1016/j.cub.2012.07.019>
- Lettvin, J. Y., Maturana, H. R., Maturana, H. R., McCulloch, W. S., & Pitts, W. H. (1959). What the frog's eye tells the frog's brain. *Proceedings of the IRE*, *47*(11), 1940–1951. <https://doi.org/10.1109/JRPROC.1959.287207>
- Livingstone, M. S., & Hubel, D. H. (1987). Psychophysical evidence for separate channels for the perception of form, color, movement, and depth. *The Journal of Neuroscience: The Official Journal of the Society for Neuroscience*, *7*(11), 3416–3468. Retrieved from <http://www.jneurosci.org/content/7/11/3416.short>
- Malik, M. H., Saeed, M., & Kamboh, A. M. (2016). Automatic threshold optimization in nonlinear energy operator based spike detection. In *2016 38th Annual International Conference of the IEEE Engineering in Medicine and Biology Society (EMBC)* (Vol. 2016, pp. 774–777). IEEE. <https://doi.org/10.1109/EMBC.2016.7590816>
- Matsuura, K., Kawano, K., Inaba, N., Miura, K., & Munoz, D. (2016). Contribution of color signals to ocular following responses. *European Journal of Neuroscience*, *44*(8), 2600–2613. <https://doi.org/10.1111/ejn.13361>
- Nieuwkoop PD, Faber J. (1994). *Normal table of Xenopus laevis (Daudin): A systematical and chronological survey of the development from the fertilized egg till the end of metamorphosis*. New York: Garland.

- Packer, O., Diller, L. C., Verweij, J., Lee, B. B., Pokorny, J., Williams, D. R., ... Brainard, D. H. (2001). Characterization and use of a digital light projector for vision research. *Vision Research*, *41*(4), 427–439. [https://doi.org/10.1016/S0042-6989\(00\)00271-6](https://doi.org/10.1016/S0042-6989(00)00271-6)
- Ramlochansingh, C., Branoner, F., Chagnaud, B. P., & Straka, H. (2014). Efficacy of tricaine methanesulfonate (MS-222) as an anesthetic agent for blocking sensory-motor responses in *Xenopus laevis* tadpoles. *PLoS ONE*, *9*(7), e101606. <https://doi.org/10.1371/journal.pone.0101606>
- Raphan, T., Matsuo, V., & Cohen, B. (1979). Velocity storage in the vestibulo-ocular reflex arc (VOR). *Experimental Brain Research*, *35*(2), 229–248. <https://doi.org/10.1007/BF00236613>
- Rinner, O., Rick, J. M., & Neuhauss, S. C. F. (2005). Contrast sensitivity, spatial and temporal tuning of the larval zebrafish optokinetic response. *Investigative Ophthalmology and Visual Science*, *46*(1), 137–142. <https://doi.org/10.1167/iovs.04-0682>
- Robinson, D. A. (1981). The Use of Control Systems Analysis in the Neurophysiology of Eye Movements. *Annual Review of Neuroscience*, *4*(1), 463–503. <https://doi.org/10.1146/annurev.ne.04.030181.002335>
- Röhlich, P., & Szél, Á. (2000). Photoreceptor cells in the *Xenopus* retina. *Microscopy Research and Technique*, *50*(5), 327–337. [https://doi.org/10.1002/1097-0029\(20000901\)50:5<327::AID-JEMT2>3.0.CO;2-P](https://doi.org/10.1002/1097-0029(20000901)50:5<327::AID-JEMT2>3.0.CO;2-P)
- Rothman, G. R., Blackiston, D. J., & Levin, M. (2016). Color and intensity discrimination in *Xenopus laevis* tadpoles. *Animal Cognition*, *19*(5), 911–919. <https://doi.org/10.1007/s10071-016-0990-5>
- Schaerer, S., & Neumeyer, C. (1996). Motion detection in goldfish investigated with the optomotor response is “color blind.” *Vision Research*, *36*(24), 4025–4034. [https://doi.org/10.1016/S0042-6989\(96\)00149-6](https://doi.org/10.1016/S0042-6989(96)00149-6)

- Straka, H., & Dieringer, N. (2004). Basic organization principles of the VOR: Lessons from frogs. *Progress in Neurobiology*, 73(4), 259–309.  
<https://doi.org/10.1016/j.pneurobio.2004.05.003>
- Witkovsky, P. (2000). Photoreceptor classes and transmission at the photoreceptor synapse in the retina of the clawed frog, *Xenopus laevis*. *Microscopy Research and Technique*, 50(5), 338–346. [https://doi.org/10.1002/1097-0029\(20000901\)50:5<338::AID-JEMT3>3.0.CO;2-I](https://doi.org/10.1002/1097-0029(20000901)50:5<338::AID-JEMT3>3.0.CO;2-I)
- Yamaguchi, S., Wolf, R., Desplan, C., & Heisenberg, M. (2008). Motion vision is independent of color in *Drosophila*. *Proceedings of the National Academy of Sciences of the United States of America*, 105(12), 4910–5.  
<https://doi.org/10.1073/pnas.0711484105>
- Zoccolan, D., Cox, D. D., & Benucci, A. (2015). *Editorial: What can simple brains teach us about how vision works. Frontiers in Neural Circuits* (Vol. 9). Frontiers.  
<https://doi.org/10.3389/fncir.2015.0005>

## 4 Manuscript 3

### I spy with my little eye: A simple behavioral assay to test color perception in animal virtual reality setups

Céline M. Gravot<sup>1,2,\*</sup>, Alexander G. Knorr<sup>3,4,\*</sup>, Stefan Glasauer<sup>3</sup> and Hans Straka<sup>1</sup>

<sup>1</sup> Department Biology II, Ludwig-Maximilians-University Munich, Großhaderner Str. 2, 82152 Planegg

<sup>2</sup> Graduate School of Systemic Neurosciences, Ludwig-Maximilians-University Munich, Großhaderner Str. 2, 82152 Planegg

<sup>3</sup> Center for Sensorimotor Research, University Hospital Großhadern, Feodor-Lynen-Str. 19, 81377 Munich

<sup>4</sup> Institute for Cognitive Systems, TUM Department of Electrical and Computer Engineering, Technical University of Munich, Karlstraße 45/II, 80333 München

\* C.M.G. and A.G.K. contributed equally to this work

**Acknowledgments:** The authors further acknowledge financial support from the German Science Foundation (CRC 870; STR 478/3-1 and GL 342/2-1), the German Federal Ministry of Education and Research under the Grant code 01 EO 0901 and the Bernstein Center for Computational Neuroscience Munich (BT-1).

**Abstract**

Virtual reality has become an increasingly popular and powerful tool to study behavior and perception in humans and – more recently – also in animals. Driven by the advances in computer animation technology, virtual realities (VR) can now closely mimic natural scenes. However, little is known about how animals (whose photoreceptors differ from those of humans) perceive colors that are presented on RGB digital screens. In this study, we present a simple behavioral assay to test color perception in an animal VR setup and demonstrate results from experiments employing semi-intact preparations of *Xenopus laevis* tadpoles at mid-larval stages. The optokinetic reflex (OKR) is a visual motion driven gaze-stabilizing motor reaction and appropriately elicited by an internal representation of the visual surround's movement. Online eye tracking permits a measurement of the OKR in response to different visual scenes in a VR setup. Optokinetic stimuli were presented at a constant velocity ( $\pm 10^\circ/\text{s}$ , 0.2 Hz) using black/color striped patterns in any of the three component colors (red, green and blue). By varying the intensity of the colored stripes, we obtained response amplitude curves for each color. The intensities required to obtain an optokinetic response above a specific threshold level were determined by the relative sensitivity to an individual RGB color and was used to estimate the relative spectral sensitivity of *Xenopus* tadpoles. Systematic employment of this technique demonstrated that the relative sensitivity ( $c_{R,G,B}$ ) to the component colors of the display were  $c_R = 0.275 \pm 0.032$  for red,  $c_G = 0.585 \pm 0.028$  for green and  $c_B = 0.140 \pm 0.017$  for blue in *Xenopus laevis* tadpoles. This relatively simple method can thus be extended to other species using other suitable visuomotor transformations as behavioral readout to validate color presentation in virtual reality setups used for animal experiments.

## Introduction

Over the last two decades, virtual reality (VR) has undergone a development that is far from being completed. Ranging from military training purposes to video game technologies, VR also reached neurosciences (Bohil et al., 2011; Tarr et al., 2002; Thurley et al., 2017) as a powerful tool that opens up new avenues of research. VR enables experimenters to present situations to their subjects without limitations by the actual laboratory's layout, and even scenarios that are impossible in the real world, thereby allowing for fundamentally new approaches to study human perception and behavior that were not feasible before (Tarr & Warren, 2002). Therefore, it is no surprise that VR setups have become more and more established as a tool also in the field of research on animals (Thurley, 2017). Driven by advances in computer processing power, visual virtual environments are getting increasingly more sophisticated and life-like.

Typically, these environments are presented to the animals using readily available display technologies, such as LCD monitors and image projectors. These digital screens reproduce natural colors by mixing three distinct component colors (red, green and blue). This provides colors that appear realistic to the human eye, although the frequency spectrum of composite colors might differ from the colors observed in nature. The exact ratio between the three primary colors was determined through intensive psychophysical experimentation (Guild, 1932).

However, since different animals have different combinations of photoreceptor types, it cannot be taken for granted that this technique of color reproduction also works in the same way for animals (D'Eath, 1998; Fleishman et al., 1998). Despite the technical advances of VR in the last years, relatively little is known about how animals perceive colors on digital monitors. This is a challenge when aiming for realistic life-like virtual environments since an animal might perceive an image presented on an RGB display differently than when looking at the same image in the real world (Chouinard-Thuly et al., 2017).

Previous efforts towards an understanding of how to adequately calibrate display devices have relied on a detailed model of the retinal photoreceptors in the target species (Tedore & Johnsen, 2017). If an approximate calibration of the visual stimulus

suffices, as is the case in most VR experiments in the behavioral neurosciences, we propose a simple method for estimating the relative sensitivities to the three component colors of a RGB screen, that can be used on already-in-place VR setups.

In this study, we demonstrate how a low-level optomotor response can be used to test how animals perceive colors presented on RGB displays: Tracking the optomotor response to visual motion stimuli presented in each of the three component colors at various intensities allows for estimating the relative sensitivities to the red, green and blue channels.

## Materials and Methods

*Animal Experiments.* Experiments were performed *in-vitro* on isolated, semi-intact preparations of *Xenopus laevis* tadpoles and comply with the National Institute of Health publication entitled "Principles of animal care", No. 86-23, revised 1985. Permission for these experiments was granted by the governmental institution at the Regierung von Oberbayern/Government of Upper Bavaria (55.2-1-54-2532.3-59-12). Animals were obtained from the in-house animal breeding facility at the Biocenter-Martinsried of the Ludwig-Maximilians-University Munich. A total of 6 *Xenopus laevis* tadpoles of developmental larval stages 53-55 (Nieuwkoop & Faber, 1967) were used for experimentation. For preparation, tadpoles were anesthetized in 0.05% 3-aminobenzoic acid ethyl ester (MS-222; Pharmaq) in frog Ringer solution (in mM: 75NaCl, 25NaHCO<sub>3</sub>, 2CaCl<sub>2</sub>, 2KCl, 0.5MgCl<sub>2</sub> and 11glucose, pH7.4). The telencephalon was removed according to the preparation procedure described by Lambert et al. (2012). Preparations were kept at 14°C for 3 hours after the preparation, allowing their central nervous system to recover (Ramlochansingh et al., 2014).

*Setup.* The semi-intact preparation was fixed with insect pins to the Sylgard floor of a Petri dish (5cm diameter). The chamber, constantly perfused with oxygenated frog Ringer solution, was fixed in the center of an open cylindrical screen, encompassing 275° with a diameter of 8cm and a height of 5cm. Three digital light processing (DLP) video projectors (Aiptek V60), installed in approximately 90° angles to each other, were fixed on the table around the screen and projected different visual motion stimuli (Packer et al., 2001) at a refresh rate of 60Hz onto the screen (Fig. 1A). A CCD camera (Grasshopper

0.3 MP Mono FireWire 1394b, PointGrey), fixed on the table, permitted on-line eye tracking by custom software following the procedure described by Beck et al. (2004). The chamber was illuminated from above using an 840 nm infrared light source. An infrared long-pass filter in the camera ensured selective transmission of the infrared light and a good contrast of the eyes for the online analysis. The exact position of the visual stimulus and both eyes was read out in the data acquisition program Spike2 (Version 7.04, Cambridge Electronic Design).

*Data acquisition.* We measured the optokinetic response of *Xenopus* tadpoles. Eye position data were preprocessed by a Gaussian low-pass filter at a frequency of 5Hz, and segmented into individual cycles of the stimulus, excluding all cycles with a peak velocity  $> 50^\circ/\text{s}$  (i.e. discarding all cycles which showed other oculomotor behavior than optokinetic slow phase response, such as spontaneous swimming). We then computed the amplitude of the optokinetic reflex from the oculomotor response by fitting the stimulus profile to individual stimulus cycles and taking the median of all individual cycle amplitudes. The stimuli consisted of a 3 different stripe patterns: Red-black, green-black and blue-black at relative intensities of 0.0, 0.031, 0.063, 0.126, 0.251, 0.377, 0.502, 1.0. The stripe patterns moved following a rectangular velocity profile with a velocity of  $\pm 10^\circ/\text{s}$  and a frequency of 0.2Hz.

## Results

A suitable optomotor response is the optokinetic reflex (see Fig. 1, text inset), a gaze-stabilizing reflex which has been shown to scale with increasing contrast of a visual motion stimulus in zebrafishes (Rinner et al., 2005) and *Xenopus* tadpoles (see chapter 1, manuscript 2). This reflex can be measured by an eye tracking setup (Fig. 1) and will be used as an example in the following study. Our method can also be applied for other optomotor responses, such as body kinematics or wing beat in insects (Duistermars et al., 2007; Gray et al., 2002).

*Experimental procedure.* The relative perceived brightness  $B$  of any color ( $R, G, B$ ) in the RGB color space can be computed as (ITU-R BT.601-7):

$$B = c_R * R + c_G * G + c_B * B; \quad 0 \leq R, G, B \leq 1; \quad c_R + c_G + c_B = 1 \quad (1)$$

with  $c_{R,G,B}$  denoting the relative sensitivities to the three component colors.

To determine the values for the parameter  $c_{R,G,B}$  we measured the optokinetic reflex of *Xenopus laevis* tadpoles in response to colored visual motion stimuli (rectangular velocity profile, triangular position profile; Fig. 1B). The stimulus consisted of a striped pattern of alternating colored and black vertical stripes. The colored stripes were presented in one of the three component colors, which were shown at 8 different intensity values (0.0, 0.031, 0.063, 0.126, 0.251, 0.377, 0.502, 1.0).

As a measure for the optokinetic reflex, we used the amplitude of the eye movement response (Fig. 1C). To find the relative sensitivities to the red, green and blue components, we chose an appropriate threshold amplitude (Fig. 2). Our threshold of 0.8 was at approximately half of the saturation amplitude observed for high-intensity stimuli. We then determined the three intensities ( $R_{Th}$ ,  $G_{Th}$ ,  $B_{Th}$ ) required for each of the three colors to reach the optomotor threshold amplitude by linear interpolation.

The relative sensitivities to the individual primary colors can then be computed as:

$$c_R = \frac{1}{R_{Th}(\frac{1}{R_{Th}} + \frac{1}{G_{Th}} + \frac{1}{B_{Th}})} \quad c_G = \frac{1}{G_{Th}(\frac{1}{R_{Th}} + \frac{1}{G_{Th}} + \frac{1}{B_{Th}})} \quad c_B = \frac{1}{B_{Th}(\frac{1}{R_{Th}} + \frac{1}{G_{Th}} + \frac{1}{B_{Th}})} \quad (2)$$

*Results of animal experiments.* The results from our experiments are shown in Fig. 2. For all below-saturation intensities in the three primary colors, the optokinetic response differs greatly between red, green and blue stripes of the same relative intensity. Green stimuli evoke relatively large responses, followed by a slightly weaker response to a purely red stimulus and the smallest response to a stimulus shown only in blue. Accordingly, the relative intensity of a blue stimulus required to reach the threshold response level is much greater than the intensity required in the red and green channels. For a threshold level of 0.8 of the mean amplitude in all trials, we obtain the following relative weights for the red, green and blue components, according to equation (2):  $c_R = 0.275 \pm 0.032$ ,  $c_G = 0.585 \pm 0.028$ ,  $c_B = 0.140 \pm 0.017$ , which is surprisingly close to the values based on human perception (ITU-R BT.601-7:  $c_R = 0.299$ ,  $c_G = 0.587$ ,  $c_B = 0.114$ ). The estimates for the relative sensitivities were consistent between animals and robust to variations in threshold.

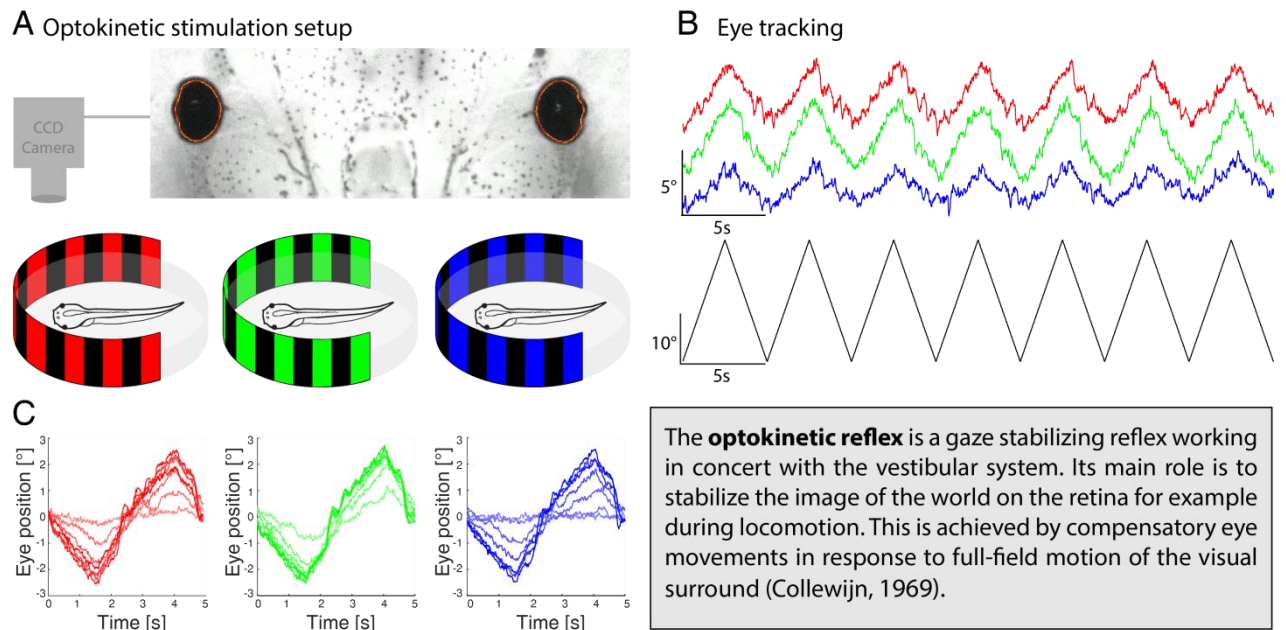


**Figure 1: Optokinetic stimulation setup.**

(A) The horizontal optokinetic reflex (hOKR) is evoked by rotation of a striped pattern projected onto a full-field cylindrical screen in a virtual reality setup. Eye movements are recorded using a monochrome CCD camera and tracked using custom-written eye tracking software (adapted from Hanzi and Straka, 2016). (B) An exemplary eye movement trace for each color (intensity level=0.1255) of the stimulus and the corresponding visual stimulus (black trace,  $v=\pm 10^\circ/s$ ,  $f=0.2\text{Hz}$ ). (C) Average OKR responses evoked by the different colors of the stimulus at different intensity levels.

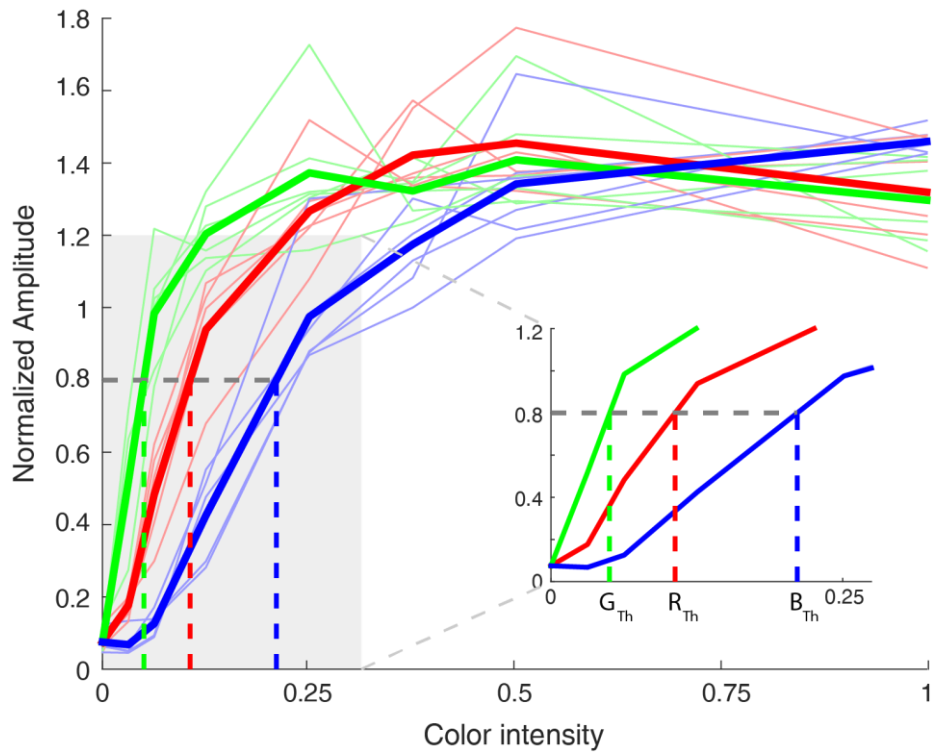


**Figure 2: Sensitivity curves for the RGB colors.**

Bold lines show averages between animals, shaded lines show individual animals' data. A threshold level was set at 0.8. The relative intensities required to obtain an optokinetic response above the threshold level are denoted with  $R_{Th}$ ,  $G_{Th}$  and  $B_{Th}$  for the three component colors, respectively (inset). These values can then be used to estimate the relative spectral sensitivities of the animal model to the three primary colors of the display.

## Discussion

Although virtual reality is becoming increasingly popular to study behavior in animals, it remains unclear if animals perceive the virtual world like we do. To validate a visual animal VR setup, we propose in this study a simple behavioral assay based on the optokinetic reflex to test color perception in a VR environment. This method can be expanded to any optomotor response which scales with subjective brightness.

Using *Xenopus laevis* tadpoles as a model, we were able to characterize animal RGB color perception in an already-in-place VR setup. An interesting observation of our results is that the relative sensitivities to the component colors of a RGB display we found in *Xenopus* tadpoles are strikingly similar to the ones used to calibrate monitors for human observers. Until now *Xenopus laevis* was mostly recognized as a model animal for developmental studies. Our results recommend *Xenopus* tadpoles as a viable species for research on the subcortical visual system.

More generally our results demonstrate that the proposed method gives consistent estimates of the spectral sensitivity between animals and is robust to the choice of the threshold level. The determined sensitivities can be used to tune VR setups adequately to provide approximately realistic color impression to the experimental animal. This is vital not only to get natural behavioral responses but also to distinguish e.g. pure color cues from combined color and intensity cues in the virtual world. On top of the optokinetic reflex as a powerful tool to gain insights into visuo-motor transformations (Benkner et al., 2013; Brockerhoff, 2006), many VR setups rely on other optomotor responses as a behavioral measure for perception, such as body kinematics (Gray et al., 2002). While our proposed method might not be as accurate as the one from Tedore and Johnsen (2016), we introduce a way to easily obtain the required data that relies only on already-in-place methods. Further, it allows for non-invasive measurements of the primary spectral sensitivity for each individual animal, this way accounting for interindividual variations in color perception. As an alternative to using our method to calibrate an RGB display, it can also be used as a rapid procedure to validate calibration according to other methods (Chouinard-Thuly et al., 2017; Tedore & Johnsen, 2017).

## References

- Beck, J. C., Gilland, E., Baker, R., & Tank, D. W. (2004). Instrumentation for Measuring Oculomotor Performance and Plasticity in Larval Organisms. *Methods in Cell Biology*, *76*, 385–413. [https://doi.org/10.1016/S0091-679X\(04\)76017-3](https://doi.org/10.1016/S0091-679X(04)76017-3)
- Benkner, B., Mutter, M., Ecke, G., & Münch, T. A. (2013). Characterizing visual performance in mice: an objective and automated system based on the optokinetic reflex. *Behavioral Neuroscience*, *127*(5), 788–96. <https://doi.org/10.1037/a0033944>
- Bohil, C. J., Alicea, B., & Biocca, F. A. (2011). Virtual reality in neuroscience research and therapy. *Nature Reviews Neuroscience*, *12*(12), 752. <https://doi.org/10.1038/nrn3122>
- Brockhoff, S. E. (2006). Measuring the optokinetic response of zebrafish larvae. *Nature Protocols*, *1*(5), 2448–51. <https://doi.org/10.1038/nprot.2006.255>
- Chouinard-Thuly, L., Gierszewski, S., Rosenthal, G. G., Reader, S. M., Rieucau, G., Woo, K. L., ... Witte, K. (2017). Technical and conceptual considerations for using animated stimuli in studies of animal behavior. *Current Zoology*, *63*(1), 5–19. <https://doi.org/10.1093/cz/zow104>
- D'Eath, Richard, B. (1998). Can video images imitate real stimuli in animal behaviour experiments? *Biological Reviews*, *73*(3), 267–292.
- Duistermars, B. J., Chow, D. M., Condro, M., & Frye, M. A. (2007). The spatial, temporal and contrast properties of expansion and rotation flight optomotor responses in *Drosophila*. *The Journal of Experimental Biology*, *210*(Pt 18), 3218–27. <https://doi.org/10.1242/jeb.007807>
- Fleishman, L. J., McClintock, W. J., D'Eath, R. B., Brainard, D. H., & Endler, J. A. (1998). Colour perception and the use of video playback experiments in animal behaviour. *Animal Behaviour*, *56*(4), 1035–1040. <https://doi.org/10.1006/anbe.1998.0894>

- Gray, J. R., Pawlowski, V., & Willis, M. A. (2002). A method for recording behavior and multineuronal CNS activity from tethered insects flying in virtual space. *Journal of Neuroscience Methods*, 120(2), 211–223. [https://doi.org/10.1016/S0165-0270\(02\)00223-6](https://doi.org/10.1016/S0165-0270(02)00223-6)
- Guild, J. (1932). The Colorimetric Properties of the Spectrum. *Philosophical Transactions of the Royal Society of London A: Mathematical, Physical and Engineering Sciences*, 230(681–693). Retrieved from <http://rsta.royalsocietypublishing.org/content/230/681-693/149.short>
- Hänzi, S., & Straka, H. (2016). Schemes of *Xenopus laevis* tadpoles. *Figshare*. Retrieved from [https://figshare.com/articles/Schemes\\_of\\_Xenopus\\_laevis\\_tadpoles/3841173](https://figshare.com/articles/Schemes_of_Xenopus_laevis_tadpoles/3841173)
- Lambert, F. M., Combes, D., Simmers, J., & Straka, H. (2012). Gaze stabilization by efference copy signaling without sensory feedback during vertebrate locomotion. *Current Biology*, 22(18), 1649–1658. <https://doi.org/10.1016/j.cub.2012.07.019>
- Nieuwkoop, P. D., & Faber, J. (1994). *Normal table of Xenopus laevis (Daudin): A Systematical and Chronological Survey of the Development from the Fertilized Egg till the end of Metamorphosis*.
- Packer, O., Diller, L. C., Verweij, J., Lee, B. B., Pokorny, J., Williams, D. R., ... Brainard, D. H. (2001). Characterization and use of a digital light projector for vision research. *Vision Research*, 41(4), 427–439. [https://doi.org/10.1016/S0042-6989\(00\)00271-6](https://doi.org/10.1016/S0042-6989(00)00271-6)
- Ramlochansingh, C., Branoner, F., Chagnaud, B. P., & Straka, H. (2014). Efficacy of tricaine methanesulfonate (MS-222) as an anesthetic agent for blocking sensory-motor responses in *Xenopus laevis* tadpoles. *PLoS ONE*, 9(7), e101606. <https://doi.org/10.1371/journal.pone.0101606>
- Rinner, O., Rick, J. M., & Neuhauss, S. C. F. (2005). Contrast sensitivity, spatial and temporal tuning of the larval zebrafish optokinetic response. *Investigative Ophthalmology and Visual Science*, 46(1), 137–142. <https://doi.org/10.1167/iovs.04-0682>

Tarr, M. J., & Warren, W. H. (2002). Virtual reality in behavioral neuroscience and beyond. *Nature Neuroscience*, 5(Supp), 1089–1092.  
<https://doi.org/10.1038/nn948>

Tedore, C., & Johnsen, S. (2017). Using RGB displays to portray color realistic imagery to animal eyes. *Current Zoology*, 63(1), 27–34. <https://doi.org/10.1093/cz/zow076>

Thurley, K., & Ayaz, A. (2017). Virtual reality systems for rodents. *Current Zoology*, 63(1), 109–119. <https://doi.org/10.1093/cz/zo>

## 5 Discussion

### 5.1 Motion information

By making use of different forms of physical quantities, the sensory systems of vertebrates and invertebrates collect information about their environment. Specialized sensors have evolved such that they selectively respond to these different physical modalities. The information that these sensors collect about a specific quantity is analyzed and processed by the central nervous system to transform e.g. the physical forces by hair cells or the movement of images across the retina into internal representations of some behaviorally meaningful state of the world and is, ultimately, used to control motor behavior. Such sensorimotor transformations are likely a defining feature that characterize how living animals interact with their environment.

#### 5.1.1 Detecting different forms of motion

One of the undoubtedly most crucial types of information that must be encoded by every living organism is motion. Whether a predator notices the movement of a prey it wants to feed on or a pedestrian infers the speed of a car to avoid a collision while crossing the road: These examples clearly illustrate that mechanisms to detect and quantify motion are vital for life. More particularly, two main types of motion cues need to be detected by living organisms: The motion of individual objects in the immediate environment around oneself, as well as one's own motion within the world.

To differentiate between these two types of motion, animals can make use of their different sensory systems and locomotor efference copies. Many aquatic species, for instance, are able to distinguish between their own and the motion of predators and preys, relying on their lateral line system that senses motion of the surrounding water. However, this system cannot give a faithful representation of self-motion with respect to the world when the surrounding medium itself is in motion. The vestibular system, on the other hand, can detect self-motion with respect to the stationary world independent of any medium but is ill-suited to detect constant motion. The visual system ideally complements these two sensory systems, as it possesses characteristics that are neither provided by the vestibular nor the lateral line system, such as the ability

to work without a high-density medium, the capability to detect constant motions, or the skill to see into the distance. This illustrates that the combination of different sensory systems is profitable for animals to obtain reliable motion information from their environment and discern between object- and self motion.

### 5.1.2 Visual motion detection

During his time as an airplane pilot during World War II, J.J. Gibson observed that the visual perception of a pilot during flight or landing periods depended on different information of a large-field image scene, such as depth cues, edges or the texture of a visual scene (Gibson, 1950). He introduced the term *optic flow field* as the spatially coherent changes of the egocentric location of image features to describe the visual stimulus provided to an observer during self-motion. Gibson's idea was that every movement has an associated optic flow pattern, permitting an observer to rely on optic flow information to reconstruct/estimate their own movement in space. And indeed, while locomoting, animals use visual motion information from a large-field image for both object detection and to guide their own movements through space. Self-motion thereby generates distinct optic flow patterns on the retina, that depend on the type of locomotor action (Krapp & Hengstenberg, 1996).

However, computationally, the extraction of motion patterns from a sequence of retinal images is not trivial. While for the lateral line and vestibular organs, there is an immediate physical coupling of the force on each individual hair cell and the motion through the medium (lateral line) or acceleration with respect to the world (vestibular system), no such direct physical coupling exists for the sense of vision. Only by comparing the activation of multiple photoreceptor cells over space and time it is possible to obtain information about motion from the sequence of retinal images.

One possible way for the visual system to discern between self- and object motion is to eliminate large-field image motion on the retina by means of eye movements that counteract the visual motion induced by self-motion through space (Lappe & Hoffmann, 2000). These eye movements have important consequences as they ensure a stable image of the environment on the retina and thereby increase visual acuity. The resulting stability of the large-field image also enhances the sensitivity for small-field object flow

patterns. Thus, compensatory eye movements are a crucial process for appropriate vision and a behavioral correlate of self-motion-related information available to the animal *via* its visual system.

In this thesis, I investigated how the eye assesses and encodes large-field motion information and how the downstream oculomotor circuitry in the midbrain controls eye movement reflexes based on these motion signals.

## 5.2 Gaze-stabilizing reflexes

To account for image displacements on the retina and achieve spatial constancy, two main gaze-stabilizing reflexes, the vestibulo-ocular reflex and the optokinetic reflex, tightly work together: While the vestibulo-ocular reflex produces compensatory eye movements in response to head motion, the optokinetic reflex elicits following eye movements in response to large-field image motion. These two reflexes ensure high visual acuity by relying on self-motion related signals from two different sensory modalities, namely the vestibular and the visual systems.

Interestingly, as demonstrated in previous work (Beraneck & Straka, 2011; DeAngelis & Angelaki, 2012) and chapters 2 and 3 of this thesis, the type of information transmitted *via* the vestibular nerve and the optic nerve population is very similar, although it originates from two qualitatively very different sensory mechanisms. Through hair cell deflection and large field optic flow, the vestibular and visual systems encode comparable information: Both nerves modulate their activity according to sensory stimuli that are likely evoked by self-motion. The notion that both nerves encode the same behavioral entity is further demonstrated by the fact that both nerves partially converge on the same central nuclei.

### 5.2.1 A behavioral correlate

To investigate how the visual system assesses and evaluates large-field motion information, the optokinetic reflex was employed as a behavioral correlate for self-motion perception. Indeed, as the optokinetic reflex is driven by the velocity of a large-field moving scene (Cohen et al., 1981; Maioli, 1988; Raphan, 1979), this reflex can give crucial insights into how the visual motion processing system assesses on the velocity of

a moving scene. The involved visuomotor circuits likely form a speed estimate of the large-field signal and translate this information into a low-level motor behavior to estimate self-motion and thereby stabilize gaze.

Typically, the percept of self-motion is acquired when animals locomote in their environments. However, large-field image motion around a stationary observer can also induce a compelling illusory sense of self-motion (Campos & Bühlhoff, 2012). In this thesis, *Xenopus* tadpoles were fixed in the center of a virtual reality setup and projectors projected different artificial virtual large-field sceneries on a cylindrical screen around the animals. Using a camera mounted on top of the setup, the optokinetic reflex of the animals could be monitored. As the moving visual images were presented with the same velocity profile, the optokinetic reflex provided an easily accessible way to compare internal speed representations in different visual scenes: A higher internal estimate of stimulus speed would translate into a stronger optokinetic response and a lower internal estimate into a lower optokinetic response. Accordingly, the magnitude of the optokinetic response in *Xenopus* tadpoles offers a convenient behavioral substrate to reveal influences of image characteristics on visual motion perception (see chapter 2, manuscript 1).

### 5.3 Speed estimation

When navigating within the environment and interacting with other animals, the ability to form an adequate internal representation of self-motion is crucial. This raises the question which signal the visual system of animals relies on to form a speed estimate of a large-field visual image scene and consequently control locomotion and navigation.

#### 5.3.1 A velocity signal present at the retinal level

One possible mechanism is that low-level motion computation is already performed at the retinal level and that motion signals are directly assessed by gaze-stabilizing visual pathways. Several studies performed on invertebrates and vertebrates showed that extensive image computation is indeed already performed at the retinal level (Gollisch & Meister, 2010). Experiments performed by Lettvin (Lettvin et al., 1959) showed for instance that optic nerve fibers of a frogs' eye report different abstract information about a visual scene (sharp edges and contrast, curvature of edges, movement of edges)

to the brain. In the seminal publication “What the frog’s eye tells the frog’s brain” (Lettvin et al., 1959), Lettvin and colleagues reported that the optic nerve does not only signal the spatial distribution of light on the different places of the retina, but rather already extracts “perceptual” features. For instance, as some cells responded preferentially to small, dark objects moving on a visual scene, they were named the “bug perceiver”.

To answer the question whether motion information of a large-field visual image is also already present at a retinal level, the optic nerve output signal transmitted from the retina to the midbrain was recorded in semi-intact *Xenopus* preparations. In the first two papers, where optic nerve activity was recorded, the results show that large-field horizontal image motion modulates the spike discharge activity in the optic nerve. These results indicate that the population signal, present at the level of the optic nerve, can already serve as an estimate of stimulus velocity and can be used to drive the optokinetic reflex (see chapter 2, manuscript 1). In the first manuscript, the strong similarity between image-related biases of the optokinetic reflex and optic nerve population activity further supports the point that the population activity at the level of the optic nerve is interpreted by the oculomotor circuitry as a velocity signal and is the basis for OKR performance (see chapter 2, manuscript 1, Figs. 3 and 5).

The aim of this thesis was to explore how the retinal signal is interpreted as a speed estimate by the visual system of *Xenopus* tadpoles, and how this signal then translates into behavior (in particular the optokinetic reflex), without explicitly studying how this speed signal is computed by retinal circuits.

### 5.3.2 The influence of visual scene parameters

Velocity signals on the retinal level are read out by certain visuomotor reflexes to ensure gaze stability during behavioral tasks. However, natural moving scenes are very complex and may possess steadily changing image characteristics. This raises the questions whether the velocity estimate is robust to the complexity of a visual scene and what impact characteristics of a moving visual image has on gaze-stabilizing reflexes. Using optokinetic reflex performance as behavioral correlate, the first two manuscripts of this

thesis demonstrate that visual speed estimation in *Xenopus* tadpoles is indeed influenced by features of a visual scene, in particular contrast polarity and color.

### Contrast polarity

In the first manuscript, the experimental manipulation of contrast polarity indicated that the optokinetic response amplitude varied strongly when inverting this parameter of the visual scene. The results suggest that for gaze-stabilizing reflexes, which are computed at early stages of visual processing, the speed estimation process is not only based on local motion of contours (Albright, 1992). Rather, the results suggested that more abstract properties of the visual surround, such as contrast polarity, heavily influence the speed estimation of a large-field visual scene. Therefore, the optokinetic reflex asymmetry must be a direct consequence of the neuronal processing underlying speed estimation, which obviously differed for different contrast polarities. Moreover, elimination of total luminance as an experimental parameter indicated that the sole inversion of contrast polarity is sufficient to elicit an asymmetric OKR.

To understand the origin of the contrast polarity bias, I recorded from the optic nerve of *Xenopus* tadpoles while presenting a single moving bar on a large-field visual screen (black bar on white background *versus* white bar on black background). Interestingly, the contrast polarity bias could be reproduced, suggesting that the velocity signal present at the retinal level is influenced by the light intensity in the vertical neighborhood of a horizontally moving edge (see chapter2, manuscript 1, Fig. 6): High uniform light intensities impinging on the receptive field of retinal ganglion cells appeared to suppress their modulation in response to the moving edge. Taken together, as a direct correlate of retinal biases could be observed in the optokinetic reflex response, this suggests that the reflex directly relies on a speed signal, which is already present at the retinal level.

### Fast phases

Interestingly, in the first study reported here, an asymmetry caused by retinal speed computations was not only observed in the immediate oculomotor following response, the optokinetic reflex, but also in a more indirect behavior, namely the number of fast phases during constant velocity stimulation (see chapter 2, manuscript 1, Fig. 4). Indeed,

a positive contrast polarity evoked both an optokinetic reflex with a higher slow phase velocity and more fast-phases. As the generation of fast phases is typically related to an internal estimate of surround velocity (Anastasio, 1996), the results suggest that the generation of fast phases is also influenced by how the central nervous system estimates the speed of image slip. The strong correlation between fast phase number and slow phase eye movements (see chapter 2, manuscript 1, Fig. 4) supports this hypothesis, suggesting that both the following response as well as the neural circuits responsible for fast phase generation draw on the same velocity estimate (see chapter 2, manuscript 1). However, how exactly the velocity signal is further processed to generate fast phases is still unclear in *Xenopus* tadpoles and in humans. Anatomical research on monkeys investigated which neural circuitries are involved in this process (Horn et al., 1996), but the question warrants further investigation.

### Color contrast

The results of the second study indicate that the color of a moving visual scene has a minor effect but also influences the optokinetic reflex in *Xenopus laevis* tadpoles. When decreasing luminance contrast in a visual moving scene (composed of two colored stripes), preparations showed a residual optokinetic response at the point of equiluminance. This indicates that pure color contrast of a moving visual image cannot be excluded to play a role - together with luminance cues - in visual motion detection mechanisms, that form the basis of and drive the optokinetic reflex. In the last years, there was a long debate about the question (Gegenfurtner & Hawken, 1996) whether color and luminance signals cooperate in the process of motion detection. Early studies claimed that color and motion cues are strictly separated (Livingstone & Hubel, 1987), such that color does not play a role in the motion detection process. However, other experiments showed that a motion percept could still be evoked in the absence of luminance contrast in human subjects (Cavanagh et al., 1984). The results of the second manuscript of this thesis support the view that color plays a role, albeit minor, in motion detecting mechanisms already in a relatively simple vertebrate species.

At high light intensity stimuli, larger responses were additionally observed when black stripes were presented together with colored than when presented together with white stripes, suggesting an influence of color on the optokinetic reflex of *Xenopus* tadpoles

(see chapter 3, manuscript 2). In experiments performed on human subjects, color has been shown to play a role in subjective speed estimation (Gegenfurtner & Hawken, 1996). Based on the results of the second study, I stipulate that color, like contrast polarity, plays a role to form a speed estimate of a large-field visual scene, and consequently influences the control of self-motion perception.

In contrast to the first manuscript, the biases observed at high intensities were not mirrored at the population level of the optic nerve. However, at a single unit level, response preferences to specific colors were present and could form the neural basis for color related biases. Since these observations are true for a large range of high-intensity luminance levels, this demonstrates that the observed differences in response amplitude are not caused by luminance artifacts, but suggests that another process explains the different increase of OKR amplitude during chromatic stimulation. It could for instance be that different retinal motion detectors with preferences for specific colors differ in how strongly they are coupled to the optokinetic reflex circuitry in the brainstem, and thereby differentially drive the reflex (Orger & Baier, 2005).

#### 5.4 Comparative aspect of visual motion processing

In the last decades, non-human primates have been used as one main animal model to investigate visual processing mechanisms (Zoccolan et al., 2015). Indeed, it was often assumed that simpler brains lack important structures to perform advanced visual processing tasks and are therefore inadequate models to draw comparisons to mammalian brains (Zoccolan et al., 2015). However, as vision is widely distributed in many species and evolutionary conserved in the animal kingdom (Sanes & Zipursky, 2010), simpler brains represent, in contrast, a very useful tool for gaining insight into common computations of visual processing. Nowadays, more and more studies are investigating visual processing mechanisms in simpler animal models, ranging from rodents (Busse et al., 2011) over simpler vertebrates (Orger & Baier, 2005) and even to nonvertebrate species (Borst, 2009), providing important findings about common computational principles in vision in general and motion vision in particular.

#### 5.4.1 Through the eye of *Xenopus laevis* tadpoles

The animal model *Xenopus laevis* developed over the last years in an excellent model to study the functional establishment of sensory-motor circuits during ontogeny (Straka & Simmers, 2012). In previous studies performed in this laboratory, the ontogenetic establishment and performance of both vestibular (Branoner et al., 2016) and optokinetic reflexes (Schuller et al., 2014) was characterized in *Xenopus laevis* tadpoles and froglets. The amphibian model hereby provides several advantages, such as the easy accessibility to both vestibular and visual systems as well as robust visuo-motor reflex responses. Further, the advantage of utilizing *in vivo*-like experimental paradigms in semi-intact *in vitro* preparations endows the experimenter with powerful opportunities for controlled manipulations of the involved circuits. Moreover, the use of these semi-intact preparations in virtual reality setups opens up valuable experimental possibilities such as the ability to isolate both sensory stimulation inputs and motor behavioral output.

In previous experiments performed by Schuller et al. (2014), large-field image motion was shown to evoke a robust optokinetic reflex in mid-larval stages of semi-intact *Xenopus* preparations with phase-coupled following movements of both eyes.

In this thesis, *Xenopus* tadpoles is the model of choice to investigate low-level visual motion perception processes. As the large-field image velocity directly determines the performance of the OKR with the purpose of minimizing retinal image slip, the OKR represents a relatively easy means to compare speed estimation for different visual scenes, provided that all experimental stimuli have the same velocity profile. Furthermore, this amphibian model species possesses a vertebrate eye and, like various other vertebrates including humans, different types of cones with three distinct absorption spectra (Witkovsky, 2000), providing the basis for potential color vision. The easy access of the eyes also enables extracellular multi-unit recordings of extraocular eye muscles or the optic nerve. Moreover, the amphibian has no fovea which other species use to focus on individual parts of an image. This facilitates the monitoring of purely optokinetic reflex eye movements without smooth pursuit eye movements like for instance in humans.

All these aspects taken together demonstrate how advantageous semi-intact preparations of *Xenopus laevis* tadpoles and their optokinetic reflex are, to provide further insight into common image processing mechanisms across species.

#### 5.4.2 Human experiments

The role of scene characteristics has been investigated extensively in human visual perception of static images (Khuu et al., 2016; Navon, 1977; Oliva, 2005). These studies demonstrated that image features, such as openness, luminance polarity or color influence perception and play a role in the interpretation of ambiguous images. However, although it is known that the perception of a visual scene depends crucially on the context in which it is presented (Stone et al., 1990; Vaziri-Pashkam & Cavanagh, 2008), it still remains unclear how motion processing in humans - in particular subjective speed estimation - is influenced by image features to form a coherent percept of full-field visual motion.

By comparing data from our *Xenopus* animal model to human subjects (see chapter 6, appendix 1), I intended to gain further insight into how context-dependent perceptual influences are represented at an early and a late processing stage along the visual pipeline, bridging the gap between brainstem computations and cognitive-level subjective perception. The influence of contrast polarity on speed perception in healthy human subjects (n=10) was tested by conducting sets of psychophysical experiments (see chapter 6, appendix 1, methods and results). Based on the results in *Xenopus* tadpoles and previous findings (Stone et al., 1990; Thompson, 1982), a similar perceptual bias in human subjective motion perception as in the animal experiment was expected, with humans slightly overestimating the speed of white dots on a black background (positive contrast polarity).

The psychophysical experiments however showed that subjective perception in human subjects is robust to a large range of visual features (total luminance and contrast polarity), except for a minor but significant individual bias with respect to contrast polarity. The functional basis of this bias could either be innate or adaptively acquired depending on lighting conditions of the recent environment.

### 5.4.3 Comparative approach

The comparative approach revealed that manipulation of image features of a visual scene influences optokinetic responses and higher cognitive functions, such as subjective speed perception. However, the results showed that the optokinetic reflex in *Xenopus* tadpoles is affected much more strongly by manipulations to the visual scene than the human subjective speed perception. These two measures provide insight into visual motion perception within two hierarchical levels. The OKR is mediated exclusively by midbrain circuits, whereas subjective perception in human subjects can be construed as a cortical process. Büchel et al. (1998) found in a human fMRI study that attention, in the absence of eye movements, modulates the activation of superior colliculus neurons in the midbrain, however, without any functional explanation of this finding. The perceptual coupling between early- and higher-level (conscious) speed estimation could relate this modulation of neural activity to a sort of “active readout” process, in which attention-related networks actively access the speed signal encoded in pretectal/midbrain circuits.

Given that cortical areas are involved in human visual motion perception (Bartels et al., 2008; Dieterich et al., 1998; Vanduffel et al., 2001), the comparative *Xenopus* and human subject results of this thesis support the notion that cortical areas appear to compensate biases, which are unaccounted for at early levels of the visual system. Boynton et al. (1999) found that contrast information is represented in the visual cortex while performing a contrast discrimination task. This information could possibly be used during motion detection to estimate the bias at brainstem visual circuitries and to compensate accordingly. The lack of consistent bias with respect to contrast polarity in human speed perception might be indicative of this compensatory process. Future experiments such as tracking of eye movements could clarify how visual motion is perceived along hierarchical levels of the visual circuitry.

### 5.4.4 Different speed estimates

Our results demonstrate that in *Xenopus* tadpoles the velocity signal encoded in the optic nerve population activity directly determines the optokinetic reflex performance.

This means that the OKR directly relies on this speed estimation signal, that may have a rather poor quality but enables a quick activation of short-latency reflex pathways.

In contrast, the fact that no systematic bias was observed in humans advocates that these subjects may rely on an additional speed signal that provides a more reliable estimate of a large-field visual scene. This is supported by the second study reported in this thesis: In contrast to the *Xenopus* OKR, which is barely present at equiluminance, humans can indeed detect motion when presented with a pure color contrast, albeit with qualitatively different discrimination thresholds for motion and direction discrimination (Derrington & Henning, 1993). This suggests that human subjects with cortical structures supplement the fast estimate at the retinal level by a second motion estimation process. For instance, human subjects could compensate for biases based on a higher-level representation of image properties. They may be able to use the different estimates for different processes, such as subjective perception or reflexes, depending on which information source appears more reliable. In this regard, human subjects could rely on (learned) a-priori information, that enable them to evaluate the correctness of the speed estimate more effectively.

## 5.5 Internal representation of self-motion

To make sense of the complex pattern of activations of sensory neurons, animals need to make an abstract internal representation about the relevant features of their environment. Indeed, perception is more than just the activation of sensory receptor cells but rather the construction of an internal representation of the state of the world. For instance, vision is not just the activation of green or blue receptors in the retina but rather an animal will perceive a tree on a green meadow in front of a blue sky. The same holds for motion vision, where animals do not only see a sequence of bright and dark spots but can infer the direction or the velocity of a whole moving image.

Sensory systems have evolved in different animals to extract biologically meaningful information from the physical world they live in. Therefore, studying these systems can be used as a vehicle to understand how animals make sense of and form an internal representation of their complex environments. In this thesis, I was particularly interested in the way the visual system of *Xenopus* tadpoles forms a speed estimate of

a large-field moving scene. As living creatures deal with diverse habitats and a large range of visual scenarios, the internal representation of their visual world needs to be robust to adequately ensure gaze stability and in a broader sense control self-motion perception.

The drastic OKR performance asymmetry with respect to contrast polarity in the first manuscript, therefore seems counterintuitive at first glance. Indeed, when coping with a large range of visual scenarios, the optokinetic reflex of sighted animals should not only be fast but also perform a robust estimate of the speed of the visual surround to maintain visual acuity. These results however suggest that a distinction based on contrast polarity assists animals in adjusting their optokinetic reflex to only relevant aspects of a large-field visual scene. The preference of specific fore- and background information (e.g. small bright objects in front of a black background) suggests that a low-level interpretation of image motion is already made at the retinal level. The observed asymmetry might functionally help the optokinetic reflex to respond predominantly to visual motion evoked by self-motion within the world, and thereby restricts eye movements in response to object motion.

This interpretation is consistent with findings in zebrafish, where large dark spots on a brighter background were shown to evoke a more efficient hunting behavior, than with a reversed stimulus. This suggests that closed contours with negative contrast are likely interpreted as prey (Bianco & Engert, 2015) and not as background (see chapter 2, manuscript 1). Almost seventy years ago, experiments performed in frogs (Barlow & Hill, 1963; Lettvin et al., 1959) showed that a prey/non-prey distinction is already made at the retinal level. Further downstream, prey-like objects were also shown to activate specific visual pathways in the predatory zebrafish (Semmelhack et al., 2014). Although *Xenopus* tadpoles are not carnivorous and thereby do not necessarily require a prey/non-prey distinction, the distinction between self-motion from the motion of other objects (animals) is ecologically advantageous. Furthermore, since adults of *Xenopus* are indeed predators, the required circuitry for prey detection might already be in place at larval stages (see chapter 2, manuscript 1).

Noteworthy in this context is that *Xenopus* changes its lifestyle during metamorphosis: this development is not only accompanied by a switch in locomotor strategy (Straka & Simmers, 2012), but also by a change in habitat. While *Xenopus* tadpoles live purely in aquatic environments, adult frogs are semi-aquatic and capture insects from the air. This transition offers a unique opportunity to gain into adaptive processes of the visual system in *Xenopus laevis*. Further experiments in adult frogs could for instance reveal, if the asymmetry caused by contrast polarity reverses in adult frog, as they are now confronted with other visual scene characteristics. It could be that the optokinetic reflex is now more sensitive to black contours on a brighter background, such as the bright (blue) sky.

Including color information from a moving visual scene to the optokinetic reflex also appears ecologically advantageous. As color is known to increase the saliency of objects, it might be assumed that color also facilitates motion perception (Dobkins & Albright, 1994). Color information could be an advantage for distinguishing between visual motion of a large-field visual scene, that is most likely caused by self-motion and should therefore elicit an OKR, and motion of small objects, such as dust or plancton moving through the water, that should be ignored by the optokinetic system. For instance, motion with respect to the blue sky could likely be interpreted as self-motion and should elicit gaze stabilizing eye movements.

As demonstrated in this thesis, features of a large-field moving scene can drastically influence the perception of the visual world in animals. Consequently, when performing experiments in different animal models, it is crucially important to control the visual environments that are presented to the laboratory animal. An incorrect calibration of the setup could distort interpretations or lead to premature conclusions regarding the behavioral data set. It is therefore important to understand how sensory systems adapt to different environmental constraints and how animals make an internal representation of these environments to support the guidance of their motor actions.

#### 5.5.1 Nature versus nurture

In the last years, there was a long debate about whether behaviors are innate (nature) or are the product of adaptations to specific environments (nurture, (Powledge, 2011)).

The results of the third manuscript revealed that color sensitivity of *Xenopus* tadpoles to the three primary colors red, green and blue, projected on the screen of our virtual reality setup, is very similar to the sensitivity of human subjects. The results are validating our animal species as a model of choice to comparatively investigate visual processes. However, the striking similarity between the sensitivities in two species raises the question whether these relative color sensitivities are genetically hard-coded in *Xenopus* tadpoles, or if the results could be the product of an adaptation process to the environmental breeding conditions of the animal model. Indeed, as the *Xenopus* tadpoles used in this study grow up under fluorescent lamps (with emission peaks in exactly the red, green and blue parts of the visible spectrum) in the animal facility, it could be that the visual system of the animal model adapted to these lighting conditions. In rats, it was shown that light can become an uncontrolled variable in experimental research by affecting the physiology and behavior of these animals (Azar et al., 2008). Therefore, further experiments in which *Xenopus* eggs and tadpoles would be raised under different lighting conditions (e.g. monochromatic red or blue light) and the spectral sensitivities of the OKR would be reassessed, could elucidate whether the spectral sensitivities are due to an adaptive process or if these sensitivities are innate to *Xenopus* tadpoles independent of rearing conditions.

## 5.6 From biology to technology

Eye movements permit to explore properties of the visual surround. In the dynamic world, animals thereby need to filter sensory information by assessing certain characteristics and events in their environments. How is the visual system extracting relevant information from the complexity of visual scenes?

The eye of *Xenopus* tadpoles can teach us much about basic computations performed in a “simpler brain” and elucidate common computation principles between species. In this thesis, I wanted to show that *Xenopus* tadpoles present a suitable animal model to help researchers from different fields understand and improve visual image analysis. Indeed, especially biophysicists and engineers try to understand design principles of biological nervous systems that enable them to design artificial neural systems. In particular, understanding the characteristics of the biological vision system, could help researchers

to overcome limitations of conventional vision sensors and develop more powerful visual sensors using bio-inspired imaging systems.

Conventional vision sensors see the world as a series of still images. However, this kind of visual processing is highly inefficient, as it uses successive frames that contain an enormous amount of redundant information. In addition, each pixel in every frame needs the same exposure time, leading to a difficult visual processing under conditions with very dark and bright regions. In contrast, event-time cameras transmit only local pixel-level brightness changes caused by movement in a scene (Mishra et al., 2017). These devices offer significant advantages, namely the processing of events in a microsecond time resolution, short-latency and consequently high-speed vision.

Similar to these technical devices, the eye of *Xenopus* tadpoles, and by extension the vertebrate eye in general, processes visual information only when changes in the image occur. The electrophysiological experiments revealed that the *Xenopus* eye responds to brightness changes and detects moving edges. The simplicity of the organisms and the easy accessibility of the visual system, could therefore provide crucial information for researchers that aim at improving visual technical devices. And especially since different features of visual scenes have a strong impact on neural activity in *Xenopus* tadpoles, this species could help in elucidating basic computations of the visual system and unraveling how image information is encoded by the retina to be sent to the visual areas of the brain. This knowledge is vital for e.g. the development of sensory prostheses. While today's commercially available cochlear implants can already restore patients' abilities to understand speech, similar solutions for e.g. blind patients are still in clinical trials.

Moreover, adult frogs could also give further insights into visual processes. By keeping their eyes still during prey detection, frogs eliminate biologically unimportant information about stationary objects (Dieringer & Daunicht, 1986). This behavior increases their ability to detect the movement of objects (food, mates, predators) amid complex environmental sceneries. When locomoting, although the stationary environment moves relative to the retina, this information can also be used to identify the location and distance of certain objects in the world (Ewert, 1970).

Taken together, simpler brains and neural circuitries such as the brain of *Xenopus laevis* can help to bridge the gap between biology and technology, and help in designing sophisticated and powerful bio-inspired visual devices, such as perhaps someday visual motion sensors on autonomous cars.

## 5.7 Outlook

Animals live in complex and dynamic environments, that require them to experience, explore and interact with their physical world (Prete, 2004). By studying simpler species, researchers of various fields can learn how the perceptual worlds of these animals are astonishingly rich and complex. To get a deeper understanding of how animals perceive their environments, scientists however first need to uncover how the sensory systems of these animals respond to and interpret different stimuli of the physical world. By introducing the term *Umwelt*, the famous biologist Jakob von Uexküll already emphasized at the beginning of the twentieth century, that the way of understanding nature is to investigate the complex relationship between the environment and an animal's internal representation (Stella & Kleisner, 2010). The technical advances of the last years and novel virtual reality setups will certainly give critical insights into many unanswered questions.

The fundamental question of how features of a visual scene influence visual speed processing have also been associated with driving performance problems on the road (Owsley & McGwin, 2010). In driving simulators, the "Thompson effect" can for instance induce faster driving in fog conditions, when subjects are asked to keep the speed constant but are deprived of speedometer reading (Snowden et al., 1998).

The visual system of *Xenopus* tadpoles therefore not only presents an ideal candidate to provide insight into common perceptual mechanisms across species, building a bridge between the well-established separate fields studying the neurophysiology of motion detection in insects on one side, and mammalian and primate visual processing on the other hand, but also to increase driving safety or to elucidate the challenge of motion detectors in autonomous cars.

## 6 Appendix 1: Human Experiments

### Methods

*Psychometric studies.* 10 healthy, naïve human subjects (9 female,  $29.6 \pm 4.6$  years) were asked to perform a speed-discrimination task. Seated in a dark room, subjects were placed in front of a 58.4 cm (23") LCD screen (ASUS VX238; 0.2652 mm pixel distance; 1920 x 1080 px) at their natural viewing distance of ~50 cm. All subjects had normal or corrected to normal vision. The experimental protocol was approved by the local ethics committee at the University Hospital Großhadern, in accordance with the standards of the Declaration of Helsinki.

*Experimental Procedure.* 480 pairs of two successive images of 400 random dots (randomly generated for each image, diameter 16 px (4.2 mm)) all moving at a speed between 25 and 75 px/s (6.6 and 19.9 mm/s) to either the left or the right were presented sequentially, with a pause of 0.75 s between two movement presentations, during which a grey screen was shown. Presentation times were drawn independently for each stimulus from a Gaussian distribution with a mean of 1.0 s and a standard deviation of 0.15 s. A red fixation point in the center of the screen was shown during the entire experiment. One of the two motion stimuli (chosen randomly) always moved at a speed of 50 px/s (13.3 mm/s), and will be referred to as *reference* stimulus. The speed of the *test* stimulus was chosen by an adaptive 1up-2down-staircase procedure starting at an absolute speed difference of 25 px/s (6.6 mm/s), with two individual staircases for each of the 4 different conditions (Table 1, Condition 1A, 1B, 2A, 2B). Each staircase was presented in 60 trials, resulting in a total of 120 trials per condition. In each trial, the sign of the speed difference with respect to the reference speed was chosen randomly and independently. Subjects were instructed to maintain fixation of the red point during the experiment and to indicate which of the two motion stimuli were perceived as moving faster by keypress on a computer keyboard. It was brought to subjects' attention that presentation times were randomized and judging displacement would not be successful. Subjects had to press the *Page Up* button, if they estimated the first stimulus as the faster one or the *Page Down* button, if they estimated the second stimulus as the faster one.

*Condition 1: role of total luminance.* The influence of total luminance on speed perception in human subjects was tested by presenting two pairs of textures with the same contrast intensity but different total luminances (Table 1). Within each pair of stimuli, the contrast polarity was identical. One pair had a positive (Condition 1A), the second pair a negative (Condition 1B) contrast polarity.

*Condition 2: role of contrast polarity.* The influence of contrast polarity on speed perception was tested by presenting two pairs of stimuli. Both pairs consisted of two stimuli with opposite contrast polarities. In one pair, which maximized contrast intensity, the total luminance differed (Condition 2A). In the other pair, the two stimuli had the same total luminance by adjusting the grey scale values of dots and background (Condition 2B).

*Data analysis and statistics.* Responses were pooled per subject for the two staircases in each experiment. Then, the speed difference between the two stimuli was computed and the ratio that subjects answered in favor of one stimulus was determined. Individual subjects' responses were fitted by cumulative Gaussian psychometric functions using the MATLAB *fit* function (MATLAB 2015b, The MathWorks Inc, Natick, MA), weighting the individual points by the number of presentations. For further analysis, the mean and standard deviation of the Gaussian fit was extracted as the point of subjective equality (PSE) and just noticeable difference (JND).

To assess potential perceptual biases in speed estimation for stimuli with different contrast polarities and luminances, *t*-tests of the recorded PSE values for all 4 conditions of the two experimental paradigms were performed. To test for individual-specific biases with respect to luminance, the correlation coefficient between subjects' PSEs in the positive contrast condition and the negative contrast (Condition 1) was computed. To test for intra-individual specific biases with respect to the contrast polarity, the correlation coefficient between the subject's PSEs during stimulation with uncontrolled-for and controlled-for total luminance (Condition 2) was computed. The critical value of significance was adjusted for multiple comparisons using Bonferroni correction.

## Results

### *Motion perception in human subjects*

A possible perceptual bias for speed estimation as observed for *Xenopus* tadpoles was tested in healthy human subjects by conducting two sets of psychophysical experiments. The different stimulus parameters and the statistics of the results are indicated in Table 1 and 2, respectively.

### *Role of total luminance on speed estimation*

The first set of experiments tested the influence of total luminance on motion perception. Subjects ( $n = 9$ ) were asked to judge and compare the respective speeds of pairs of stimuli (see Methods for details) with the same contrast polarity and contrast intensity but different total luminances. As main result, neither a consistent bias with respect to the total luminance nor a correlation between the PSEs of the two pairs of stimuli was observed (Fig. 1A). This indicates that subjective motion perception in humans is largely unaffected by changes in total luminance for the brightness levels used in this study (Fig. 1A; Table 2).

### *Role of contrast polarity on speed estimation*

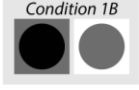
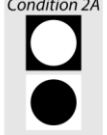
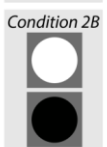
The second set of experiments tested the influence of contrast polarity on motion perception, by presenting two pairs of stimuli with opposite contrast polarities (Table 1). In one pair, the total luminance differed between both stimuli; in the other pair the total luminance was the same. On average, there was no consistent bias related to contrast polarity (Fig. 1B). Since the distribution of PSEs was non-normal in the equi-luminant pair of stimuli (Lilliefors test,  $p = 0.019$ ), a rank correlation analysis using Kendall's  $\tau$  was performed to reveal a potential association between individual biases in the two stimulus conditions with different contrast polarities. Interestingly, a significant strong association ( $\tau = 0.64$ ,  $p < 0.01$ ) between PSEs in both conditions was encountered, suggesting a consistent *intra-individual* perceptual bias related to contrast polarity (scatter plot in Fig. 1C<sub>2</sub>).

In summary, psychophysical experiments showed that subjective perception in humans is robust to a large range of visual features, however, with the exception of a minor individual bias with respect to contrast polarity.

Features		<i>contrast intensity</i>	<i>total luminance</i>	<i>contrast polarity</i>	
contrast polarity	positive		<i>Condition 1A</i> 	<i>Condition 2A</i> 	<i>Condition 2B</i> 
	negative		<i>Condition 1B</i> 		
		see Stone et al., 1990	<i>Condition 1</i>	<i>Condition 2</i>	

**Table 1: Stimulus conditions for experiments in human subjects.**

*Contrast intensity, contrast polarity* and *total luminance* were manipulated to test the respective influence of these scene features on speed perception. Pictograms indicate the intensity and contrast polarity between the random-dot pattern and the background.

<i>Conditions</i>	PSE	<i>t</i> (9)	<i>p</i>	
<i>Condition 1</i>	<i>Condition 1A</i> 	0.44 ± 4.74	0.29	0.78
	<i>Condition 1B</i> 	-1.32 ± 3.67	-1.14	0.28
<i>Condition 2</i>	<i>Condition 2A</i> 	1.65 ± 3.17	1.64	0.13
	<i>Condition 2B</i> 	1.01 ± 3.11	1.03	0.33

**Table 2: Statistical results from experiments in human subjects.**

PSE values are indicated as mean (±SD). *t* and *p* are the t-statistics and p-values for the different pairs of stimulus conditions.

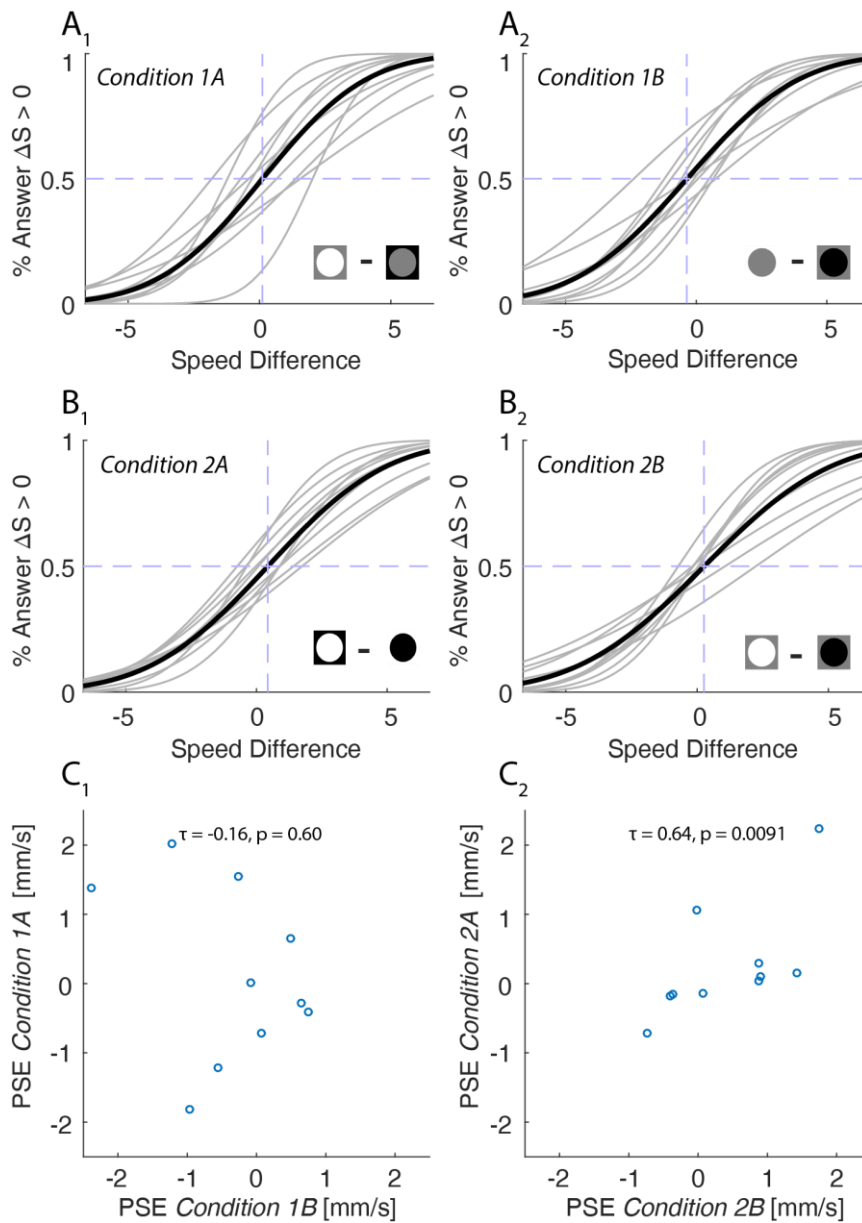


**Figure 1: Psychometric functions of human visual speed perception.**

(A,B) Dependency of speed estimation on speed difference ( $\Delta S$ , mm/s) under experimental conditions that tested the role of *total luminance* (A<sub>1,2</sub>) and *contrast polarity* (B<sub>1,2</sub>) (see pictograms in the lower right corner, respectively); grey lines represent data from individual subjects ( $n = 9$ ); black lines indicate the mean psychometric functions; the point (purple dotted line transecting the x-axis) at which individuals subjectively perceived the speed between pairs of stimuli as equal defines the *Point of Subjective Equality* (PSE). (C) Correlation of PSE values from individual subjects ( $n = 9$ ) obtained from testing *total luminance* (C<sub>1</sub>) and *contrast polarity* (C<sub>2</sub>); the high  $\tau$  value in C<sub>2</sub> indicates an association of PSE values, suggesting an intra-individual perceptual bias between the two conditions.

## 7 References

- Albright, T. D. (1992). Form-cue invariant motion processing in primate visual cortex. *Science*, 255(5048), 1141–1143. <https://doi.org/10.1126/science.1546317>
- Anastasio, T. J. (1996). A random walk model of fast-phase timing during optokinetic nystagmus. *Biol. Cybern*, 75(19), 1–9. <https://doi.org/10.1007/BF00238734>
- Angelaki, D. E., & Cullen, K. E. (2008). Vestibular System: The Many Facets of a Multimodal Sense. *Annual Review of Neuroscience*, 31(1), 125–150. <https://doi.org/10.1146/annurev.neuro.31.060407.125555>
- Appelboom, G., Yang, A. H., Christophe, B. R., Bruce, E. M., Slomian, J., Bruyère, O., ... Sander Connolly, E. (2014). The promise of wearable activity sensors to define patient recovery. *Journal of Clinical Neuroscience*. <https://doi.org/10.1016/j.jocn.2013.12.003>
- Azar, T. A., Sharp, J. L., & Lawson, D. M. (2008). Effect of housing rats in dim light or long nights on heart rate. *Journal of the American Association for Laboratory Animal Science : JAALAS*, 47(4), 25–34. Retrieved from <http://www.ncbi.nlm.nih.gov/pubmed/18702448>
- Barlow, H. B., & Hill, R. M. (1963). Evidence for a physiological explanation of the waterall phenomenon and figural after-effects. *Nature*, 200, 1345–7. <https://doi.org/10.1038/2001345A0>
- Barnes, G. R. (1983). Physiology of visuo-vestibular interactions: discussion paper. *Journal of the Royal Society of Medicine*, 76. Retrieved from <http://pubmedcentralcanada.ca/pmcc/articles/PMC1439428/pdf/jrsocmed00232-0035.pdf>
- Bartels, A., Zeki, S., & Logothetis, N. K. (2008). Natural vision reveals regional specialization to local motion and to contrast-invariant, global flow in the human brain. *Cerebral Cortex*, 18(3), 705–717. <https://doi.org/10.1093/cercor/bhm107>

- Basili, P., Huber, M., Brandt, T., Hirche, S., & Glasauer, S. (2009). Investigating Human-Human Approach and Hand-Over (pp. 151–160). Springer Berlin Heidelberg.  
[https://doi.org/10.1007/978-3-642-10403-9\\_16](https://doi.org/10.1007/978-3-642-10403-9_16)
- Bayat, B., Crasta, N., Crespi, A., Pascoal, A. M., & Ijspeert, A. (2017). Environmental monitoring using autonomous vehicles: a survey of recent searching techniques. *Current Opinion in Biotechnology*. <https://doi.org/10.1016/j.copbio.2017.01.009>
- Beck, J. C., Gilland, E., Tank, D. W., & Baker, R. (2004). Quantifying the Ontogeny of Optokinetic and Vestibuloocular Behaviors in Zebrafish, Medaka, and Goldfish. *Journal of Neurophysiology*, 92(6). Retrieved from  
<http://jn.physiology.org/content/92/6/3546>
- Benkner, B., Mutter, M., Ecke, G., & Münch, T. A. (2013). Characterizing visual performance in mice: an objective and automated system based on the optokinetic reflex. *Behavioral Neuroscience*, 127(5), 788–96.  
<https://doi.org/10.1037/a0033944>
- Beraneck, M., & Straka, H. (2011). Vestibular signal processing by separate sets of neuronal filters. *Journal of Vestibular Research : Equilibrium & Orientation*, 21(1), 5–19. <https://doi.org/10.3233/VES-2011-0396>
- Bianco, I. H., & Engert, F. (2015). Visuomotor Transformations Underlying Hunting Behavior in Zebrafish. *Current Biology*, 25(7), 831–846.  
<https://doi.org/10.1016/j.cub.2015.01.042>
- Bohil, C. J., Alicea, B., & Biocca, F. A. (2011). Virtual reality in neuroscience research and therapy. *Nature Reviews Neuroscience*, 12(12), 752.  
<https://doi.org/10.1038/nrn3122>
- Borst, A. (2009). Drosophila's View on Insect Vision. *Current Biology*, 19(1), R36–R47.  
<https://doi.org/10.1016/j.cub.2008.11.001>
- Borst, A., & Egelhaaf, M. (1993). Detecting visual motion: theory and models. *Reviews of Oculomotor Research*, 5, 3–27. Retrieved from  
<http://www.ncbi.nlm.nih.gov/pubmed/8420555>

- Borst, A., & Helmstaedter, M. (2015). Common circuit design in fly and mammalian motion vision. *Nature Neuroscience*, *18*(8), 1067–76.  
<https://doi.org/10.1038/nn.4050>
- Boynton, G. M., Demb, J. B., Glover, G. H., & Heeger, D. J. (1999). Neuronal basis of contrast discrimination. *Vision Research*, *39*(2), 257–269.  
[https://doi.org/10.1016/S0042-6989\(98\)00113-8](https://doi.org/10.1016/S0042-6989(98)00113-8)
- Branoner, F., Chagnaud, B. P., & Straka, H. (2016). Ontogenetic Development of Vestibulo-Ocular Reflexes in Amphibians. *Frontiers in Neural Circuits*, *10*, 91.  
<https://doi.org/10.3389/fncir.2016.00091>
- Brockhoff, S. E. (2006). Measuring the optokinetic response of zebrafish larvae. *Nature Protocols*, *1*(5), 2448–51. <https://doi.org/10.1038/nprot.2006.255>
- Büchel, C., Josephs, O., Rees, G., Turner, R., Frith, C. D., & Friston, K. J. (1998). The functional anatomy of attention to visual motion. A functional MRI study. *Brain*, *121*(7), 1281–1294. <https://doi.org/10.1093/brain/121.7.1281>
- Busse, L., Ayaz, A., Dhruv, N. T., Katzner, S., Saleem, A. B., Scholvinck, M. L., ... Carandini, M. (2011). The Detection of Visual Contrast in the Behaving Mouse. *Journal of Neuroscience*, *31*(31), 11351–11361.  
<https://doi.org/10.1523/JNEUROSCI.6689-10.2011>
- Butler, A. B., & Hodos, W. (2005). *Comparative vertebrate neuroanatomy : evolution and adaptation*. Wiley-Interscience. Retrieved from <https://books.google.de/books?hl=de&lr=&id=6kGARvykJKMC&oi=fnd&pg=PR5&ots=JMKSQj5XU&sig=d0OJB1LFyA2ghHXdjTSCceGqffo#v=onepage&q&f=false>
- Campos, J. L., & Bühlhoff, H. H. (2012). *Multimodal Integration during Self-Motion in Virtual Reality. The Neural Bases of Multisensory Processes*. CRC Press/Taylor & Francis. Retrieved from <http://www.ncbi.nlm.nih.gov/pubmed/22593878>
- Cavanagh, P., Tyler, C. W., & Favreau, O. E. (1984). Perceived velocity of moving chromatic gratings. *Journal of the Optical Society of America. A, Optics and Image Science*, *1*(8), 893–9. <https://doi.org/10.1364/JOSAA.1.000893>

- Chouinard-Thuly, L., Gierszewski, S., Rosenthal, G. G., Reader, S. M., Rieucau, G., Woo, K. L., ... Witte, K. (2017). Technical and conceptual considerations for using animated stimuli in studies of animal behavior. *Current Zoology*, *63*(1), 5–19. <https://doi.org/10.1093/cz/zow104>
- Cochran, S. L., Dieringer, N., & Precht, W. (1984). Basic optokinetic-ocular reflex pathways in the frog. *The Journal of Neuroscience : The Official Journal of the Society for Neuroscience*, *4*(1), 43–57. Retrieved from <http://www.ncbi.nlm.nih.gov/pubmed/6198496>
- Cohen, B., Henn, V., Raphan, T., & Dennett, D. (1981). Velocity storage, nystagmus, and visual-vestibular interactions in Humans. *Annals of the New York Academy of Sciences*, *374*(1), 421–433. <https://doi.org/10.1111/j.1749-6632.1981.tb30888.x>
- Cullen, K. E. (2012). The vestibular system: multimodal integration and encoding of self-motion for motor control. *Trends in Neurosciences*, *35*(3), 185–196. <https://doi.org/10.1016/j.tins.2011.12.001>
- D'Eath, Richard, B. (1998). Can video images imitate real stimuli in animal behaviour experiments? *Biological Reviews*, *73*(3), 267–292.
- de Burlet, H. M. (1929). Zur Vergleichenden Anatomie der Labyrinthinnervation. *The Journal of Comparative Neurology*, *47*(2), 155–169. <https://doi.org/10.1002/cne.900470202>
- DeAngelis, G. C., & Angelaki, D. E. (2012). *Visual–Vestibular Integration for Self-Motion Perception. The Neural Bases of Multisensory Processes*. CRC Press/Taylor & Francis. Retrieved from <http://www.ncbi.nlm.nih.gov/pubmed/22593867>
- Derrington, A. M., & Henning, G. B. (1993). Detecting and discriminating the direction of motion of luminance and colour gratings. *Vision Research*, *33*(5–6), 799–811. Retrieved from <http://www.ncbi.nlm.nih.gov/pubmed/8351851>
- Dichgans, J., & Brandt, T. (1978). Visual-Vestibular Interaction: Effects on Self-Motion Perception and Postural Control. In *Perception* (pp. 755–804). Berlin, Heidelberg: Springer Berlin Heidelberg. [https://doi.org/10.1007/978-3-642-46354-9\\_25](https://doi.org/10.1007/978-3-642-46354-9_25)

- Dieringer, N., & Daunicht, W. J. (1986). Image fading - a problem for frogs? *Naturwissenschaften*, *73*(6), 330–332. <https://doi.org/10.1007/BF00451484>
- Dieterich, M., Bucher, S. F., Seelos, K. C., & Brandt, T. (1998). Horizontal or vertical optokinetic stimulation activates visual motion-sensitive, ocular motor and vestibular cortex areas with right hemispheric dominance. An fMRI study. *Brain*, *121*(8), 1479–1495. <https://doi.org/10.1093/brain/121.8.1479>
- Dobkins, K. R., & Albright, T. D. (1994). What happens if it changes color when it moves?: the nature of chromatic input to macaque visual area MT. *The Journal of Neuroscience : The Official Journal of the Society for Neuroscience*, *14*(8), 4854–70. Retrieved from <http://www.ncbi.nlm.nih.gov/pubmed/8046456>
- Donaghy, M. (1980). The contrast sensitivity, spatial resolution and velocity tuning of the cat's optokinetic reflex. *The Journal of Physiology*, *300*(1), 353–65. <https://doi.org/10.1113/jphysiol.1980.sp013166>
- Duistermars, B. J., Chow, D. M., Condro, M., & Frye, M. A. (2007). The spatial, temporal and contrast properties of expansion and rotation flight optomotor responses in *Drosophila*. *The Journal of Experimental Biology*, *210*(Pt 18), 3218–27. <https://doi.org/10.1242/jeb.007807>
- Dvorak, D., Srinivasan, M. V., & French, A. S. (1980). The contrast sensitivity of fly movement-detecting neurons. *Vision Research*, *20*(5), 397–407. [https://doi.org/10.1016/0042-6989\(80\)90030-9](https://doi.org/10.1016/0042-6989(80)90030-9)
- Enright, J. M., Toomey, M. B., Sato, S., Temple, S. E., Allen, J. R., Fujiwara, R., ... Corbo, J. C. (2015). Cyp27c1 Red-Shifts the Spectral Sensitivity of Photoreceptors by Converting Vitamin A1 into A2. *Current Biology*, *25*(23), 3048–3057. <https://doi.org/10.1016/j.cub.2015.10.018>
- Erwin, D. H., Laflamme, M., Tweedt, S. M., Sperling, E. A., Pisani, D., & Peterson, K. J. (2011). The Cambrian Conundrum: Early Divergence and Later Ecological Success in the Early History of Animals. *Science*, *334*(6059). Retrieved from <http://science.sciencemag.org/content/334/6059/1091>

- Ewert, J.-P. (1970). Neural Mechanisms of Prey-catching and Avoidance Behavior in the Toad (*Bufo bufo* L.). *Brain, Behavior and Evolution*, 3(1–4), 36–56.  
<https://doi.org/10.1159/000125462>
- Fleishman, L. J., McClintock, W. J., D'Eath, R. B., Brainard, D. H., & Endler, J. A. (1998). Colour perception and the use of video playback experiments in animal behaviour. *Animal Behaviour*, 56(4), 1035–1040.  
<https://doi.org/10.1006/anbe.1998.0894>
- Fritzsche, B., & Straka, H. (2014). Evolution of vertebrate mechanosensory hair cells and inner ears: toward identifying stimuli that select mutation driven altered morphologies. *Journal of Comparative Physiology. A, Neuroethology, Sensory, Neural, and Behavioral Physiology*, 200(1), 5–18. <https://doi.org/10.1007/s00359-013-0865-z>
- Gegenfurtner, K. R., & Hawken, M. J. (1996). Interaction of motion and color in the visual pathways. *Trends in Neurosciences*, 19(9), 394–401.  
[https://doi.org/10.1016/S0166-2236\(96\)10036-9](https://doi.org/10.1016/S0166-2236(96)10036-9)
- Gestri, G., Link, B. A., & Neuhauss, S. C. F. (2012). The visual system of zebrafish and its use to model human ocular Diseases. *Developmental Neurobiology*, 72(3), 302–327. <https://doi.org/10.1002/dneu.20919>
- Gibson, J. J. (1950). *The perception of the visual world*. Houghton Mifflin. Retrieved from <http://psycnet.apa.org/psycinfo/1951-04286-000>
- Gibson, J. J. (1979). *The ecological approach to visual perception*. Houghton Mifflin. Retrieved from <http://library.wur.nl/WebQuery/clc/102810>
- Goldberg, J. M. (2000). Afferent diversity and the organization of central vestibular pathways. *Experimental Brain Research*, 130(3), 277–297.  
<https://doi.org/10.1007/s002210050033>
- Gollisch, T., & Meister, M. (2010). Eye Smarter than Scientists Believed: Neural Computations in Circuits of the Retina. *Neuron*, 65(2), 150–164.  
<https://doi.org/10.1016/j.neuron.2009.12.009>

- Goulet, J., Engelmann, J., Chagnaud, B. P., Franosch, J.-M. P., Suttner, M. D., & van Hemmen, J. L. (2008). Object localization through the lateral line system of fish: theory and experiment. *Journal of Comparative Physiology A*, *194*(1), 1–17. <https://doi.org/10.1007/s00359-007-0275-1>
- Graf, W. M. (2007). 3.26 – Vestibular System. In *Evolution of Nervous Systems* (pp. 341–359). <https://doi.org/10.1016/B0-12-370878-8/00095-1>
- Gray, J. R., Pawlowski, V., & Willis, M. A. (2002). A method for recording behavior and multineuronal CNS activity from tethered insects flying in virtual space. *Journal of Neuroscience Methods*, *120*(2), 211–223. [https://doi.org/10.1016/S0165-0270\(02\)00223-6](https://doi.org/10.1016/S0165-0270(02)00223-6)
- Guild, J. (1932). The Colorimetric Properties of the Spectrum. *Philosophical Transactions of the Royal Society of London A: Mathematical, Physical and Engineering Sciences*, *230*(681–693). Retrieved from <http://rsta.royalsocietypublishing.org/content/230/681-693/149.short>
- Hain, T., Ramaswamy, T., Hillman, M., & Herdman, S. (2007). Anatomy and physiology of the normal vestibular system. *Vestibular Rehabilitation*.
- Hawken, M. J., Gegenfurtner, K. R., & Tang, C. (1994). Contrast dependence of colour and luminance motion mechanisms in human vision. *Nature*, *367*(6460), 268–270. <https://doi.org/10.1038/367268a0>
- Hirasaki, E., Moore, S. T., Raphan, T., & Cohen, B. (1999). Effects of walking velocity on vertical head and body movements during locomotion. *Experimental Brain Research*, *127*(2), 117–130. <https://doi.org/10.1007/s002210050781>
- Horn, A. K. E., Büttner-Ennever, J. A., & Büttner, U. (1996). Saccadic premotor neurons in the brainstem: functional neuroanatomy and clinical implications. *Neuro-Ophthalmology*, *16*(4), 229–240. <https://doi.org/10.3109/01658109609044631>
- Hudspeth, A. J. (2005). How the ear's works work: mechano-electrical transduction and amplification by hair cells. *Comptes Rendus Biologies*, *328*(2), 155–162. <https://doi.org/10.1016/j.crv.2004.12.003>

- Huterer, M., & Cullen, K. E. (2002). Vestibuloocular Reflex Dynamics During High-Frequency and High-Acceleration Rotations of the Head on Body in Rhesus Monkey. *Journal of Neurophysiology*, *88*(1). Retrieved from <http://jn.physiology.org/content/88/1/13.short>
- Kaas, J. H. (1989). The evolution of complex sensory systems in mammals. *The Journal of Experimental Biology*, *146*, 165–76. Retrieved from <http://www.ncbi.nlm.nih.gov/pubmed/2689560>
- Keeley, B. L. (2002). Making Sense of the Senses. *Journal of Philosophy*, *99*(1), 5–28. <https://doi.org/10.5840/jphil20029915>
- Khuu, S. K., Honson, V., & Kim, J. (2016). The perception of three-dimensional contours and the effect of luminance polarity and color change on their detection. *Journal of Vision*, *16*(3), 31. <https://doi.org/10.1167/16.3.31>
- Kihara, A. H., Tsurumaki, A. M., & Ribeiro-do-Valle, L. E. (2006). *Effects of ambient lighting on visual discrimination, forward masking and attentional facilitation. Neuroscience Letters* (Vol. 393). <https://doi.org/10.1016/j.neulet.2005.09.033>
- Komban, S. J., Kremkow, J., Jin, J., Wang, Y., Lashgari, R., Li, X., ... Alonso, J.-M. (2014). Neuronal and Perceptual Differences in the Temporal Processing of Darks and Lights. *Neuron*, *82*(1), 224–234. <https://doi.org/10.1016/j.neuron.2014.02.020>
- Krapp, H. G., & Hengstenberg, R. (1996). Estimation of self-motion by optic flow processing in single visual interneurons. *Nature*, *384*(6608), 463–466. <https://doi.org/10.1038/384463a0>
- Lamb, T. D., Collin, S. P., & Pugh, E. N. (2007). Evolution of the vertebrate eye: opsins, photoreceptors, retina and eye cup. *Nature Reviews Neuroscience*, *8*(12), 960–976. <https://doi.org/10.1038/nrn2283>
- Lappe, M., & Hoffmann, K. P. (2000). Optic flow and eye movements. *International Review of Neurobiology*, *44*, 29–47. Retrieved from <http://www.ncbi.nlm.nih.gov/pubmed/10605640>

- Lettvin, J., Maturana, H., McCulloch, W., & Pitts, W. (1959). What the Frog's Eye Tells the Frog's Brain. *Proceedings of the IRE*, 47(11), 1940–1951. <https://doi.org/10.1109/JRPROC.1959.287207>
- Levy, K., Lerner, A., & Shashar, N. (2014). Mate choice and body pattern variations in the Crown Butterfly fish *Chaetodon paucifasciatus* (Chaetodontidae). *Biology Open*, 3(12), 1245–1251. <https://doi.org/10.1242/bio.20149175>
- Lisberger, S. G., & Westbrook, L. E. (1985). Properties of visual inputs that initiate horizontal smooth pursuit eye movements in monkeys. *The Journal of Neuroscience : The Official Journal of the Society for Neuroscience*, 5(6), 1662–1673. Retrieved from <http://www.jneurosci.org/content/5/6/1662>
- Livingstone, M. S., & Hubel, D. H. (1987). Psychophysical evidence for separate channels for the perception of form, color, movement, and depth. *The Journal of Neuroscience : The Official Journal of the Society for Neuroscience*, 7(11), 3416–3468. Retrieved from <http://www.jneurosci.org/content/7/11/3416.short>
- Macior, L. W. (1971). Co-Evolution of Plants and Animals. Systematic Insights from Plant-Insect Interactions. *Taxon*, 20(1), 17. <https://doi.org/10.2307/1218530>
- Maioli, C. (1988). Optokinetic nystagmus: modeling the velocity storage mechanism. *Journal of Neuroscience*, 8(3), 821–832. Retrieved from <http://jneurosci.org/content/8/3/821>
- Masseck, O. A., & Hoffmann, K.-P. (2009). Comparative Neurobiology of the Optokinetic Reflex. *Annals of the New York Academy of Sciences*, 1164(1), 430–439. <https://doi.org/10.1111/j.1749-6632.2009.03854.x>
- Mishra, A., Ghosh, R., Principe, J. C., Thakor, N. V., & Kukreja, S. L. (2017). A Saccade Based Framework for Real-Time Motion Segmentation Using Event Based Vision Sensors. *Frontiers in Neuroscience*, 11, 83. <https://doi.org/10.3389/fnins.2017.00083>
- Navon, D. (1977). Forest before trees: The precedence of global features in visual perception. *Cognitive Psychology*, 9(3), 353–383. <https://doi.org/10.1016/0010->

0285(77)90012-3

- Nieuwkoop, P. D., & Faber, J. (1967). *Normal Tables of Xenopus laevis: A Systematical and Chronological Survey of the Development from the Fertilized Egg Till the End of Metamorphosis*. Retrieved from <http://agris.fao.org/agris-search/search.do?recordID=US19960044123>
- Nityananda, V., Tarawneh, G., Jones, L., Busby, N., Herbert, W., Davies, R., & Read, J. C. A. (2015). The contrast sensitivity function of the praying mantis *Sphodromantis lineola*. *Journal of Comparative Physiology A: Neuroethology, Sensory, Neural, and Behavioral Physiology*, 201(8), 741–750. <https://doi.org/10.1007/s00359-015-1008-5>
- Oakley, B. (1977). Potassium and the photoreceptor-dependent pigment epithelial hyperpolarization. *The Journal of General Physiology*, 70(4). Retrieved from <http://jgp.rupress.org/content/70/4/405>
- Oliva, A. (2005). Gist of the Scene. In L. Itti, G. Rees, & J. K. Tsotsos (Eds.), *Neurobiology of Attention* (pp. 696–64). Academic Press. Retrieved from <internal-pdf://0.0.1.10/undefined.html>
- Orger, M. B., & Baier, H. (2005). Channeling of red and green cone inputs to the zebrafish optomotor response. *Visual Neuroscience*, 22(3), 275–281. <https://doi.org/10.1017/S0952523805223039>
- Osorio, D., & Vorobyev, M. (2008). A review of the evolution of animal colour vision and visual communication signals. *Vision Research*, 48(20), 2042–2051. <https://doi.org/10.1016/j.visres.2008.06.018>
- Owsley, C., & McGwin, G. (2010). Vision and driving. *Vision Research*, 50(23), 2348–2361. <https://doi.org/10.1016/j.visres.2010.05.021>
- Packer, O., Diller, L. C., Verweij, J., Lee, B. B., Pokorny, J., Williams, D. R., ... Brainard, D. H. (2001). Characterization and use of a digital light projector for vision research. *Vision Research*, 41(4), 427–439. [https://doi.org/10.1016/S0042-6989\(00\)00271-6](https://doi.org/10.1016/S0042-6989(00)00271-6)

- Parker, A. (2003). *In the blink of an eye*. Perseus Pub. Retrieved from [https://books.google.de/books/about/In\\_The\\_Blink\\_Of\\_An\\_Eye.html?id=bhgQC92kxNOC&redir\\_esc=y](https://books.google.de/books/about/In_The_Blink_Of_An_Eye.html?id=bhgQC92kxNOC&redir_esc=y)
- Pfeiffer, C., Serino, A., Blanke, O., Ferri, F., & Wong, H. Y. (2014). The vestibular system: a spatial reference for bodily self-consciousness. *Frontiers in Integrative Neuroscience* <https://doi.org/10.3389/fnint.2014.00031>
- Pinto, L. H., & Enroth-Cugell, C. (2000). Tests of the mouse visual system. *Mammalian Genome*, *11*(7), 531–536. <https://doi.org/10.1007/s003350010102>
- Powledge, T., (2011). Behavioral epigenetics: How Nurture shapes Nature. *BioScience*, *61*(8), 588-592. <https://doi:10.1525/bio.2011.61.8.4>
- Prete, F. R. (2004). *Complex worlds from simpler nervous systems*. MIT Press.
- Ramlochansingh, C., Branoner, F., Chagnaud, B. P., & Straka, H. (2014). Efficacy of tricaine methanesulfonate (MS-222) as an anesthetic agent for blocking sensory-motor responses in *Xenopus laevis* tadpoles. *PLoS ONE*, *9*(7), e101606. <https://doi.org/10.1371/journal.pone.0101606>
- Raphan, T., Matsuo, V., & Cohen, B. (1979). Velocity storage in the vestibulo-ocular reflex arc (VOR). *Experimental Brain Research*, *35*(2), 229–248. <https://doi.org/10.1007/BF00236613>
- Rinner, O., Rick, J. M., & Neuhauss, S. C. F. (2005). Contrast sensitivity, spatial and temporal tuning of the larval zebrafish optokinetic response. *Investigative Ophthalmology and Visual Science*, *46*(1), 137–142. <https://doi.org/10.1167/iovs.04-0682>
- Robinson, D. A. (1968). Eye Movement Control in Primates. *Science*, *161*(3847). Retrieved from <http://science.sciencemag.org/content/161/3847/1219>
- Sadeghi, S. G., Chacron, M. J., Taylor, M. C., & Cullen, K. E. (2007). Neural variability, detection thresholds, and information transmission in the vestibular system. *The Journal of Neuroscience : The Official Journal of the Society for Neuroscience*,

- 27(4), 771–81. <https://doi.org/10.1523/JNEUROSCI.4690-06.2007>
- Sanes, J. R., & Zipursky, S. L. (2010). Design principles of insect and vertebrate visual systems. *Neuron*, *66*(1), 15–36. <https://doi.org/10.1016/j.neuron.2010.01.018>
- Schiller, P. H., Sandell, J. H., & Maunsell, J. H. R. (1986). Functions of the ON and OFF channels of the visual system. *Nature*, *322*(6082), 824–825. <https://doi.org/10.1038/322824a0>
- Schuller, J. M., Knorr, A. G., Glasauer, S., & Straka, H. (2014). Task-specific activation of extraocular motoneurons in *Xenopus laevis*. In *Society for Neuroscience Abstracts*, *40*, 247.06.
- Semmelhack, J. L., Donovan, J. C., Thiele, T. R., Kuehn, E., Laurell, E., & Baier, H. (2014). A dedicated visual pathway for prey detection in larval zebrafish. *eLife*, *3*. <https://doi.org/10.7554/eLife.04878>
- Seymour, K., Clifford, C. W. G., Logothetis, N. K., & Bartels, A. (2009). The Coding of Color, Motion, and Their Conjunction in the Human Visual Cortex. *Current Biology*, *19*(3), 177–183. <https://doi.org/10.1016/j.cub.2008.12.050>
- Shichida, Y., & Matsuyama, T. (2009). Evolution of opsins and phototransduction. *Philosophical Transactions of the Royal Society of London. Series B, Biological Sciences*, *364*(1531), 2881–95. <https://doi.org/10.1098/rstb.2009.0051>
- Snowden, R. J., Stimpson, N., & Ruddle, R. A. (1998). Speed perception fogs up as visibility drops. *Nature*, *392*(6675), 450. <https://doi.org/10.1038/33049>
- Stella, M., & Kleisner, K. (2010). Uexküllian Umwelt as science and as ideology: the light and the dark side of a concept. *Theory in Biosciences = Theorie in Den Biowissenschaften*, *129*(1), 39–51. <https://doi.org/10.1007/s12064-010-0081-0>
- Stone, L. S., Watson, A. B., & Mulligan, J. B. (1990). Effect of contrast on the perceived direction of a moving plaid. *Vision Research*, *30*(7), 1049–1067. Retrieved from <http://www.ncbi.nlm.nih.gov/pubmed/2392834>
- Straka, H., & Baker, R. (2013). Vestibular blueprint in early vertebrates. *Frontiers in*

- Neural Circuits*, 7, 182. <https://doi.org/10.3389/fncir.2013.00182>
- Straka, H., & Dieringer, N. (2004). Basic organization principles of the VOR: lessons from frogs. *Progress in Neurobiology*, 73(4), 259–309. <https://doi.org/10.1016/j.pneurobio.2004.05.003>
- Straka, H., Holler, S., & Goto, F. (2002). Patterns of Canal and Otolith Afferent Input Convergence in Frog Second-Order Vestibular Neurons. *Journal of Neurophysiology*, 88(5). Retrieved from <http://jn.physiology.org/content/88/5/2287.short>
- Straka, H., & Simmers, J. (2012). *Xenopus laevis*: An ideal experimental model for studying the developmental dynamics of neural network assembly and sensory-motor computations. *Developmental Neurobiology*, 72(4), 649–663. <https://doi.org/10.1002/dneu.20965>
- Straw, A. D., Rainsford, T., & O'Carroll, D. C. (2008). Contrast sensitivity of insect motion detectors to natural images. *Journal of Vision*, 8(3), 32.1-9. <https://doi.org/10.1167/8.3.32>
- Sung, C., Makino, C., Baylor, D., & Nathans, J. (1994). A rhodopsin gene mutation responsible for autosomal dominant retinitis pigmentosa results in a protein that is defective in localization to the photoreceptor outer segment. *Journal of Neuroscience*, 14(10). Retrieved from <http://www.jneurosci.org/content/14/10/5818.short>
- Tarr, M. J., & Warren, W. H. (2002). Virtual reality in behavioral neuroscience and beyond. *Nature Neuroscience*, 5(Supp), 1089–1092. <https://doi.org/10.1038/nn948>
- Tedore, C., & Johnsen, S. (2017). Using RGB displays to portray color realistic imagery to animal eyes. *Current Zoology*, 63(1), 27–34. <https://doi.org/10.1093/cz/zow076>
- Thompson, P. (1982). Perceived rate of movement depends on contrast. *Vision Research*, 22(3), 377–380. [https://doi.org/10.1016/0042-6989\(82\)90153-5](https://doi.org/10.1016/0042-6989(82)90153-5)

- Thurley, K., & Ayaz, A. (2017). Virtual reality systems for rodents. *Current Zoology*, 63(1), 109–119. <https://doi.org/10.1093/cz/zow070>
- Vanduffel, W., Fize, D., Mandeville, J. B., Nelissen, K., Van Hecke, P., Rosen, B. R., ... Orban, G. A. (2001). Visual Motion Processing Investigated Using Contrast Agent-Enhanced fMRI in Awake Behaving Monkeys. *Neuron*, 32(4), 565–577. [https://doi.org/10.1016/S0896-6273\(01\)00502-5](https://doi.org/10.1016/S0896-6273(01)00502-5)
- Vaziri-Pashkam, M., & Cavanagh, P. (2008). Apparent speed increases at low luminance. *Journal of Vision*, 8(16), 9.1-912. <https://doi.org/10.1167/8.16.9>
- Wersäll, J. (1956). Studies on the structure and innervation of the sensory epithelium of the cristae ampulares in the guinea pig; a light and electron microscopic investigation. *Acta Oto-Laryngologica. Supplementum*, 126, 1–85. Retrieved from <http://www.ncbi.nlm.nih.gov/pubmed/13326368>
- Witkovsky, P. (2000). Photoreceptor classes and transmission at the photoreceptor synapse in the retina of the clawed frog, *Xenopus laevis*. *Microscopy Research and Technique*, 50(5), 338–346. [https://doi.org/10.1002/1097-0029\(20000901\)50:5<338::AID-JEMT3>3.0.CO;2-I](https://doi.org/10.1002/1097-0029(20000901)50:5<338::AID-JEMT3>3.0.CO;2-I)
- Zoccolan, D., Cox, D. D., & Benucci, A. (2015). Editorial: What can simple brains teach us about how vision works. *Frontiers in Neural Circuits*, 9, 51. <https://doi.org/10.3389/fncir.2015.00051>

## 8 Acknowledgements

First of all, I would like to thank my supervisor Prof. Straka for having given me the chance to perform my PhD thesis in his laboratory. Thank you for providing the basis that gave me the opportunity to establish a new setup and for being open to the new directions that my studies took.

I would like to thank my TAC committee, Prof. Horn-Bochtler, PD Dr. Lars Kunz and Prof. Straka for fruitful discussions during the meetings, and Prof. Büschges for reviewing this thesis.

A great thank you to Prof. Grothe and to the GSN for all the great opportunities offered by the graduate school and for the financial support during my travels to India. I also want to thank the BCCN and the RTG2175 for financial support during all these years.

I want to thank the mechanical workshop of the Biocenter Martinsried for their help in assembling the experimental setup.

A big thank to all my lab members: I had a wonderful time with you all! Particularly, thank you Francisco for always diffusing good mood, Roberto for showing me the art of operating microscopes, Sara for great scientific discussions, and Johanna for the shared salads.

A special thank to Boris, from whom I learned a lot about myself, what kind of scientist I want to be and how to recognize irony. I wish you all the best!

Thank you to my friends Katha, Johanna and Nadine: Thanks for always being there during all these years and for making the time besides work so enjoyable. I am looking forward to all the great adventures in the next years!

Merci à ma famille pour le soutien pendant toutes ces années!

And last but not least, thank you Alex! Thank you for the wonderful last years of team working. These years were the best I had during my time in science. Full of work, night shifts and analysis but also of great scientific discussions, new ideas and fun. Thank you for your amazing patience, your support and for being the best team worker one can imagine. Without you and our bio-engineering team, I would never be where I am now!

## 9 List of publications

Trattner, B., Gravot, C. M., Grothe, B., & Kunz, L. (2013). **Metabolic maturation of auditory neurones in the superior olivary complex.** *PloS one*, 8(6), e67351.

### **In press:**

Gravot C.M.\* , Knorr A.G.\* , Glasauer S. and Straka H. **It's not all black and white: Contrast polarity influences optokinetic reflex performance in *Xenopus laevis* tadpoles.**

The aforementioned manuscript is in press now (6.11.2017) in the *Journal of Experimental Biology*, doi:10.1242/jeb.16770, with a slightly modified title: "It's not all black and white: Visual scene parameters influence optokinetic reflex performance in *Xenopus laevis* tadpoles."

### **In preparation:**

Knorr A.G.\* , Gravot C.M.\* , Glasauer S. and Straka H. **Add a splash of color: Interaction of luminance and color information in the optokinetic reflex system of *Xenopus laevis* tadpoles.**

Gravot C.M.\* , Knorr A.G.\* , Glasauer S. and Straka H. **I spy with my little eye: A simple behavioral assay to test color perception in animal virtual reality setups.**

## 10 Eidesstattliche Versicherung

Hiermit versichere ich an Eides statt, dass ich die vorliegende Dissertation „**I can see it in your eyes: What the *Xenopus* eye can teach us about motion perception**“ selbstständig angefertigt habe, mich außer der angegebenen keiner weiteren Hilfsmittel bedient und alle Erkenntnisse, die aus dem Schrifttum ganz oder annähernd übernommen sind, als solche kenntlich gemacht und nach ihrer Herkunft unter Bezeichnung der Fundstelle einzeln nachgewiesen habe.

München, den 25.10.2017

---

Céline Gravot

## 11 Author contributions

Die Autoren leisteten folgende Beiträge zu den Manuskripten:

1) Céline M. Grivot\*, Alexander G. Knorr\*, Stefan Glasauer and Hans Straka. **It's not all black and white: Contrast polarity influences optokinetic reflex performance in *Xenopus laevis* tadpoles.**

C.M.G. and A.G.K. contributed equally to the present study.

Contribution of C.M.G.:

- Biological design of the study
- Performed all animal preparations
- Conducted all behavioral and electrophysiological experiments
- Data analysis of the behavioral part of the study (Fig. 1, Fig. 2)
- Data analysis for the electrophysiological parts of the study (Fig. 5B, D; Fig. 6C)
- Writing, revising and submitting the manuscript

Contribution of A.G.K.:

- Technical design of the study
- Programmed the experimental software of the setup
- Statistical analysis of the behavioral part of the study (Fig. 3, Fig. 4)
- Statistical analysis for the electrophysiological parts of the study (Fig. 5C; Fig. 6B, D)
- Programmed psychophysical experiments
- Writing, revising and submitting the manuscript

H.S. contributed to writing of the manuscript. S.G. and H.S. supervised the study and edited the manuscript.

2) Alexander G. Knorr\*, Céline M. Gravot\*, Stefan Glasauer and Hans Straka. **Add a splash of color: Interaction of luminance and color information in the optokinetic reflex system of *Xenopus laevis* tadpoles.**

A.G.K. and C.M.G. contributed equally to the present study.

Contribution of C.M.G.:

- Biological design of the study
- Performed all animal preparations
- Conducted all behavioral and electrophysiological experiments
- Data analysis of the behavioral part of the study (Fig. 1)
- Data analysis of the electrophysiological parts of the study (Fig. 3A)
- Writing, revising and submitting the manuscript

Contribution of A.G.K.:

- Technical design of the study
- Programmed the experimental software of the setup
- Statistical analysis of the behavioral part of the study (Fig. 2)
- Statistical analysis of the electrophysiological parts of the study (Fig. 3B, C)
- Performed statistical analysis
- Writing, revising and submitting the manuscript

S.G. and H.S. supervised the study.

3) Céline M. Gravot\*, Alexander G. Knorr\*, Stefan Glasauer and Hans Straka. **I spy with my little eye: A simple behavioral assay to test color perception in animal virtual reality setups.**

C.M.G. and A.G.K. contributed equally to the present study.

Contribution of C.M.G.:

- Biological design of the study
- Performed all animal preparations
- Conducted all behavioral experiments
- Data analysis of the behavioral part of the study (Fig. 1)
- Writing, revising and submitting the manuscript

Contribution of A.G.K.:

- Technical design of the study
- Programmed the experimental software of the setup
- Statistical analysis of the behavioral part of the study (Fig. 2)
- Writing, revising and submitting the manuscript

S.G. and H.S. supervised the study.

#### 4) Appendix 1: Human experiments

C.M.G. and A.G.K. contributed equally to the present study.

Contribution of C.M.G.:

- Design of the study
- Conducted human experiments

Contribution of A.G.K.:

- Design of the study
- Data analysis

S.G. and H.S. supervised the study.

Hiermit bestätige ich die angegebenen Beiträge zur Erstellung der Manuskripte.

München, den \_\_\_\_\_

Céline M. Gravot

Alexander G. Knorr  
(shared first author)

Prof. Hans Straka  
(supervisor)